MECHANISMS OF SYNAPSE FORMATION AND MAINTENANCE: INSIGHTS FROM THE DEVELOPING AND DISEASED NERVOUS SYSTEM

Ethan G. Hughes

A DISSERATION

in

Neuroscience

Presented to the Faculties of the University of Pennsylvania

in

Partial fulfillment of the Requirements for the

Degree of Doctor of Philosophy

2009

Supervisor of Dissertation

Rita J. Balice-Gordon, Ph.D.

Graduate Group Chairperson

Rita J. Balice-Gordon, Ph.D.

Dissertation Committee

Steven S. Scherer, M.D., Ph.D.

Harry Ischiropoulos, Ph.D.

Tom D. Parsons, V.M.D., Ph.D.

Michael B. Robinson, Ph.D.

Josep Dalmau, M.D., Ph.D.

ABSTRACT

MECHANISMS OF SYNAPSE FORMATION AND MAINTENANCE: INSIGHTS FROM THE DEVELOPING AND DISEASED NERVOUS SYSTEM

Ethan G. Hughes

Rita J. Balice-Gordon, Ph.D.

The formation and maintenance of synapses is essential for the central nervous system (CNS) to function. In the developing nervous system, the assembly of synaptic circuits is a complex and dynamic process, requiring the coordinated exchange of signals between pre- and postsynaptic neurons and surrounding glia. The maintenance and modulation of synaptic connections is required for normal CNS function and ongoing plasticity. The structural and functional integrity of synaptic connections is often modified or lost in the diseased nervous system, resulting in profound cognitive and behavioral deficits. While some aspects of the mechanisms underlying the formation, maintenance and plasticity of CNS synapses in the developing and diseased nervous system have been elucidated, many more remain to be understood.

In my thesis work, I have examined the role of astrocytes in the development of GABAergic hippocampal synapses in *in vitro* models. I have also examined the maintenance of glutamatergic synapses in *in vitro* and *in vivo* models of anti-NMDAR

encephalitis, an immune-mediated disorder of memory and behavior. First, I demonstrate that secreted factors released from astrocytes specifically increase GABAergic axon length, branching, and synaptogenesis, that these effects are not mediated by several well-known candidates, and that the secreted factors from astrocytes are proteins. Second, I examined the identity of the proteins released from astrocytes that affect GABAergic neurons using size fractionation, mass spectroscopy, and computational analyses. Third, I examined the cellular and synaptic mechanisms underlying anti-NMDAR encephalitis and investigated the effects of autoantibodies from patients with this disorder on the maintenance and function of CNS excitatory synapses. Together, my work extends our understanding of how neuron-glial communication modulates the formation of synapses in the developing brain, and how the disruption of synapse maintenance may underlie cognitive deficits in the diseased nervous system.

TABLE OF CONTENTS

LIST OF TABLES

Chapter 2

Chapter 3

LIST OF ILLUSTRATIONS

Chapter 2

Chapter 3

Chapter 4

Introduction

Part 1: Neuron-glia signaling in CNS synapse formation

The assembly of central nervous system (CNS) synaptic circuits is a complex and dynamic process, requiring the coordinated exchange of signals between pre- and postsynaptic neurons and surrounding glia. Astrocytes, one of the main glial cell types in the CNS, have been traditionally considered to act passively in the brain, maintaining ionic homeostasis in the extracellular milieu, removing neurotransmitters from the synaptic cleft, and providing trophic factors for neurons. Recently, this view has been challenged by evidence that astrocytes can respond to and modulate neuronal signaling. While astrocytes participate in the function of neuronal circuitry, other studies implicate astrocytes in neuronal process outgrowth and the development and maintenance of synaptic connections. However, until recently the mechanisms by which astrocytes affect neurite outgrowth and synapse formation, function and maintenance have been poorly understood.

Role of astrocytes in neurite outgrowth

The surface of astrocytes and astrocyte precursors are prominent substrates for neurite growth during development, and also play an active role in directing axons to targets by both promoting and inhibiting axonal outgrowth. Astrocytes express and release numerous factors that promote and inhibit neurite outgrowth. Studies

investigating the signals that promote axon growth along astroglia surfaces as in the developing optic pathway, have identified cell surface adhesion molecules, such as N-cadherin and integrins, to be expressed on the surface of astrocytes promote neurite outgrowth (Neugebauer et al., 1991). Interestingly, other cell-surface proteins also present on astrocytes, such as chondroitin sulfate proteoglycans, have been shown to restrict neurite outgrowth (Smith-Thomas et al., 1994). In addition to contact-mediated factors, astrocytes have also been shown to promote neurite outgrowth through the release of diffusible factors. Biochemical fractionation and purification of astrocyte conditioned media has identified extracellular matrix proteins, laminin and fibronectin, are released by astrocytes and act to promote neurite outgrowth (Matthiessen et al., 1989). Furthermore, astrocytes release trophic factors, such as fibroblast growth factor, that stimulate both axonal and dendritic growth of dissociated neurons grown *in vitro* (Le and Esquenazi, 2002).

How do astrocytes both promote and inhibit neurite outgrowth? First, there may be regional differences in the ability of astrocytes to modulate neurite outgrowth such that local astrocytes support outgrowth in a manner distinct from target-derived or other cues (Qian et al., 1992). Second, populations of astrocytes within the same region of the nervous system may be composed of functionally distinct subtypes, some of which support and others that restrict neurite outgrowth (Meiners et al., 1995). Recent work shows that astrocyte subtypes in the spinal cord are positionally distinct and are determined by the expression of certain homeodomain transcription factors (Hochstim et

al., 2008). Third, neurite promoting properties of astrocytes may be a balance between the expression of promoting and blocking molecules (Smith-Thomas et al., 1994). Understanding how astrocytes affect neurite outgrowth will not only give us a better understanding of how the nervous system develops but also provide insights into the diseased nervous system, as astrocytic responses to injury are thought to negatively affect axon regeneration (Benfey and Aguayo, 1982; Smith et al., 1986; Tomaselli et al., 1988; Silver and Miller, 2004; Rolls et al., 2009). Together, these studies show that astrocytes use both soluble and contact-mediated mechanisms to both promote and inhibit the outgrowth of processes from neurons.

Role of astrocytes in the development of synapse structure and function

Several lines of evidence suggest that astrocytes also affect the development of synapses. First, astrocytes extend thousands of fine processes that enwrap synapses and blood vessels (Ventura and Harris, 1999; Bushong et al., 2002). Second, the peak of astrocyte development overlaps with the formation of synapses during the development in vivo (Ullian et al., 2001). Third, experimental evidence has shown that in purified retinal ganglion cell cultures, the presence of astrocytes and/or astrocyte conditioned media (ACM) dramatically increases the number of presynaptic contacts, the quantal size and efficacy of neurotransmitter release, and the number of postsynaptic AMPA receptor clusters (Pfrieger and Barres, 1997; Nagler et al., 2001; Ullian et al., 2001; Ullian et al., 2004). Fourth, astrocyte-like glia in *C elegans* are important for synapse specification

and the source of soluble factors that both increase and decrease synapse formation (Shen and Bargmann, 2003; Shen et al., 2004; Colon-Ramos et al., 2007; Poon et al., 2008). These data suggest that astrocytes, in addition their roles in neurite outgrowth, modulate the formation of synapses in the developing nervous system.

Role of astrocytes in the development of inhibitory synapses

Since a majority of studies investigating synaptogenesis have focused on the formation of excitatory synapses, much less is known inhibitory synaptogenesis. While the components of the inhibitory synapse are clearly defined, the mechanisms regulating the construction of inhibitory synapses are less understood. Recent studies have implicated several different processes involving secreted factors, trans-synaptic signaling molecules, and transcription factors in mediating the formation of inhibitory synapses. The secretion of the neurotrophic factor BDNF not only increases the formation of excitatory synapses, but also increases the number of inhibitory synapses formed by developing neurons (Vicario-Abejon et al., 1998; Marty et al., 2000). The trans-synaptic adhesion molecule, Neuroligin-2, is localized to inhibitory synapses and induces the formation of inhibitory presynaptic terminals when expressed in heterologous cells (Graf et al., 2004; Varoqueaux et al., 2004). In addition, the transcription factor NPAS4 regulates the expression of activity-dependent genes, which in turn control the number of GABA-releasing synapses that form on excitatory neurons (Lin et al., 2008).

Though many studies have investigated the role of astrocytes at excitatory synapses, the role of astrocyte signaling in inhibitory synapse formation and function is largely unknown. Astrocytes influence inhibitory synaptic transmission in hippocampal slices, where perisynaptic astrocytes release glutamate in response to $GABA_B$ receptor activation potentiating interneuron GABA release onto pyramidal neurons (Kang et al., 1998). Recent work has demonstrated that Bergmann glia of the cerebellum express L1 family immunoglobulin protein Close Homologue of L1 (CHL1) which directs the innervation of inhibitory stellate cells onto their postsynaptic targets (Ango et al., 2008). In addition, cortical astrocytes increase the GABA-induced Cl- currents and contribute to the maintenance of surface $GABA_A$ receptors ($GABA_ARs$), the major inhibitory ionotropic receptor, in developing hippocampal neurons (Liu et al., 1996; Liu et al., 1997). Recent work has shown that astrocytes increase inhibitory synaptogenesis by augmenting the number of inhibitory presynaptic terminals and frequency of miniature IPSCs, through the modulation neurotrophin signaling between neurons (Elmariah et al., 2005). These findings support a role for astrocytes in the formation and function of inhibitory synapses as well as excitatory synapses, as previously appreciated.

Role of astrocyte-neuron contact in synapse structure and function

The intimate proximity of neurons and astrocytes in the brain raises the question of what role astrocyte contact plays in synapse formation and function. Astrocytes ensheathe synapses throughout the hippocampus (Ventura and Harris, 1999) and recent

work showed that astrocytes regulate postsynaptic spine morphology through signaling between ephrinA3 in astrocyte processes and ephA4 in dendritic spines (Murai et al., 2003). Time-lapse microscopy has revealed that astrocytes rapidly extend and retract fine processes to engage and disengage motile postsynaptic dendritic spines (Haber et al., 2006). This activity of astrocytic processes during development can act to stabilize dendritic filapodia and possibly lead to their maturation into spines (Nishida and Okabe, 2007).

In addition to playing a role in maintaining synaptic structure and number by regulating spine shape, astrocyte contact is important in the plasticity of synaptic circuits. In the hypothalamus, withdrawal of astrocyte processes increases the number of synapses on the postsynaptic neuron (Theodosis and Poulain, 2001). Astrocyte contact also increases neuronal voltage-gated calcium currents (Mazzanti and Haydon, 2003), and is thought to be required for the potentiation of synaptic inputs by D-serine secreted from astrocytes (Yang et al., 2003).

Beyond roles in regulating synaptic structural and functional plasticity, recent work has shown that astrocyte contact with neurons increases excitatory synaptogenesis through an integrin-mediated PKC-dependent mechanism (Hama et al., 2004). These and other studies highlight the importance the physical interactions of neurons and astrocytes in regulating synapse formation and function.

Role of astrocyte-derived soluble factors in synapse structure and function

Several lines of evidence suggest that astrocytes coordinately modulate the pre- and postsynaptic development of excitatory synapses by soluble as well as contact-mediated factors. Glial-derived soluble and contact factors enhance neurite outgrowth and synapse formation and function (Pfrieger and Barres, 1997; Ullian et al., 2001; Le and Esquenazi, 2002; Ullian et al., 2004). In purified retinal ganglion cell and spinal motor neuron cultures, glia-conditioned medium increased the number of presynaptic contacts made between neurons, quantal size and the efficacy of transmitter release and increased the number of postsynaptic AMPA receptor clusters (Pfrieger and Barres, 1997; Nagler et al., 2001; Ullian et al., 2001; Ullian et al., 2004). Recent work from the Balice-Gordon lab has shown that astrocytes also enhance inhibitory synaptogenesis by releasing soluble factors that enhance BDNF to TrkB signaling in neurons (Elmariah et al., 2005). Additionally, the secretion of the cytokine tumor necrosis factor-α (TNF-α) from astrocytes increases postsynaptic efficacy in hippocampal cultures and slices by regulating the number of surface AMPA receptors (Beattie et al., 2002).

Once mature synapses have formed, astrocytes continue to provide soluble factors that regulate synaptic transmission. Several studies have shown that neuronal transmitters evoke the release of soluble factors from astrocytes that in turn modulate excitatory and inhibitory transmission (Kang et al., 1998; Yang et al., 2003; Zhang et al., 2003; Fiacco and McCarthy, 2004). These effects are mediated in part by astrocyte factors that are released via a SNARE-dependent mechanism of vesicular release (Bezzi et al., 2004; Mothet et al., 2005; Pascual et al., 2005).

Role of astrocytes in synapse maintenance

Astrocytes role in synapse formation has been well studied; however, what role astrocytes play in the maintenance of synapses is less understood. In the peripheral nervous system Schwann cells, a glial cell type that is essential for the development and function of neuromuscular junctions (NMJ), are crucial for the maintenance of NMJs. Schwann cell ablation at NMJs causes reduced synaptic efficacy of motor nerve terminals and retraction after 1 week showing that Schwann cells are essential for the long-term maintenance of synaptic structure and function of the adult NMJ (Feng and Ko, 2008).

While the role of astrocytes in the maintenance of CNS synapses has not been specifically examined, astrocytes have been implicated in playing a role in synapse elimination. Stevens and colleges have shown that immature astrocytes release a soluble factor that increases the expression and release of C1q, a protein in the classical complement cascade, from neurons and possibly microglia. C1q then associates with synapses and is thought to initiate the complement cascade at unwanted synapses to mediate synapse elimination (Stevens et al., 2007).

At motor nerve terminals, several candidate molecules are necessary for the maintenance of NMJs. While collagen IV chains alpha 2 are necessary for the proper development and function of motor nerve terminals, synapse-specific alpha3-6 (IV) chains accumulate only after synapses are mature and are required for synaptic maintain synaptic terminals (Fox et al., 2007). Collagens are an essential part of the extracellular

matrix and previously have also been shown to be expressed by astrocytes (Heck et al., 2003). Future studies examining the role of astrocyte-derived collagens may lead to insights into how astrocytes affect the maintenance of CNS synapses.

Identification of astrocyte-factors involved in synaptogenesis

Since the initial observations that glia enhance excitatory synaptogenesis (Pfrieger and Barres, 1997), investigators have been in search for the candidate molecules mediating these effects. Mauch et al. found that astrocyte-derived cholesterol complexed to ApoE was both necessary and sufficient to increase the number of functional presynaptic terminals in retinal ganglion cells (RGC) (Mauch et al., 2001). Recent work has also demonstrated that thrombospondin-1 and -2 expressed by immature astrocytes can also increase excitatory synapses between RGCs *in vitro* and *in vivo*. These immature synapses are presynaptically active but postsynaptically silent, suggesting that other, as yet unknown, factors may coordinate pre- and postsynaptic maturation (Christopherson et al., 2005).

Identification of astrocyte factors that regulate synapse formation has been limited by the lack of characterization of the genes and proteins expressed by astrocytes. Without efficient purification methods to obtain a sufficiently pure population of astrocytes, gene array analyses were not possible. Using different purification strategies approaches, two groups have recently profiled the gene expression of in vitro and in vivo astrocytes (Lovatt et al., 2007; Cahoy et al., 2008). These “astrocyte transcriptomes”

provide a view into the inter-workings of astrocytes and show many interesting pathways and candidates that can now be examined for their roles in synaptogenesis. Taking a different approach, several other groups have used proteomic approaches to analyze the proteins released by astrocytes, or the "astrocyte secretome" (Dowell et al., 2009; Keene et al., 2009; Moore et al., 2009). Translational profiling approaches (Doyle et al., 2008; Heiman et al., 2008) and analysis of secreted and membrane-bound molecules by signal-sequence trap (Spiegel et al., 2006) may yield even more interesting and useful data if applied to study astrocytes. These gene and secreted protein profiles of astrocytes will be invaluable tools in proceeding forward in the identification of new astrocyte factors and their roles in synapse formation.

With the discovery of larger numbers of new candidates from genomic and proteomic profiles of astrocytes, the evaluation of these potentially interesting candidates will be necessary. Several groups have used large-scale screens to identify new molecules implicated in synapse formation and synapse specificity (Kurusu et al., 2008; Linhoff et al., 2009). One of these approaches was an unbiased expression screen, where a cDNA library screen yielded a new family of trans-synaptic molecules that mediate synapse formation (Linhoff et al., 2009). This type of approach on a large and small scale will be invaluable to evaluate new candidates identified by the gene expression and secreted protein profiles of astrocytes.

Conclusions and future directions

The studies described above begin to define the cellular and molecular mechanisms that underlie the communication between neurons and glia that modulates synapse formation, function and maintenance. Evaluating these newly defined pathways in intact animals represents an important challenge for future research. Examining neuron-glia communication will be critical to understand how synaptic connections are formed and function in the developing and mature brain and will greatly contribute to disorders of development such as epilepsy, autism and mental retardation, in which synapse formation, function, maintenance are aberrant or reduced.

Thesis rationale and goals

Though many studies have investigated the role of astrocytes at excitatory synapses, the role of astrocyte signaling in inhibitory synapse formation and function is largely unknown. Previous work from our lab has suggested that astrocytes increase inhibitory synaptogenesis by modulating postsynaptic $GABA_A$ receptors via BDNF to TrkB signaling (Elmariah et al., 2005). Based on these findings, I examined the effects of astrocytes on presynaptic aspects of inhibitory synaptogenesis and have identified the proteins released by astrocytes that affect GABAergic neurons (Chapters 2, 3). Using biochemical, proteomics, and imaging techniques, I tested the hypothesis that a*strocyte*

secreted proteins specifically increase GABAergic axon length, branching, and synaptogenesis.

My work demonstrates the identity of astrocyte proteins that selectively increase GABAergic axon length, branching and the density of functional synapses. Moreover, I show that these proteins differentially affect GABAergic axon outgrowth compared to glutamatergic neurons. Together this work characterizes new roles for astrocytes in mediating GABAergic synaptogenesis, highlighting the importance of this glial type in the development and maintenance of neural circuits.

Part 2: Glutamate receptors in immune-mediated encephalitis

Glutamate ionotropic receptors, NMDARs and AMPARs, play essential roles in synaptic transmission and plasticity and underlie numerous brain functions, including learning and memory. The dysfunction of NMDA and AMPA receptors has been proposed to result in several well known cognitive disorders, including schizophrenia and addiction. However, the mechanisms linking changes in glutamate receptor function to changes in behavior remain controversial. Recently, two new disorders of behavior and cognition, anti-NMDAR and anti-AMPAR encephalitis, have been identified and are mediated by autoantibodies against glutamate receptors (Dalmau et al., 2007; Lai et al., 2009). Patient autoantibodies bind to surface glutamate receptors, leading to their internalization and a decrease in receptor mediated synaptic currents, resulting in glutamate receptor hypofunction. The reduction or removal of autoantibodies results in a recovery of behavioral and cognitive dysfunctions suggesting that the blockade of glutamate receptors by autoantibodies is responsible for observed changes in cognition and behavior (Dalmau et al., 2008); Hughes et al., in preparation). Thus these new disorders have the potential to provide important insights into the functional roles of these receptors in memory, behavior and cognition of the normal and diseased brain.

Autoimmunity to synaptic proteins

While there are numerous diseases where synaptic dysfunction correlates to a neurological condition, autoimmune disorders provide an opportunity to link a defined disease that causes synaptic dysfunction, to circuit dysfunction and, ultimately, behavioral dysfunction, and in particular to understand how each recovers once autoantibodies are reduced or eliminated. In the peripheral nervous system, immune-mediated alterations in synaptic structure and physiology are known to cause specific neurological disorders. Two well known examples are Myasthenia gravis and Lambert-Eaton syndrome (Sanders, 2002; Conti-Fine et al., 2006). Patients with these disorders develop antibodies that alter the function and density of acetylcholine receptors or voltage-gated calcium channels, resulting in characteristic muscle weakness due to synaptic dysfunction. Both of these usually improve with immunotherapy and other treatments. The autoantibodies that cause these disorders affect synaptic proteins by at least three different mechanisms. First, they have been shown to functionally block receptors or channels resulting in decreased synaptic function (Gomez and Richman, 1985; Kim and Neher, 1988). Second, autoantibodies crosslink synaptic proteins which lead to their removal from the synaptic membrane by internalization and degradation, a process called antigenic modulation (Drachman et al., 1978; Rich et al., 1994). A third mechanism is antibody-mediated activation of the complement cascade which has been shown to cause a large portion of the effects of myasthenia gravis. Autoantibodies bind the acetylcholine receptor and trigger the complement cascade, which leads to the focal destruction of postsynaptic membrane through the recruitment of the membrane attack

complex (Lennon and Lambert, 1981; Tuzun et al., 2003). While these and other studies have extensively characterized autoimmune disorders affecting neuromuscular synaptic proteins, much less is known about autoimmunity to synaptic proteins in the central nervous system.

Autoimmunity to glutamate receptors

Autoimmunity to glutamate receptors (both NMDA and AMPA receptor subunits) has been previously described in patients with epilepsy, systemic lupus erythematosus (SLE) and encephalitis. Autoantibodies against the GluR3 subunit of the AMPA receptor have been implicated in mediating Rasmussen's encephalitis, a severe epileptic disorder, and several other epilepsies (Rogers et al., 1994; Levite and Ganor, 2008), although the association of GluR3 autoantibodies and encephalitis has been controversial (Pleasure, 2008). Previous work has suggested that some autoantibodies against GluR3 can act as AMPA receptor agonists and evoke ion currents (Twyman et al., 1995) which can lead to excitotoxic cell death (Levite et al., 1999). However, other groups have been unable to find autoantibodies against GluR3 in patients with Rasmussen's encephalitis and intractable epilepsy, or, when autoantibodies are present; these antibodies did not affect AMPA receptor function (Watson et al., 2004). These results suggest that although GluR3 autoantibodies may have pathogenic effects, their presence is not characteristic of Rasmussen's encephalitis or epilepsy.

Some studies show that autoantibodies against double-stranded DNA also cross-react to the NR2A or NR2B subunits of the NMDA receptor in SLE (DeGiorgio et al., 2001). These autoantibodies that bind DNA and the NR2 subunit of NMDA receptors can cause apoptotic death of neurons *in vivo* and *in vitro* through an excitotoxic and complement-independent mechanisms (DeGiorgio et al., 2001). However, while other groups have confirmed the presence of NR2 autoantibodies in some patients with SLE, these studies have not found an association of the presence of autoantibodies and cognitive dysfunction (Hanly et al., 2006; Harrison et al., 2006; Lapteva et al., 2006). These findings suggest that although autoantibodies against NR2 subunits exist in some patients with SLE, however, their function and correlation with SLE is less well defined.

Autoantibodies against the metabotropic glutamate receptor mGluR1 have been identified in two patients diagnosed with cerebellar ataxia after being in remission from Hodgkin's lymphoma (Sillevis Smitt et al., 2000). These autoantibodies have been shown to reduce the basal activity of Purkinje cells and block induction of long-term depression (Coesmans et al., 2003). Another patient with cerebellar ataxia has autoantibodies to Homer3, an mGluR1 interacting protein (Zuliani et al., 2007). This work suggests that autoimmunity to synaptic metabotropic proteins may result in cerebellar dysfunction.

Taken together, these studies suggest that autoantibodies against glutamate receptors may be present in epilepsy, systemic lupus erythematosus (SLE) and some

types of encephalitis. However, more work is needed to establish a causative pathogenic effect of these autoantibodies in mediating the symptoms of these disorders.

Anti-NMDAR encephalitis: Human model of NMDA receptor dysfunction

Recently, a new disorder has been described by Dalmau and colleges where the presence of autoantibodies against the NR1 subunit of the NMDA receptor confirms the diagnosis of the behavioral and cognitive dysfunctions associated with the disorder. This disorder, anti-NMDA receptor encephalitis, is a severe, potentially lethal, but treatment responsive encephalitis that affects children and young adults, predominantly women, and manifests with a predictable set of symptoms (Dalmau et al., 2007; Dalmau et al., 2008); Florance et al., 2009). Two large cohorts of patients comprising 181 cases show that the disorder presents with sudden behavioral and personality changes for which patients are often admitted to psychiatric centers and are often misdiagnosed with acute schizophrenia (Dalmau et al., 2007; Dalmau et al., 2008); Florance et al., 2009). Similar to autoimmune disorders of the neuromuscular synapse, anti-NMDA receptor encephalitis may also occur as a paraneoplastic manifestation of a systemic tumor, mostly commonly ovarian teratomas. Studies show that the frequency of tumor association is age- and gender-dependant (Florance et al., 2009). Despite the severity of the neurological syndrome, 75% of patients respond to immunotherapy and when appropriate, tumor removal. The recovery occurs over months, with initial resolution of

the movement and autonomic symptoms, and then gradual improvement of behavioral and memory deficits.

To investigate the cellular mechanisms underlying the behavioral deficits in anti-NMDAR encephalitis, the effects of autoantibodies from patients were examined in *in vitro* and *in vivo* studies of rats. These studies show that autoantibodies decrease the surface density and synaptic localization of NMDA receptor clusters via antibody mediated capping and internalization, that the magnitude of these changes depends on antibody titer, and that these changes are reversible when antibody titer is reduced (Dalmau et al., 2008); Hughes et al., in preparation). Moreover, patient anti-NMDA receptor antibodies decrease NMDA but not AMPA receptor mediated synaptic currents, consistent with selective loss of surface NMDA receptors (Hughes et al., in preparation). These data show that NR1 autoantibodies reversibly alter the number and distribution of NMDA receptors in neurons, resulting in a decrease in excitatory synapse function. Therefore, the recovery seen in human patients may be due to reversible alterations in glutamate receptor synaptic localization and function without wholesale synapse loss. Together these results suggest that the cognitive and behavioral deficits in patients are the result of autoantibodies causing NMDA receptor hypofunction.

Previously, NMDA receptor dysfunction has been implicated in several other cognitive disorders, including schizophrenia (Olney et al., 1999). Studies investigating the effects of phencyclidine (PCP) and ketamine, noncompetitive antagonists of NMDA receptors, in human subjects have shown these drugs induce behaviors similar to the

positive and negative symptoms of schizophrenia (Luby et al., 1959; Krystal et al., 1994). In rodents, these same drugs that block NMDA receptor function also induce schizophrenic-like symptoms (Jentsch and Roth, 1999; Mouri et al., 2007). Furthermore, mice with reduced NMDA receptor expression show behaviors related to schizophrenia (Mohn et al., 1999). Interestingly, patients with anti-NMDAR encephalitis show symptoms such as psychotic behavior, signs of involvement of dopaminergic pathways, and autonomic instability (Dalmau et al., 2007; Dalmau et al., 2008) that are also caused by ketamine and PCP and seen in patients with schizophrenia. This suggests that the symptoms of anti-NMDAR encephalitis patients most likely results from NMDA receptor hypofunction and may provide new insights into the role of NMDA receptors in behavior and cognition.

Anti-AMPAR encephalitis: Human model of AMPA receptor dysfunction

Anti-AMPAR encephalitis is another recently identified disorder in which behavioral and memory deficits are associated with autoantibodies against the GluR1and 2 subunits of the AMPA receptor (Lai et al., 2009). This disease is thought to be a disorder of learning and memory, as these patients develop seizures and very severe short-term memory deficits. The median age of the first characterized cohort of 10 patients was 60 years (range 38 - 87); 9 were women; 7 had tumors of the lung, breast or thymus. Nine patients responded to immunotherapy or oncological therapy but with frequent neurologic relapses, without tumor recurrence. The presence of neurological

relapses and their frequency was correlated with neurological outcome of the patient. None of these patient autoantibodies reacted with GluR3, a subunit identified as an auto-antigen in some patients with Rasmussen's encephalitis (Rogers et al., 1994; Lai et al., 2009).

To begin to characterize the cellular mechanisms underlying anti-AMPAR encephalitis, dissociated rat hippocampal neurons were treated with GluR1/2 autoantibodies. GluR1/2 autoantibodies decreased the synaptic localization of AMPA receptors without affecting overall synapse density. Moreover, as for autoantibodies from patients with anti-NMDAR encephalitis, these effects were reversible. Although these disorders share some similar aspects, they are associated with a different clinical phenotype. Anti-AMPAR encephalitis patients did not have ovarian teratomas, experienced dyskinesias, autonomic dysfunction, or hypoventilation, which are all hallmarks of anti-NMDAR encephalitis (Dalmau et al., 2008; Iizuka and Sakai, 2008).

The trafficking of AMPA receptors to and from synapses mediates the long-term potentiation (LTP) and depression (LTD) of synaptic strength, which are thought to underlie the cellular basis for learning and memory (Kessels and Malinow, 2009). Since the major effect of GluR1/2 autoantibodies was on AMPA receptor synaptic localization, these findings suggest that receptor trafficking/turnover is disrupted in this disorder and AMPA receptors are moved from the synaptic to the extrasynaptic/intracellular pool similar to LTD paradigms. We are currently exploring the cellular mechanisms mediating

the effects of GluR1/2 autoantibodies on neurons and synapse function to gain insight into the cognitive and behavioral dysfunction in these patients.

New disorders of autoimmunity to synaptic proteins

Through ongoing screening of patients diagnosed with limbic encephalitis, Dalmau and colleagues have identified several new autoimmune disorders with autoantibodies against other CNS synaptic proteins. Autoantibodies against $GABA_B$ receptors (15 patients to date), neurexin (1 patient) and a potassium channel accessory subunit (6 patients) have been found in the serum and CSF (Dalmau unpublished data). While all of these patients have immune-mediated encephalitis, it is clear that each of these emerging groups have distinct neurological symptoms and behavioral manifestations. The generation of animal models of these disorders and further study into their underlying mechanisms will be required as these studies move forward. Given the importance of synapses in cognition and behavior, the discovery of these disorders may provide important human models of synaptic protein dysfunction which may could provide greater understanding of the function of synapses in human behavior as well as lead to important advances in the treatment of these patients.

Conclusions and future directions

The identification of anti-NMDAR and anti-AMPAR encephalitis will provide a greater understanding of the role of glutamate receptors in learning, memory and

behavior in several different ways. First, the continued generation and examination of animal models and patients will help to better understand, recognize, and treat this and other immunological diseases that affect cognitive functions. This is essential because not only are these disorders fatal if not recognized and treated appropriately, but earlier treatment results in better patient outcomes (Dalmau et al., 2008). Therefore understanding the underlying mechanisms may facilitate development of novel therapeutic strategies that can more easily identify and treat patients. Second, these disorders provide new human models of glutamate receptor function. Since these disorders have an identified pathogenic mechanism and their behavioral and cognitive phenotypes can be reversed, they provide a unique opportunity to study these receptors and their function in humans. Finally, understanding the mechanisms that result in behavioral deficits in anti-NMDAR and anti-AMPAR encephalitis may provide new insights into disease pathways of other psychiatric disorders involving the dysfunction of glutamate receptors.

Thesis rationale and goals

While the pathogenesis of autoimmune disorders of the peripheral nervous system has been well defined, the mechanisms underlying the newly identified disorder, anti-NMDAR encephalitis, remain poorly understood. Whether this CNS autoimmune disorder utilizes similar mechanisms as in the PNS to cause its characteristic cognitive and behavioral deficits is unknown. Previous work from our lab has suggested that

autoantibodies against the NR1 subunit of the NMDA receptor present in the CSF of patients with the disorder may mediate the deficits of this disorder (Dalmau et al., 2008). Based on these observations, I examined the effects of autoantibodies in patients with anti-NMDAR encephalitis on NMDA receptors *in vitro* and *in vivo* (Chapter 4). Using biochemical, electrophysiology and imaging techniques, I tested the hypothesis that *autoantibodies present in patients with anti-NMDAR encephalitis underlie the cellular mechanism of this disorder of cognition and behavior*.

My work demonstrates that patient anti-NR1 antibodies reversibly alter the number and distribution of glutamate receptors in neurons, resulting in a decrease in excitatory synapse function. Moreover, this work has extended our understanding of the cellular mechanisms underlying anti-NMDAR encephalitis and, in the future, may facilitate a better understanding of the role of NMDA receptors in learning, memory and behavior.

Submitted to MCN

Astrocyte secreted proteins selectively increase hippocampal GABAergic axon length, branching, and synaptogenesis

Ethan G. Hughes, Sarina B. Elmariah and Rita J. Balice-Gordon

Department of Neuroscience, University of Pennsylvania School of Medicine

Philadelphia, PA, 19104

Abstract / Intro / Discussion / Figures / Tables: 143 / 251 / 1023 / 5 / 0

Supplemental Figures / Tables: 3 / 1

Key words: Astrocyte, inhibitory neuron, GABA, axon, synaptogenesis, hippocampus

Address correspondence to: Rita Balice-Gordon, Ph.D., Dept. of Neuroscience, University of Pennsylvania School of Medicine, 215 Stemmler Hall, Philadelphia, PA 19104-6074

(215) 898-1037; FAX (215) 573-9122, rbaliceg@mail.med.upenn.edu

Abstract

Astrocytes modulate the formation and function of glutamatergic synapses in the CNS, but whether astrocytes modulate GABAergic synaptogenesis is unknown. We demonstrate that media conditioned by astrocytes, but not other cells, enhanced GABAergic but not glutamatergic axon length and branching, and increased the number and density of presynaptically active GABAergic synapses in dissociated hippocampal cultures. Candidate mechanisms and factors, such as activity, neurotrophins, and cholesterol were excluded as mediating these effects. While thrombospondins secreted by astrocytes are necessary and sufficient to increase hippocampal glutamatergic synaptogenesis, they do not mediate astrocyte effects on GABAergic synaptogenesis. We show that the factors in astrocyte conditioned media that selectively affect GABAergic neurons are proteins. Taken together, our results show that astrocytes increase glutamatergic and GABAergic synaptogenesis via different mechanisms and release one or more proteins with the novel functions of increasing GABAergic axon length, branching and synaptogenesis.

Introduction

The development of CNS synapses requires not only the exchange of signals between pre- and postsynaptic neurons but also communication with adjacent glia. Astrocytes up-regulate the formation of functional glutamatergic synapses through a variety of signaling mechanisms; both pre- and postsynaptic effects have been identified (Mauch et al., 2001; Hama et al., 2004; Christopherson et al., 2005). In purified retinal ganglion cell cultures, astrocyte-conditioned medium (ACM) dramatically increases the number of presynaptic contacts made between neurons, the quantal size and efficacy of neurotransmitter release, and the number of postsynaptic AMPA receptor clusters (Nagler et al., 2001; Ullian et al., 2001; Ullian et al., 2004). Some of the factors released by astrocytes that mediate these effects have been identified. Astrocyte-derived cholesterol complexed to apolipoprotein E (ApoE) increases the number of functional glutamatergic presynaptic terminals in retinal ganglion cell autaptic cultures (Mauch et al., 2001). In the cerebral cortex, immature astrocytes express thrombospondins (TSPs), which increase the number of ultrastructually normal glutamatergic synapses that are presynaptically active but postsynaptically silent (Christopherson et al., 2005). Thus soluble factors, including proteins and lipids, released by astrocytes enhance glutamatergic synaptogenesis.

By contrast, little is known about whether and how astrocytes modulate the development of GABAergic synapses. In earlier work, astrocytes increase GABA-mediated currents in neurons prior to synaptogenesis (Liu et al., 1996; Liu et al., 1997),

but the basis of these effects was not shown. Here we demonstrate that astrocytes increase glutamatergic and GABAergic synaptogenesis via distinct mechanisms and release one or more proteins that specifically increase GABAergic axon length, branching and synaptogenesis.

Results

Astrocytes selectively increase GABAergic neuron axon length and branching

GABAergic neuron morphology and neurite outgrowth was examined in hippocampal neurons cultured alone or with astrocytes. At all ages examined, neuron co-culture with astrocytes or ACM had a profound effect on the length and branching of GABAergic axons. In both culture conditions, GABAergic neurons underwent significant growth and maturation during the first two weeks *in vitro* (Fig. 1; Supp. Table 1). In contrast, GAD-negative glutamatergic axons were not significantly longer when neurons were cultured with astrocytes or ACM relative to neurons cultured alone (Fig. 1; Supp. Table 1). Cell survival, density, soma size and number and length of primary dendrites of GABAergic neurons or glutamatergic neurons were similar among all culture conditions (Supp. Table 1). Thus, while neither glutamatergic nor GABAergic axons require the presence of astrocytes for growth, astrocyte-derived cues specifically enhance the outgrowth of GABAergic axons.

GABAergic neurons co-cultured with astrocytes or ACM showed significantly increased axon branching compared to neurons cultured alone (Fig. 1, Supp. Table 1). In the absence of astrocytes, most GABAergic axons remained unbranched at 4 *div* and exhibited relatively few secondary or tertiary branches at 7 *div* (Fig. 1; Supp. Table 1). In contrast, GABAergic neurons cultured with astrocytes or ACM had more complex axonal arbors than neurons cultured alone during the first 2 weeks in vitro, exhibiting 2 to 3 secondary branches as early as 4 *div* (Supp. Table 1). These effects on branching were

not seen for glutamatergic neurons (Fig. 1; Supp. Table 1). These results demonstrate that astrocytes release soluble factors that increase the length and branching of GABAergic but not glutamatergic axons.

Astrocytes increase GABAergic synaptogenesis

We next asked whether astrocytes or ACM caused an increase in GABAergic synaptogenesis by assaying the number of GABAergic synapses per length of GABAergic axon. Neurons cultured with ACM or astrocytes had ~2-fold more GABAergic synapses per 20 μm of axon length than did neurons cultured in the absence of astrocytes (Fig. 2A). ACM increased total GABAergic axon length (sum of the length of primary, secondary, and tertiary axon branches) by ~3-fold (Fig. 2B) and the total number of synapses by ~7-fold (Fig. 2C). Thus astrocytes secrete factors that increase GABAergic synapse density, independent of increasing GABAergic axon length and branching.

Soluble factors specifically released by astrocytes increase GABAergic axon length, branching and synaptogenesis

To determine whether these soluble factors are released specifically from astrocytes, we examined the ability of media conditioned by another cell type - primary meningeal fibroblasts - to increase GABAergic axon length, branching, and synapse density. We found that 3 days of treatment with fibroblast conditioned media (FCM) did

not significantly affect GABAergic axon length or branching at 4 or 7 *div* compared to neurons cultured alone (Supp. Fig. 2 A, B). Immunostaining for synaptic markers showed that FCM treatment did not significantly increase GABAergic synapse density at 4 or 7 *div* compared to neurons cultured alone (Supp. Fig. 2C), assayed by the colocalization of presynaptic synaptophysin and postsynaptic $GABA_AR$ clusters. Taken together, these results suggest that astrocytes, but not fibroblasts, release factors that increase GABAergic axon length, branching and synaptogenesis.

ACM increases the number of presynaptically active GABAergic synapses

To determine whether astrocytes also promote the function of newly formed hippocampal synapses, we examined the number of synapses which were labeled with an antibody directed to the luminal domain of the vesicular GABA transporter (VGAT), which can be used to mark the sites of synaptic vesicle release and recycling (Martens et al., 2008). In neuron-only cultures, there are few GABAergic synapses and both neuron-astrocyte co-culture and ACM significantly increase the number of GABAergic synapses (Fig. 3A, B; see also Fig. 2). The number of GABAergic synapses labeled with the anti-VGAT-C luminal antibody (and thus were identified as presynaptically active GABAergic synapses) also was significantly increased in neuron-astrocyte co-cultures and ACM, compared to neuron only cultures (Fig. 3C). To examine whether astrocytes increase the proportion of functional GABAergic synapses in addition to increasing GABAergic synapse number, we plotted the number of functional GABAergic synapses

against total GABAergic synapse number per neuron. Although there are fewer GABAergic synapses on neurons cultured alone, the same proportion of GABAergic synapses are functional compared to neurons cultured with astrocytes or ACM (Fig. 3 D). These data show that astrocytes increase the number but not the proportion of synapses that are functional. Taken together, these results suggest that soluble factors released by astrocytes increase the number of GABAergic synapses, and these newly formed synapses are functional.

The effects of ACM on GABAergic neurons do not require neurotrophin signaling, action potential activity, or cholesterol

We evaluated several candidate mechanisms mediated by astrocyte soluble factors that increase GABAergic axon length, branching and synaptogenesis. First, we blocked action potential activity using TTX which had no effect on GABAergic axon length, branching, or presynaptic terminal density in neuron-only cultures, and did not alter the effect of astrocytes or ACM on GABAergic axon length, branching, presynaptic terminal density (Supp. Fig. 3A). To examine whether neurotrophin signaling mediates the effects of astrocytes, we scavenged endogenous BDNF or NT3 using TrkB- or TrkC-IgG fusion protein, which did not prevent the increase in GABAergic axon length, branching, or presynaptic terminal density in neurons cultured with astrocytes or with ACM compared to neurons cultured alone at 7 *div* (Supp. Fig. 3B, see also (Elmariah et al., 2005)). Finally, we examined the role of cholesterol. We found that cholesterol did not increase

GABAergic axon length, branching or GABAergic synapse density when compared to untreated and vehicle treated cultures (Supp. Fig. 3C; see also (Elmariah et al., 2005)). Parallel cultures of neurons grown on astrocytes showed the expected increase in axon length, branching, and synapse density. Taken together, these results suggest that the effects of ACM on GABAergic neurons do not require neuronal activity, are neurotrophin-independent, and cannot be mimicked by addition of exogenous cholesterol.

Effects of astrocytes on GABAergic neurons are not mediated by TSPs

Recent work has shown that TSPs, in particular TSP-1 and -2, are released by astrocytes and mediate the increase in glutamatergic synaptogenesis in retinal ganglion cells *in vitro* and *in vivo* (Christopherson et al., 2005). TSPs have also been previously shown to increase retinal neurite outgrowth (Neugebauer et al., 1991; DeFreitas et al., 1995); but see (Christopherson et al., 2005). Because much of the work on TSPs has been done in retinal ganglion cell cultures, we first examined the effects of TSPs on hippocampal glutamatergic synapse density. Treating neuron-only cultures with purified TSP-1 increased the number of glutamatergic synapses, by 2-fold at 4 *div*, mimicking the effects of ACM on glutamatergic synaptogenesis (Fig. 4E). Moreover, immunodepletion of endogenously released TSPs from ACM using a combination of antibodies against TSP-1 and TSP-2 (Supp. Fig. 4) abolished the increase in glutamatergic synapse density mediated by ACM (Fig. 4E). These results show that TSPs released by astrocytes

increase hippocampal glutamatergic synaptogenesis *in vitro*, similar to previous observations in retinal ganglion cells and cortical neurons (Christopherson et al., 2005).

To examine the role of TSPs on GABAergic axon length, branching and synaptogenesis, neuron-only cultures were treated with purified TSP-1. TSP-1 treatment did not significantly increase GABAergic axon length or branching at 7 *div* compared to neuron-only cultures, whereas parallel cultures of neurons and ACM showed the expected increases (Fig. 4A, B). This result shows that TSPs do not mediate these effects of astrocytes on GABAergic neurons.

We next determined whether TSPs could account for the effects of astrocytes on GABAergic synapse density. TSP-1 treatment of neuron-only cultures from 1 to 7 *div* did not affect the density of VGAT+ presynaptic terminals or postsynaptic $GABA_AR$ clusters per dendrite length, whereas cultures treated with ACM showed the expected increases (Fig. 4C, D). TSP treatment of neuron-only cultures did slightly increase GABAergic synapse density. This increase, however, was significantly less than that observed in neurons treated with ACM (Fig. 4 C, D). Thus, TSPs may increase the density of GABAergic synapses, but this does not account for the complete activity in ACM that increases GABAergic synapse density by ~4-fold.

As an additional test of whether TSPs released by astrocytes increase GABAergic synapse density, endogenous TSPs were immunodepleted from ACM using a combination of antisera against TSP-1 and TSP-2 (Fig. 4C, D). The density of GABAergic synapses in neuron-only cultures at 7 *div* that were treated from 1 to 7 *div*

with TSP-depleted ACM was significantly higher than in untreated neuron-only cultures, but not significantly different in neuron-only cultures treated with ACM. Thus, in contrast to glutamatergic synaptogenesis, TSPs do not appear to be necessary or sufficient to increase GABAergic synaptogenesis, suggesting that another factor(s) released from astrocytes increase GABAergic axon length, branching, and synaptogenesis.

Soluble factors released by astrocytes that increase GABAergic axon length, branching and synaptogenesis are proteins

To further examine how astrocytes tested whether the biological activity of ACM was sensitive to trypsin. Astrocytes, ACM, ACM + trypsin inhibitor and ACM + trypsinized ACM all significantly increased GABAergic axon length, branching, and synapse density, compared to neuron-only cultures (Fig. 5). In contrast, trypsinized ACM did not change GABAergic axon length, branching, and the density of GABAergic synapses compared to neuron only cultures at 7 *div*. Together, these results show that factors released by astrocytes that increase GABAergic axon length, branching and synapse density are proteins.

Discussion

Here we demonstrate for the first time that astrocytes release proteins that selectively increase GABAergic axon length, branching and synapse density. Neurotrophins, neuronal activity, cholesterol and TSPs were eliminated as candidate mechanisms underlying these effects. These results show that astrocytes utilize different mechanisms to affect glutamatergic compared to GABAergic neurons. That trypsin abolishes the effects of ACM on GABAergic neurons shows that astrocytes release proteins that selectively affect GABAergic neurons, expanding the repertoire of glial function in the development of neural circuits.

Astrocyte soluble factors increase GABAergic neuron axon length, branching, synapse formation and function

We report for the first time that astrocytes release proteins that selectively enhance the development of hippocampal GABAergic neurons by increasing GABAergic axon length, branching, synapse density and synapse function. In the context of previous work, our results highlight several important features of astrocyte-neuron signaling during development. First, astrocytes express and release numerous factors, including proteins, some of which stimulate neurite outgrowth, including laminin, fibronectin and N-cadherins, among others (Tomaselli et al., 1988; Matthiessen et al., 1989; Aoyagi et al., 1994). Recent work suggests that cortical astrocytes also release trophic factors, such as fibroblast growth factor, that stimulate both axonal and dendritic growth in postnatal

mouse cortical neurons (Le and Esquenazi, 2002). We found that astrocytes release one or more proteins that increase GABAergic axon but not dendrite length and branching. Previously identified proteins have not been shown to differentially increase axon compared to dendrite length and branching in GABAergic neurons.

Second, astrocytes secrete proteins that differentially modulate glutamatergic compared to GABAergic axonal projections. We found that astrocytes or ACM did not increase hippocampal glutamatergic dendrite or axon length or branching, whereas astrocytes and ACM significantly increased GABAergic axon length and branching. Consistent with this, retinal ganglion cell neurite length and branching are not affected by astrocytes or ACM (Ullian et al., 2001). Third, we found that astrocytes increase GABAergic synapse density in addition to increasing axon outgrowth. Together with recent studies on glutamatergic synaptogenesis, these results suggest that astrocyte signaling that influences axon length and synaptogenesis are separable (Mauch et al., 2001; Christopherson et al., 2005). Finally, our results show that astrocyte secreted proteins increase the density of functional GABAergic synapses. These findings are consistent with previous work which showed that astrocyte soluble factors and contact increased the number of functional glutamatergic synapses (Ullian et al., 2001; Hama et al., 2004; Ullian et al., 2004). Thus, our works shows that, while astrocytes have some similar affects on glutamatergic and GABAergic neurons, they also secrete one or more proteins that have differential effects that may lead to key differences in the development of these two cell types.

The effects of astrocyte soluble factors on GABAergic neurons are not mediated by action potential activity, neurotrophins, cholesterol or TSPs

While previous studies have reported a decrease in GABAergic synaptogenesis after chronic blockade of synaptic transmission (Kilman et al., 2002; Hartman et al., 2006), TTX treatment from 1 to 7 *div* had no effect on GABAergic synapse number in neuron-only cultures, and did not alter the effect of ACM on GABAergic synaptogenesis. These different results might be explained by the developmental ages of neurons when treated with TTX. In our experiments, activity was blocked from 1 to 7 *div*, while in previous studies, activity blockade began on or after 5 *div* (Kilman et al., 2002; Hartman et al., 2006). Thus our work suggests that astrocytes increase GABAergic axon length, branching and synaptogenesis via mechanism(s) that are independent of neuronal activity during early stages of development.

Neurotrophin and Trk signaling have been shown to modulate neurite outgrowth (Cohen-Cory and Fraser, 1995; McAllister et al., 1996, 1997) and regulate GABAergic synapse development (Rutherford et al., 1997; Marty et al., 2000; Seil and Drake-Baumann, 2000; Yamada et al., 2002). Moreover, we previously showed that astrocytes increase postsynaptic clustering of $GABA_A$Rs by releasing soluble factors that up-regulate BDNF-TrkB signaling among neurons (Elmariah et al., 2005). In the present work, we found that after scavenging endogenous BDNF and NT3, ACM still increased GABAergic neuron axon length, branching and presynaptic terminal number. These data

demonstrate that neurotrophins do not account for the effects of ACM on GABAergic axon length, branching and presynaptic terminal number.

Mauch et al. (2001) found that astrocyte-derived cholesterol complexed to ApoE was both necessary and sufficient to increase the number of functional presynaptic terminals in retinal ganglion cell autaptic cultures. However, recent studies have found that cholesterol is not sufficient to increase hippocampal glutamatergic synaptogenesis (Hama et al., 2004), or necessary for retinal ganglion cell glutamatergic synaptogenesis (Christopherson et al., 2005). We find that the addition of cholesterol does not increase GABAergic axon length, branching or synaptogenesis. Therefore, we have eliminated cholesterol as a candidate that mediates the effects of ACM on GABAergic neurons.

TSP-1 and -2 expressed by immature astrocytes increase the number of glutamatergic synapses between retinal ganglion cells *in vitro* and *in vivo* (Christopherson et al., 2005). While we confirm that TSPs are required for hippocampal glutamatergic synaptogenesis, exogenous TSPs do not mimic the effects of ACM on GABAergic neurons. Furthermore, depletion of TSPs from ACM does not abrogate the effect of ACM on GABAergic synaptogenesis. Thus, TSPs are essential for hippocampal glutamatergic synaptogenesis but other astrocyte proteins modulate GABAergic axon length, branching and synaptogenesis. Importantly, these experiments show for the first time that hippocampal glutamatergic and GABAergic synaptogenesis are regulated by different mechanisms.

We have shown that astrocytes release one or more proteins that selectively increase GABAergic axon length, branching and the density of functional synapses. Moreover, we show that these proteins differentially affect GABAergic compared to glutamatergic neurons. Identifying the proteins that selectively increase GABAergic axon length, branching, synapse formation and function, and the relevant downstream signaling pathways, is the focus of ongoing work. Together our results characterize new roles for astrocytes in mediating GABAergic synaptogenesis, highlighting the importance of this glial type in the development and maintenance of neural circuits.

Materials and Methods

Cell cultures

Primary neurons co-cultured with astrocytes were prepared as described previously (Elmariah et al., 2005), with minor modifications. Briefly, hippocampi were dissected from embryonic day (E) 18 rats, dissociated in HBSS (Earls Buffered Saline Solution (EBSS) with $MgCl_2$ and HEPES) containing 1% papain for 20 min., triturated in BME (Basal Medium Eagle), and plated at 75,000-100,000 cells/ml in Neurobasal medium (Invitrogen, Grand Island, NY) on poly-L-lysine (1 mg/ml; Sigma, St. Louis, MO) coated coverslips in 24-well plates. Cells were grown at 37°C, 5% CO_2, 95% humidity in Neurobasal medium plus B27 (Invitrogen) that was changed weekly.

Approximately 15% of the neurons in these cultures have small soma size, less branched dendritic arbors, and express GAD. We have previously shown that, in our culture system, activation of $GABA_A$Rs is depolarizing until 4-5 *div*; after this time, activation of $GABA_A$Rs is hyperpolarizing (Elmariah et al., 2004). Since the experiments reported here were performed at 4 *div* and older, for simplicity's sake, cells and synapses that express GABA-related markers are referred to as inhibitory.

Primary astrocyte cultures were prepared as described previously (Duan et al., 2003; Zhang et al., 2003). Briefly, hippocampi were dissected from E18 rats, dissociated in HBSS containing 0.25% trypsin for 20 min, triturated in BME, and plated in T25 flasks in MMEM (Modified Minimum Essential Medium; Invitrogen) supplemented with 10% heat-inactivated FBS (HyClone, Logan, UT), 2 mM L-glutamine, 14 mM sodium

bicarbonate, 40 mM D-glucose, 1% sodium pyruvate and 1% penicillin and streptomycin. Astrocytes proliferated for 10 – 14 days; after reaching confluence, they were rinsed in cold EBSS and shaken at 260 rpm for 18 - 20 hours in MMEM to remove neurons and other cells. Purified astrocytes were then plated onto poly D-lysine coated coverslips at 400,000 cells/ml in MMEM. Medium was changed to Neurobasal medium and coverslips used for ACM experiments within 1 - 3 days. Coverslips were immunostained with an antibody against GFAP (Chemicon, Temecula, CA) to assess purity prior to use; in the experiments described here, > 98% of the cells were GFAP+.

For neuron-only cultures, cytosine arabinoside (Ara-C; 10 μM; Sigma) was added to cultures 18 – 20 hours after plating to prevent glial proliferation. For neuron-astrocyte co-cultures, the effects of acutely isolated and mature astrocytes (14 – 21 *div*) were compared. For mature astrocyte co-cultures, neurons were plated onto confluent monolayers of astrocytes grown on coverslips and maintained up to 21 *div* in Neurobasal medium. For neurons cultured with acute astrocytes, neurons were prepared in Neurobasal plus B27 supplemented with 5% FBS, 1% L-glutamine, and 1% penicillin and streptomycin as described above without the addition Ara-C, allowing astrocyte proliferation. At 4 *div*, when astrocytes composed approximately 75-80% of cells (N = 35 coverslips), culture media was changed to Neurobasal medium with B27 and co-cultures were maintained up to 21 *div*. No differences were observed in the effects of acutely isolated and mature astrocytes on GABAergic neuron axon length or branching at 4 *div* (length: acute 303.9 ± 16.5 (N = 85 neurons), mature 291.7 ± 12.9 (24); # of 2°

branches: acute 3.24 ± 0.33 (85), mature 3.79 ± 0.41 (24); not significantly different, Student's t-test). Thus, acutely isolated astrocyte co-cultures were used for experiments.

For neurons cultured with ACM, neurons were plated in Neurobasal medium that had been conditioned by astrocytes (14-21 days old) during the previous 72 hours. Sterile inserts with 3 μm high pore density polyethylene terephthalate membranes (Becton Dickinson Labware, Franklin Lakes, NJ) were placed into each well, and coverslips with astrocyte monolayers were inverted 0.9 mm above neurons. Inserts remained in place for the duration of culture. Neuron-only cultures treated with astrocyte inserts or ACM both had increased GABAergic axon length, branching and synaptogenesis that were not significantly different from each other (data not shown); depending on the experiment, these conditions are interchangeably referred to as ACM. Cell survival and density were similar among neurons co-cultured with astrocytes or ACM or cultured alone (data not shown, see (Elmariah et al., 2005)). In addition, neuron co-culture with astrocytes or ACM produced no change in the number or length of primary dendrites or in the soma size of GABAergic neurons or glutamatergic neurons compared to neurons cultured alone (Supp. Table 1).

Primary meningeal fibroblast cultures were prepared from E18 rat meninges, which were dissociated in 0.25% trypsin for 20 min. and plated in T25 flasks in modified MMEM supplemented with 10% heat-inactivated FBS, 2 mM L-glutamine, 14 mM sodium bicarbonate, 40 mM D-glucose, 1% sodium pyruvate and 1% penicillin and streptomycin for 4-7 days before use. For neurons cultured with fibroblast conditioned

media (FCM), neuron-only cultures were plated in Neurobasal medium that had been conditioned by fibroblasts for 48 hours. Sterile inserts with 3 μm high pore density polyethylene terephthalate membranes (Becton Dickinson Labware, Franklin Lakes, NJ) were placed into each well, and coverslips with fibroblast monolayers were inverted 0.9 mm above neurons. Inserts remained in place for the duration of culture. At 1 and 4 *div*, neuron cultures were treated with FCM for 3 days, and immunostained at 4 and 7 *div*.

Immunostaining and confocal microscopy

Coverslips were fixed in 4% paraformaldehyde and 4% sucrose for 15 min., permeabilized with cold 0.25% Triton X-100 for 5 min., and blocked in 5% normal goat serum (Invitrogen) for 1 hour at RT. Triple labeling was performed with combinations of primary antibodies: A2B5 (1:5 dilution, polyclonal; gift of Dr. J. Grinspan), GAD-6 (1:10, monoclonal; Developmental Studies Hybridoma Bank, Iowa), GalC (1:500, monoclonal, gift of Dr. Judy Grinspan), GFAP (1:1000, rabbit antiserum; Sigma), MAP2 (1:1000, rabbit antiserum; gift of Dr. V. Lee), synaptophysin (1:200, rabbit antiserum; NeoMarkers, Fremont, CA), tau (1:1000, rabbit antiserum; gift of Dr. V. Lee), VGAT-N (1:200, guinea pig antiserum; Synaptic Systems, Goettingen, Germany), VGAT-C (1:200, rabbit antiserum; Synaptic Systems, Goettingen, Germany), and gephryin (1:200, mouse antiserum; Synaptic Systems, Goettingen, Germany). Antibodies were visualized after staining with the appropriate FITC-, TRITC- or CY5-conjugated secondary antibodies (all used at 1:200, Jackson ImmunoResearch, Inc., West Grove, PA). Immunostaining

was performed at 4, 7 and 10 *div* or later ages *in vitro* with antibodies against glutamic acid decarboxylase (GAD), the synthetic enzyme for GABA, to identify GABAergic neurons, and tau, to visualize axons. Because synaptophysin labels both glutamatergic and GABAergic synapses, and because $GABA_A$Rs can be transiently clustered beneath both types of terminals during development (Rao et al., 2000), immunostaining was performed at 7 *div* with antibodies against the presynaptic vesicular GABA transporter (VGAT) and postsynaptic $GABA_A$Rs or gephyrin to label GABAergic synapses. Images were obtained using a confocal microscope (Leica TCS SP2). In each image, laser light levels and detector gain and offset were adjusted so that no pixel values were saturated in regions analyzed.

VGAT-C luminal antibody labeling

Labeling was performed as described previously (Martens et al., 2008). GABAergic synapses were identified as clusters in which VGAT-N terminus and gephyrin immunostaining were colocalized. Functional GABAergic synapses were identified as clusters in which these markers were also colocalized with VGAT-C terminus immunostaining and thus underwent vesicle recycling during stimulation.

Neurotrophin scavenging and TTX, cholesterol and TSP treatment

Cultures were treated with 2 μg/ml TrkB-IgG, TrkC-IgG or control IgG (gift of Regeneron Pharmaceuticals, Inc., Tarrytown, NY) to scavenge neurotrophins. This

scavenger concentration blocked the neurotrophin mediated increase in postsynaptic $GABA_AR$ clusters (Elmariah et al., 2004, 2005). 1 μM tetrodotoxin (TTX, Sigma) was used to block action potentials (Elmariah et al., 2004, 2005). Treatments began after the first day in culture and were replenished every 24 hours until immunostaining was performed at 4 or 7 *div*. For experiments investigating the role of cholesterol, neuron-only cultures were treated with 10 μg/ml cholesterol (a concentration that increased the number of glutamatergic presynaptic terminals in retinal ganglion cell autaptic cultures (Mauch et al., 2001); Sigma) or vehicle (EtOH) from 4 -7 *div*. For experiments investigating the role of TSPs, neuron-only cultures were treated with 5 μg/ml purified TSP-1 (Christopherson et al., 2005); Haematological Tech., Essex Junction, VT) from 1 to 7 *div*.

TSP immunodepletion

Confluent purified astrocyte monolayers were washed with EBSS and treated with serum-free medium (Neurobasal plus B27 supplemented with 1% L-Glutamine, and 1% penicillin and streptomycin) for 5-7 days. ACM was filtered to remove cell debris and was concentrated 5-10x on Amicon Ultra columns (3-5 kDa; Millipore, Wilmington, DE). Fresh ACM was maintained at 4°C for no longer than 7 days prior to use in the bioassays and other samples were stored at -80°C until use. Concentrated ACM was incubated with 50 μl protein A beads (Pierce, Rockford, IL) and 50 μl protein G beads (Amersham, Piscataway, NJ) for 1 hour at RT. Beads were washed 1x with PBS

followed by incubation with a cocktail of the following anti-TSP-1 and -2 antibodies: 0.2 µg/ml Ab-8 (rabbit antiserum; Neomarkers); 1 µg/ml Ab-2 (monoclonal; Neomarkers); 10 µl anti-mTSP-1 (monoclonal; gift of Dr. D. Mosher), 10 µl anti-mTSP-2 (monoclonal; gift of Dr. D. Mosher) overnight at 4º C. Antibody bound beads were washed 3x with PBS and were added to 300 µl concentrated ACM for 1-3 hours at RT. Beads were spun down and the supernatant was removed and used as TSP-depleted ACM. To determine the amount of TSP depletion, a sample was saved for Western blot analysis before addition to neuron-only cultures. To determine the amount of TSP pulldown, beads were washed 3 times with PBS, 3 times with PBS plus 0.25 M NaCl, and 3 times with PBS, 50 µl loading dye was added, samples were boiled and analyzed by Western blot.

Trypsinized ACM

Trypsinized ACM was prepared by treating concentrated 1 ml of ACM with 10-100 ng of trypsin for 1 hour at 37 degrees followed by 1 hour incubation with equivalent amount of soybean trypsin inhibitor to stop the enzymatic digestion. SDS-PAGE followed by silverstain analysis showed that proteins in ACM were digested by trypsin treatment (data not shown). Neuron-only cultures were treated from 1-7 div with ACM inserts, ACM media, trypsinized ACM, ACM + trypsin inhibitor or ACM inserts+ trypsinized ACM, then immunostained. Astrocytes, ACM, ACM + trypsin inhibitor and ACM + trypsinized ACM all significantly increased GABAergic axon length, branching,

and synapse density, compared to neuron-only cultures showing that there are no secondary effects of trypsin inhibitor on these cultures (see Fig. 5).

Western blot analyses

Samples of concentrated ACM, TSP-depleted ACM or TSP bound to beads were resolved by SDS-PAGE, transferred to nitrocellulose membranes and probed with antibodies against TSP-1 (1.5 µg/ml Ab-2; monoclonal, Neomarkers) or TSP-2 (1:250; monoclonal, BDTransduction, San Jose, CA) followed by alkaline phosphatase-conjugated secondary antibody (1:5000; polyclonal, Applied Biosystems, Foster City, CA). Signals were visualized using chemiluminescence (Western*Star* Detection System, Applied Biosystems). Films were digitally scanned and signals were quantified using ImageJ software (available at http://rsb.info.nih.gov/ij/).

Quantification and statistical analysis

For all experiments, 6-15 neurons in each condition were examined on each of 2-3 coverslips in 3-5 independent experiments**.** Neurons were randomly selected for analysis. GABAergic neurons were distinguished from glutamatergic neurons by anti-GAD immunoreactivity. In a majority of experiments, the number and proportion of glutamatergic and GABAergic neurons were determined by counting GAD+ and GAD- neurons in a minimum of 5 randomly chosen fields on each coverslip (750 x 750 microns). To assess neuronal morphology, GAD+ soma diameter was measured and the

number and length of MAP2+ dendrites and the length of tau+ axons were determined from confocal fluorescence images using interactive software (MetaMorph, Molecular Devices, Downingtown, PA; or ImageJ). The number of immunostained pre- or postsynaptic clusters was determined from confocal images using interactive software (MetaMorph or ImageJ). To measure synapse density per axon, the longest neurite which formed synapses was identified as the axon. Because of limitations of spectral overlap among secondary antibodies and three fluorescence channels, pre- and postsynaptic specializations of GABAergic neurons were labeled with VGAT, GABAAR-β3, and GAD antibodies; tau antibody wasn't used to specifically label axons. Confocal images of neurons were threshold automatically using an iterative thresholding technique (Bergsman et al., 2006), and the number and area of individual clusters were determined using interactive software (MetaMorph, Molecular Devices, Downingtown, PA; or custom-written ImageJ macros). Clusters with more than 20% pixel overlap of pre- and postsynaptic markers were considered colocalized and thus synaptic.

Values for axon length, branch number and cluster number were compared across conditions using the Kruskal-Wallis nonparametric ANOVA test followed by Dunn's pairwise multiple comparison test, unless otherwise indicated. All values are presented as mean ± s.e.m.

Acknowledgements

We thank M. Maronski and M.O. Scott for technical assistance; and Drs. B. Barres, H. Ischiropoulos and S. Scherer, and members of the Balice-Gordon lab for helpful discussions. This work was supported by grants from the NIH (NS046490 and MH057683) to R.B.-G. and an NIH NRSA (NS056549) to E.G.H.

Figures and Legends

Figure 2.1 Astrocytes selectively increase GABAergic axon length and branching.

Hippocampal neurons were cultured alone, with astrocytes or ACM and were immunostained at 4, 7, and 10 *div* with antibodies against tau (red) and glutamic acid decarboxylase (GAD; green). (A), GABAergic axon length and branching were significantly increased in neurons cultured with astrocytes (middle) or ACM (right) compared to neurons cultured alone (left) at 4 *div* (Supp. Table 1). Areas within white boxes are shown below at higher magnification. Note that GAD expression is dimmer in neuron-only cultures compared to neurons cultured with astrocytes or with ACM, as represented in these representative figure panels, and confirmed by Western blot analyses (data not shown). Scale bar = 25 (top), 10 (bottom) μm. (B, C), Quantification of the effect of astrocytes or ACM on GABAergic axon length (B, left) and branching (B, right) or on glutamatergic axon length (C, left) and branching (C, right). Asterisk indicates significant difference compared to neuron-only cultures ($p < 0.001$).

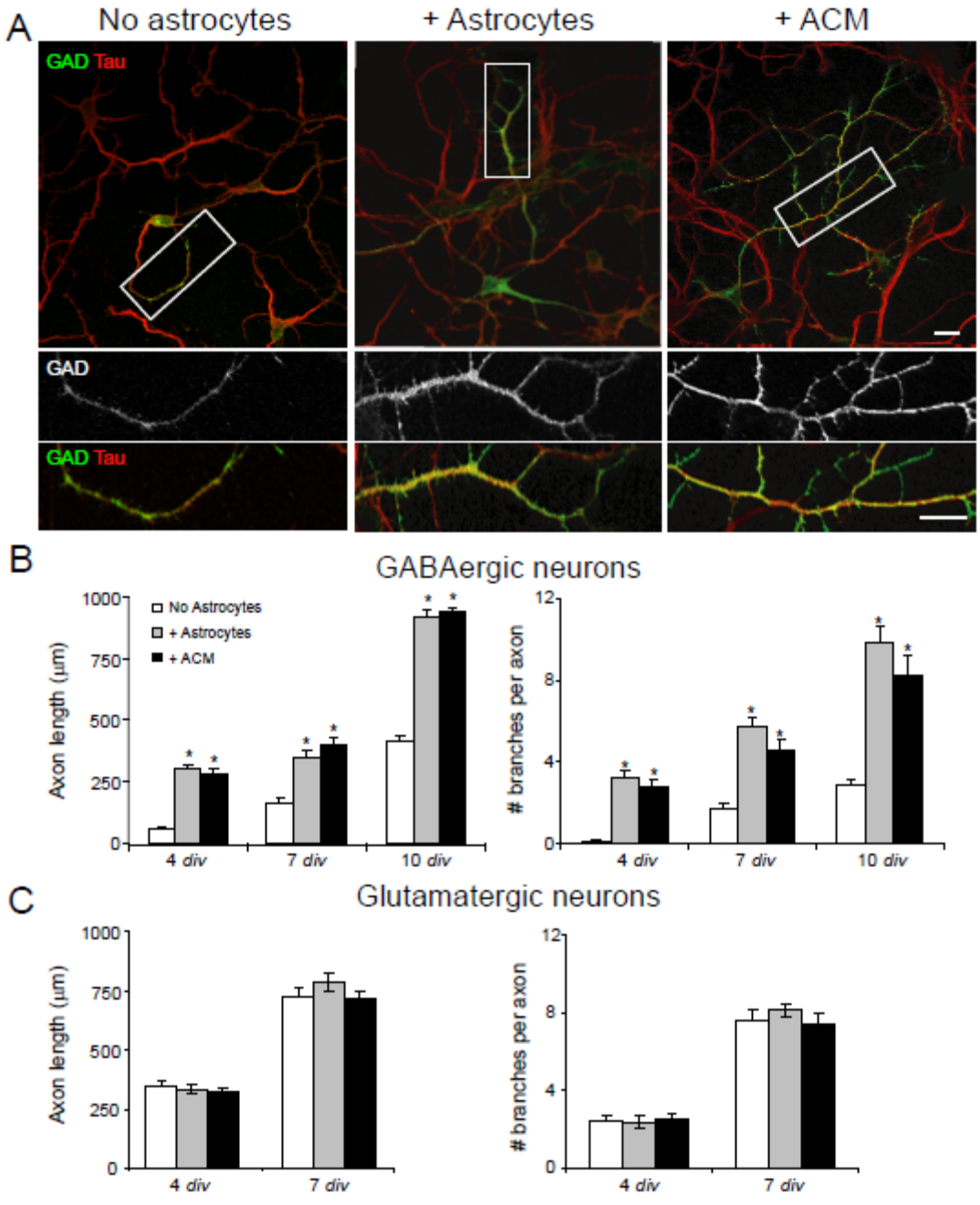
A
No astrocytes
+ Astrocytes
+ ACM
GAD Tau
GAD
GAD Tau
B
GABAergic neurons
No Astrocytes
+ Astrocytes
+ ACM
Axon length (µm)
branches per axon
4 div
7 div
10 div
C
Glutamatergic neurons
Axon length (µm)
branches per axon
4 div
7 div

Figure 2.2 Astrocyte soluble factors increase GABAergic synapse density.

(A), GABAergic axon length and branching was significantly increased in neurons cultured alone (left) compared to neurons cultured with ACM (right) at 7 *div* (see also Fig. 1, Supp. Table 1). Scale bar = 10 μm. Areas within red boxes, shown to the right at higher magnification, show presynaptic VGAT (top), postsynaptic $GABA_ARs$ (middle) and their colocalization (bottom). Neurons cultured with ACM (right) have a significantly greater synaptic density than neurons cultured alone (left). Scale bar = 10 μm. (B, C, D), Neurons cultured with ACM have significantly increased GABAergic synapse density (B), axon and branch length (C) and total number of GABAergic synapses (D) compared to neurons cultured alone. Asterisk indicates significant difference ($p < 0.05$, Student's t test).

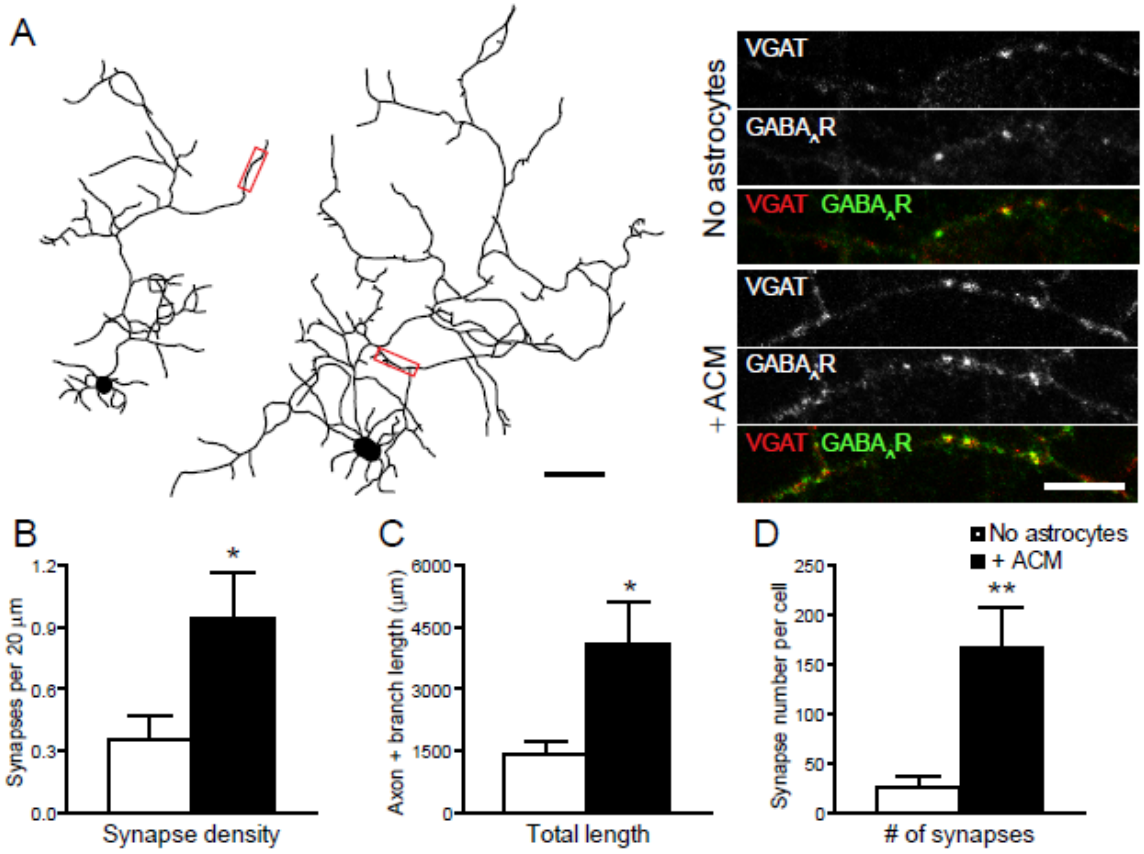
A
No astrocytes
+ ACM
VGAT
GABA$_A$R
VGAT GABA$_A$R
B
Synapses per 20 µm
Synapse density
C
Axon + branch length (µm)
Total length
D
No astrocytes
+ ACM
Synapse number per cell
# of synapses

Figure 2.3 Astrocyte soluble factors increase GABAergic synapse function.

(A), Neurons cultured with astrocytes of ACM have a significantly greater number of GABAergic synapses (colocalization of blue and green clusters) labeled by the VGAT-C luminal antibody (red) after stimulation compared to neurons cultured alone. Scale bar = 10 μm. (B, C), Quantification of the effect of astrocytes or ACM on GABAergic synapse density (B) and functional GABAergic synapse density (C). Asterisk indicates significant difference compared to neuron-only cultures ($p < 0.001$). (D), Quantification of the number of GABAergic synapses plotted against the number of functional synapses per cell. Data from each condition was fit with a straight line ($R^2 > 0.98$).

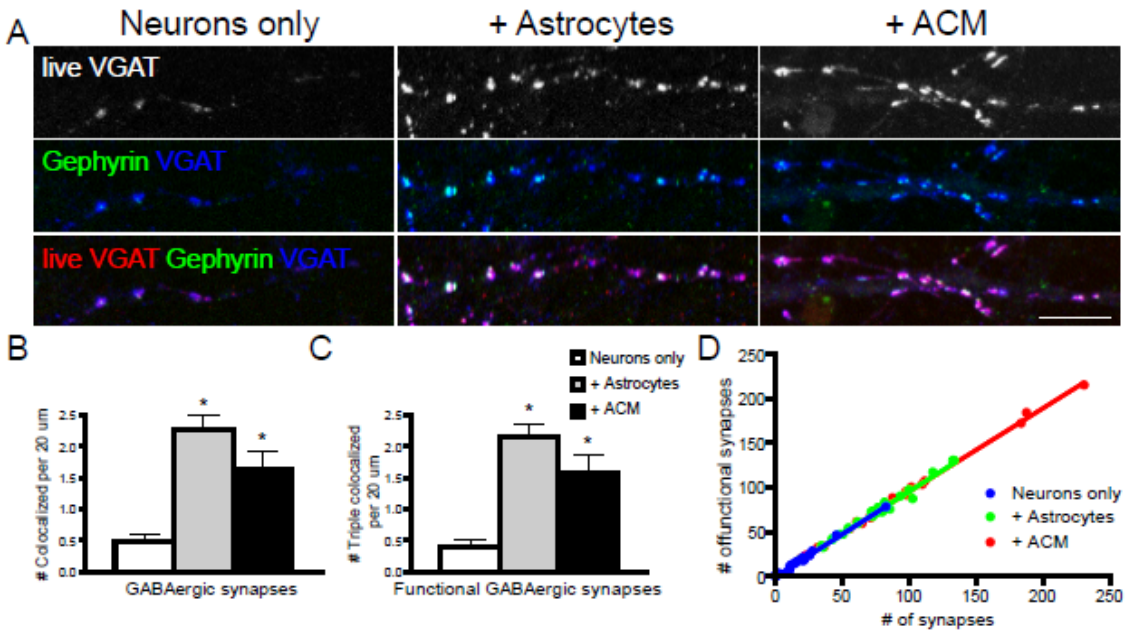
A
Neurons only
+ Astrocytes
+ ACM
live VGAT
Gephyrin VGAT
live VGAT Gephyrin VGAT
B
Colocalized per 20 um
GABAergic synapses
C
Neurons only
+ Astrocytes
+ ACM
# Triple colocalized per 20 um
Functional GABAergic synapses
D
offunctional synapses
of synapses
Neurons only
+ Astrocytes
+ ACM

Figure 2.4 TSPs do not increase GABAergic axon length, branching, or synaptogenesis.

Hippocampal neurons were cultured alone, with ACM, with TSP-1, or with TSP-depleted ACM, and were immunostained at 7 *div* with antibodies against GAD (green) and tau (red) to label GABAergic axons. (A), GABAergic axon length and branching were increased in neurons cultured with ACM (middle) but not when neurons were treated with TSP-1 (right) compared to neurons cultured alone (left) at 4 *div*. Scale bar = 25 μm. (B), Quantification shows that GABAergic axon length and branching were significantly increased in neurons cultured with ACM compared to neurons treated with TSP-1 and neurons cultured alone. ** indicates significant difference compared to neuron-only cultures ($p < 0.001$). (C), Hippocampal neurons were cultured alone, with ACM, with TSP-1, or with TSP-depleted ACM, and were immunostained at 7 *div* with antibodies against VGAT (red), and $GABA_AR$ β3 subunit (green) to label GABAergic synapses. An increase in presynaptic VGAT clusters, postsynaptic $GABA_AR$ clusters and GABAergic synapse density were observed at 7 *div* in neurons cultured with ACM (middle left) or with TSP-depleted ACM (right) but not when neurons were treated with TSP-1 (middle right) compared to neurons cultured alone (left). Scale bar = 10 μm. (D), Quantification of increase in presynaptic VGAT clusters (left), postsynaptic $GABA_AR$ clusters (middle) and GABAergic synapse density (right) per length dendrite in neurons treated with ACM, TSP-1, or TSP-depleted ACM. Single asterisk indicates significant difference compared to neuron-only cultures ($p < 0.050$); ** indicates significant

difference compared to neuron-only cultures ($p < 0.001$). (E), Quantification of increase in glutamatergic synapse number per dendrite length in neurons treated with ACM, TSP-1 but not TSP-depleted ACM. ** indicates significant difference compared to neuron-only cultures ($p < 0.001$).

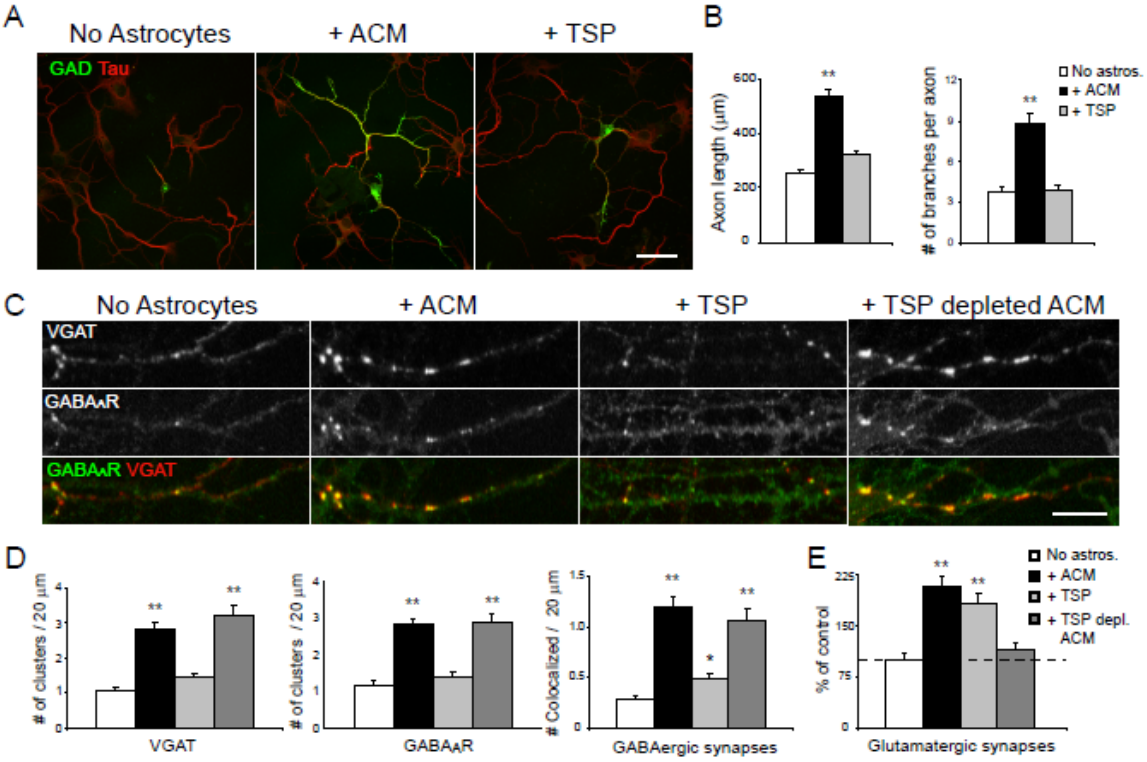
A
No Astrocytes
+ ACM
+ TSP
GAD Tau
B
Axon length (μm)
# of branches per axon
No astros.
+ ACM
+ TSP
C
No Astrocytes
+ ACM
+ TSP
+ TSP depleted ACM
VGAT
GABAAR
GABAAR VGAT
D
# of clusters / 20 μm
VGAT
GABAAR
Colocalized / 20 μm
GABAergic synapses
E
% of control
No astros.
+ ACM
+ TSP
+ TSP depl. ACM
Glutamatergic synapses

Figure 2.5 Astrocyte soluble factors are trypsin-sensitive.

Hippocampal neurons were cultured alone, with ACM or with trypsinized ACM and were immunostained at 4 *div* with antibodies against GAD and tau to label GABAergic axons and VGAT to label GABAergic presynaptic terminals. (A, B), GABAergic axon length and branching (A) and GABAergic synapse density (B) were significantly increased in neurons cultured with astrocytes (middle) but not with trypsinized ACM compared to neurons cultured alone (left). Scale bar = 25 (top), 10 (bottom) μm. (C), Quantification of GABAergic axon length, branching and synapse density in neuron-only cultures cultured with astrocytes, treated with ACM, trypsinized ACM, ACM + trypsin inhibitor or ACM + trypsinized ACM. * indicates significant difference compared to neuron-only cultures ($p < 0.001$).

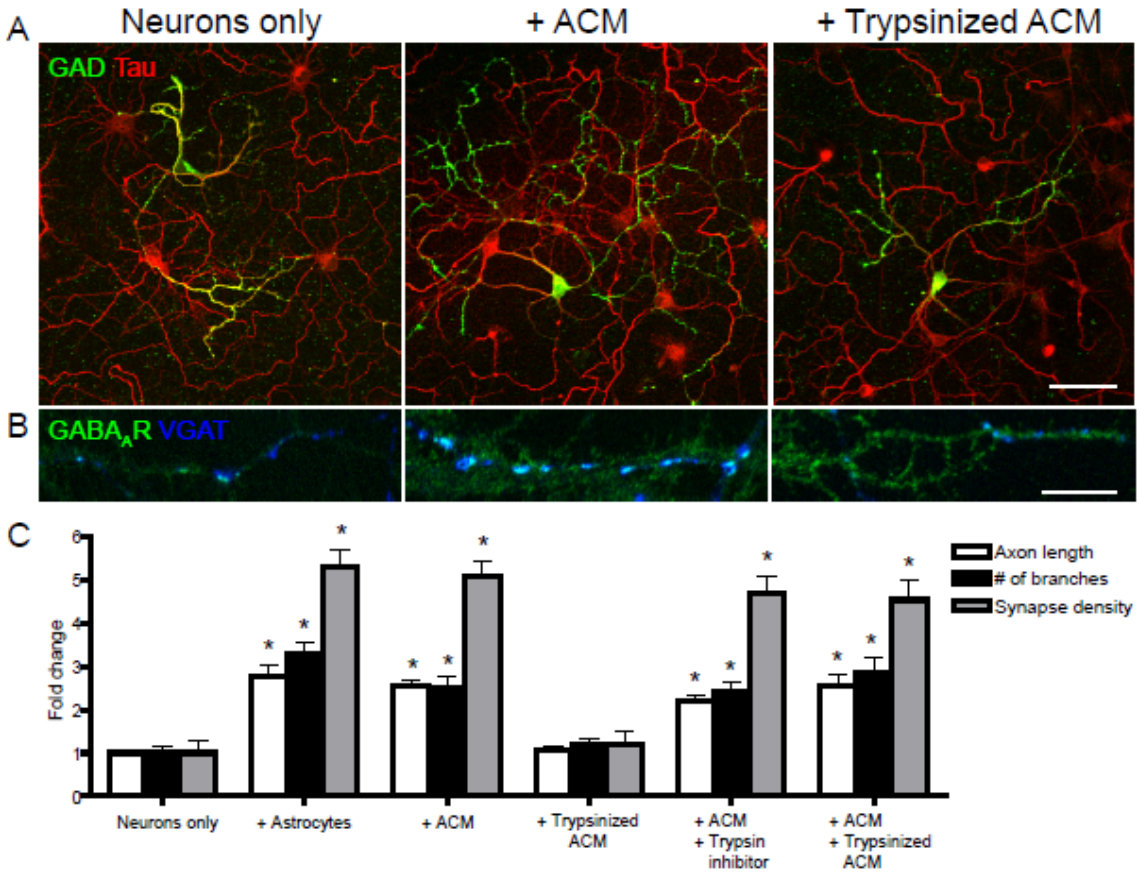
A
Neurons only
+ ACM
+ Trypsinized ACM
GAD Tau
B
GABA$_A$R VGAT
C
Fold change
Axon length
# of branches
Synapse density
Neurons only
+ Astrocytes
+ ACM
+ Trypsinized ACM
+ ACM + Trypsin inhibitor
+ ACM + Trypsinized ACM

Supplemental Figure 2.1 Soluble factors released specifically from astrocytes mediate affects on GABAergic neurons.

Hippocampal neurons were cultured alone, with astrocytes conditioned medium (ACM), or with fibroblast conditioned medium (FCM), and were immunostained at 4 and 7 *div* with antibodies against GAD (green) and tau (red) to label GABAergic axons. (A) , GABAergic axon length and branching were increased in neurons cultured with ACM (middle) but not when neurons were cultured with FCM (right) compared to neurons cultured alone (left) at 4 *div*. Areas within white boxes are shown below at higher magnification. Scale bar = 25 (top), 10 (bottom) μm. (B), Quantification of the effect of ACM or FCM on GABAergic axon length (left) and branching (right). Asterisk indicates significant difference compared to neuron-only cultures ($p < 0.001$). (C), Hippocampal neurons were cultured alone, with ACM, or with FCM, and were immunostained at 4 and 7 *div* with antibodies against presynaptic synaptophysin (red), and postsynaptic $GABA_AR$ β3 subunit (green) to label GABAergic synapses. An increase in the percent of $GABA_AR$ colocalization with synaptophysin was observed at 4 and 7 *div* in neurons cultured with ACM (middle) but not when neurons were treated with FCM (bottom) compared to neurons cultured alone (top). Scale bar = 5 μm. (D), Quantification of the effect of ACM or FCM on GABAergic synapses. Asterisk indicates significant difference compared to neuron-only cultures ($p < 0.001$).

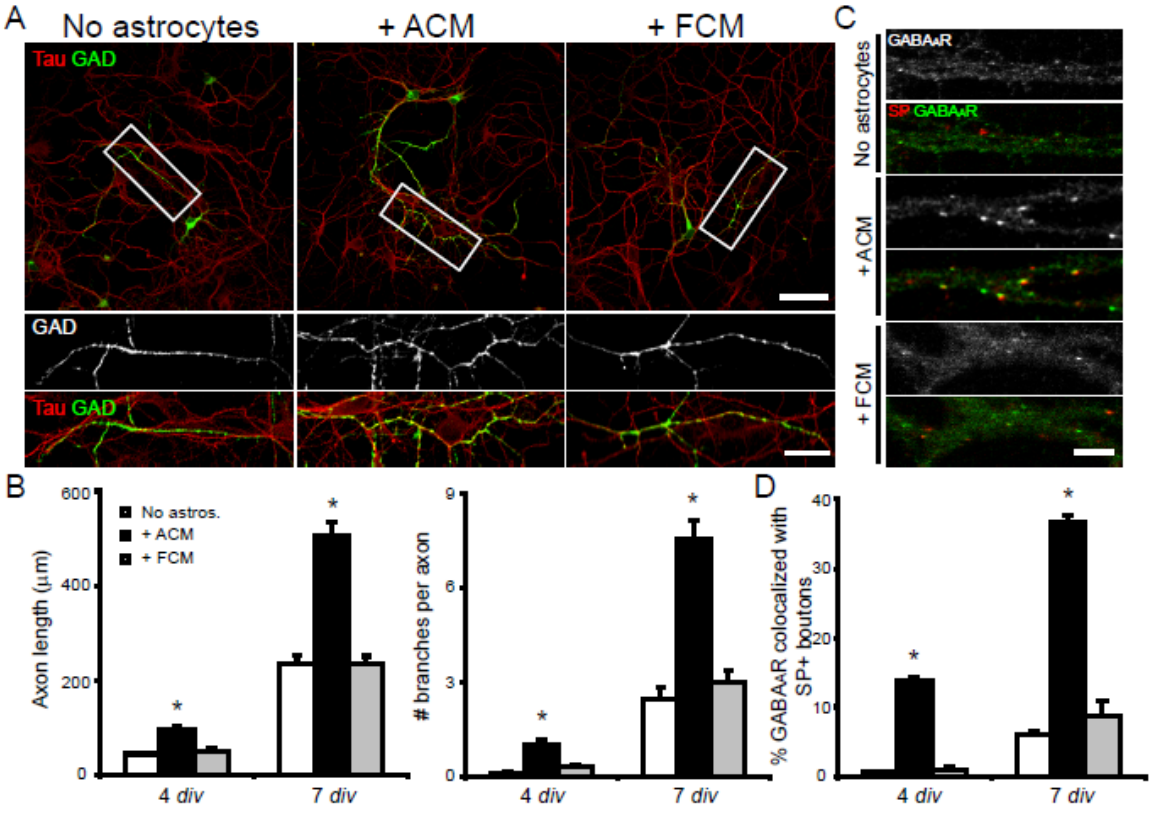
A
No astrocytes
+ ACM
+ FCM
Tau GAD
GAD
Tau GAD
C
GABAAR
SP GABAAR
No astrocytes
+ ACM
+ FCM
B
No astros.
+ ACM
+ FCM
Axon length (µm)
600
400
200
0
4 div
7 div
branches per axon
9
6
3
0
4 div
7 div
D
% GABAAR colocalized with SP+ boutons
40
30
20
10
0
4 div
7 div

Supplemental Figure 2.2 Astrocyte affects on GABAergic neurons do not require action potential activity, BDNF or NT3 signaling or cholesterol.

(A), Hippocampal neurons were cultured alone, with astrocytes, or with ACM, treated with tetrodotoxin (TTX) were immunostained with antibodies against GAD, tau, and VGAT. TTX treatment had no effect on GABAergic axon length (top), branching (middle), or presynaptic terminal density (bottom) in neurons cultured with astrocytes or ACM compared to neurons cultured alone. Asterisk indicates significant difference compared to neuron-only cultures ($p < 0.001$). (B), Hippocampal neurons were cultured alone, with astrocytes, or with ACM, treated with TrkB-IgG or TrkC-IgG were immunostained with antibodies against GAD, tau, and VGAT. Compared to control cultures treated with IgG (2.0 μg/ml final concentration), TrkB-IgG or TrkC-IgG had no effect on GABAergic axon length (top), branching (middle), or presynaptic terminal density (bottom) in neurons cultured with astrocytes or ACM at 7 *div* compared to neurons cultured alone. Asterisk indicates significant difference compared to neuron-only cultures ($p < 0.001$). (C), Hippocampal neurons were cultured alone, with cholesterol or vehicle were immunostained with antibodies against GAD, tau, VGAT and $GABA_AR$. Cholesterol treatment had no effect on GABAergic axon length (top), branching (middle), or GABAergic synapses (bottom) compared to neurons cultured alone. Asterisk indicates significant difference compared to neuron-only cultures ($p < 0.001$).

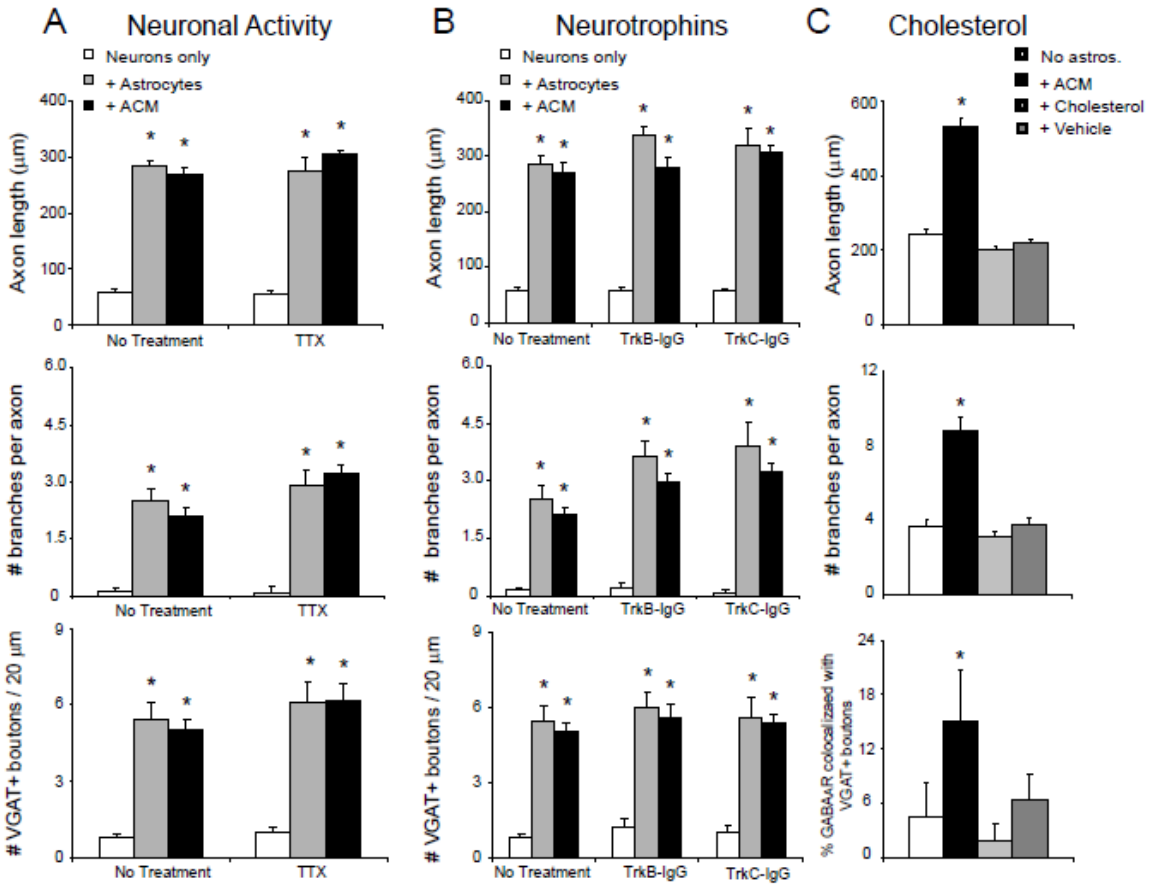
A
Neuronal Activity
Neurons only
+ Astrocytes
+ ACM
Axon length (µm)
branches per axon
VGAT+ boutons / 20 µm
No Treatment
TTX
B
Neurotrophins
Neurons only
+ Astrocytes
+ ACM
Axon length (µm)
branches per axon
VGAT+ boutons / 20 µm
No Treatment
TrkB-IgG
TrkC-IgG
C
Cholesterol
No astros.
+ ACM
+ Cholesterol
+ Vehicle
Axon length (µm)
branches per axon
% GABAAR colocalized with VGAT+ boutons

Supplemental Figure 2.3 TSPs are reduced in immunodepleted ACM.

TSP antibodies were incubated with protein A/G beads, then added to 10-fold concentrated ACM. After incubation, equivalent samples of TSP-depleted ACM were compared to ACM incubated with protein A/G beads alone, along with the TSP that was bound to the beads. (A), Immunoblotting with TSP-1 specific antibodies shows that TSP-1 is depleted by 80% from ACM, and was bound to protein A/G beads. Asterisk indicates significant difference ($p < 0.05$). (B), Immunoblotting with TSP-2 specific antibodies shows that TSP-2 is depleted by 70% from ACM and remains bound to protein A/G beads. Asterisk indicates significant difference ($p < 0.05$).

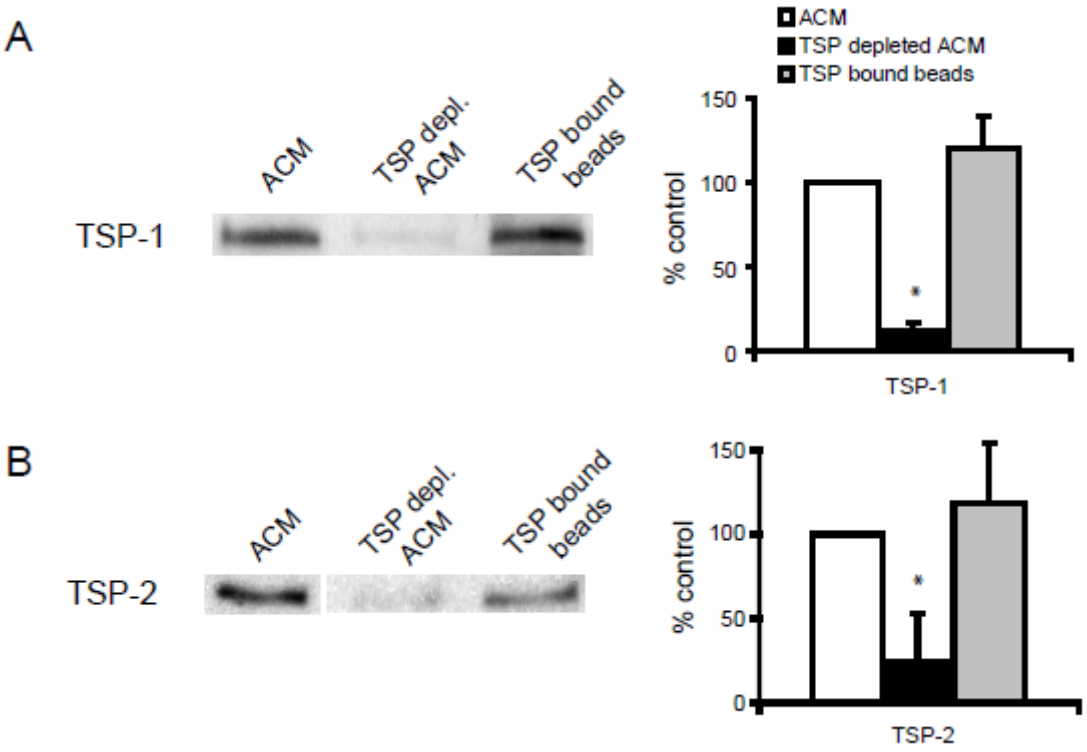
A
ACM
TSP depl. ACM
TSP bound beads
TSP-1
ACM
TSP depleted ACM
TSP bound beads
% control
150
100
50
0
*
TSP-1
B
ACM
TSP depl. ACM
TSP bound beads
TSP-2
% control
150
100
50
0
*
TSP-2

Supplemental Table 2.1 Astrocytes increase inhibitory axon length and branching.

TABLE 1	1° axon length (µm)	# of 2° branches.	# of 3° branches	# of 1° dendrites	Dendrite length (µm)	Soma area (µm^2)
4 *div*						
No astrocytes						
GABAergic neurons	57.9 ± 5.4 (88)	0.2 ± 0.1	0	3.4 ± 0.1	38.0 ± 1.8	198.0 ± 7.8
Glutamatergic neurons	348.7 ± 22.2 (45)	2.4± 0.2	n.d.	5.0 ± 0.4	37.7 ± 3.7	265.0 ± 20.0
+ Astrocytes						
GABAergic neurons	303.9 ± 16.5 (85)**	3.2 ± 0.3**	2.95 ± 0.24	3.4 ± 0.1	35.2 ± 1.1	208.6 ± 9.4
Glutamatergic neurons	335.8 ± 22.1 (45)	2.4 ± 0.3	n.d.	4.7 ± 0.3	35.3 ± 4.4	253.7 ± 21.3
+ ACM						
GABAergic neurons	284.0 ± 19.0 (82)**	2.8 ± 0.3**	2.17 ± 0.18	3.6 ± 0.2	34.4 ± 1.3	208.4 ± 6.4
Glutamatergic neurons	322.0 ± 15.0 (42)	2.54 ± 0.3	n.d.	4.8 ± 0.3	33.3 ± 3.1	234.0 ± 22.9
7 *div*						
No astrocytes						
GABAergic neurons	168.3 ± 19.2 (65)	1.8 ± 0.2	1.01 ± 0.20	5.1 ± 0.2	48.0 ± 1.6	289.9 ± 12.6
Glutamatergic neurons	723.0 ± 42.1 (40)	7.6 ± 0.6	n.d.	5.9 ± 0.4	44.3 ± 4.9	347.9 ± 26.4
+ Astrocytes						
GABAergic neurons	344.0 ± 33.1 (62)**	5.7 ± 0.5 **	5.31 ± 0.48**	5.1 ± 0.3	47.1 ± 2.1	273.2 ± 12.0
Glutamatergic neurons	787.3 ± 22.3 (38)	8.1 ± 0.3	n.d.	5.6 ± 0.5	41.7 ± 5.1	387.5 ± 26.2
+ ACM						
GABAergic neurons	400.6 ± 32.6 (56)**	4.5 ± 0.5*	5.17 ± 0.30**	5.0 ± 0.2	49.3 ± 1.5	303.7 ±13.5
Glutamatergic neurons	718.4 ± 24.6 (40)	7.4 ± 0.6	n.d.	5.7 ± 0.4	51.1 ± 4.2	336.5 ± 36.2
10 *div* GABAergic neurons						
No astrocytes	419.9 ± 22.8 (40)	3.9 ± 0.3	n.d.			
+ Astrocytes	923.8 ± 29.1 (35)**	9.9 ± 0.7**	n.d.			
+ ACM	938.7 ± 16.7 (35)**	8.3 ± 0.9**	n.d.			
16 *div* GABAergic neurons						
No astrocytes	671.6 ± 66.2 (25)	6.0 ± 0.4	n.d.			
+ Astrocytes	1435.4 ± 33.1 (25)**	14.2 ± 0.6**	n.d.			
+ ACM	1476.8 ± 32.6 (24)**	12.8 ± 0.9**	n.d.			

Identification of astrocyte proteins that affect hippocampal GABAergic axon length, branching, and synaptogenesis

Ethan G. Hughes[1], Todd M. Greco[1,3], Harry Ischiropoulos[2,3] and Rita J. Balice-Gordon[1]

[1]Dept. of Neuroscience

[2] Dept. of Pharmacology, Univ. of Pennsylvania School of Medicine

[3]Dept. of Pediatrics, Children's Hospital of Pennsylvania, Philadelphia, PA, 19104 USA

Abstract / Intro / Discussion / Figures / Tables: 185 / 400 / 1131 / 3 / 1

Supplemental Figures / Tables: 0 / 1

Key words: Astrocyte, inhibitory neuron, GABA, mass spectroscopy, synaptogenesis, proteomics

Address correspondence to: Rita Balice-Gordon, Ph.D., Dept. of Neuroscience, University of Pennsylvania School of Medicine, 215 Stemmler Hall, Philadelphia, PA 19104-6074

(215) 898-1037; FAX (215) 573-9122, rbaliceg@mail.med.upenn.edu

Abstract

Several molecules are released from astrocytes that increase the formation and function of glutamatergic synapses but the molecules that astrocytes secrete to modulate GABAergic synaptogenesis are unknown. We demonstrate that media conditioned by astrocytes can be separated by gel filtration and biologically assayed for effects on GABAergic axon length, branching and synaptogenesis. We found that gel filtration fractions containing high molecular mass proteins and protein complexes mediate the effects of astrocytes on GABAergic axon length, branching and synaptogenesis. The protein composition of these bioactive fractions was examined using mass spectroscopy and computational analyses. We show that these fractions contain at least 223 astrocyte secreted proteins. We selected and ranked 34 of these secreted proteins as candidates of interest, based on literature searches and biological pathway analysis. I describe the approaches we are taking to evaluate these candidates as proteins that mediate the effects of astrocytes on GABAergic axon length, branching, and synaptogenesis. Taken together, these results show that we have identified a list of proteins that are released from astrocytes and that may modulate the formation and function of GABAergic circuitry.

Introduction

The development of CNS synapses requires not only the exchange of signals between neurons but also communication with adjacent glia. Astrocytes increase the formation of functional glutamatergic and GABAergic synapses through a variety of signaling mechanisms including both secreted and contact-mediated factors (Mauch et al., 2001; Hama et al., 2004; Christopherson et al., 2005). Recently, several factors that increase excitatory synaptogenesis have been identified. Mauch et al. found that astrocyte-derived cholesterol complexed to ApoE was both necessary and sufficient to increase the number of functional presynaptic terminals in retinal ganglion cells (RGC) (Mauch et al., 2001). Thrombospondin-1 and -2 (TSP) expressed by immature astrocytes can also increase excitatory synapses between RGCs *in vitro* and *in vivo*. These TSP induced synapses are presynaptically active but postsynaptically silent, suggesting that other, as yet unknown, factors may coordinate pre- and postsynaptic maturation (Christopherson et al., 2005). While astrocyte proteins that increase excitatory synaptogenesis have been identified, astrocyte factors that increase GABAergic synaptogenesis remain unknown.

The identification of astrocyte factors that regulate synapse formation has been limited by the lack of characterization of the genes and proteins expressed by astrocytes. Two groups have recently profiled the gene expression of astrocytes both *in vitro* and *in vivo* (Lovatt et al., 2007; Cahoy et al., 2008). Several other groups have used proteomic approaches to analyze the proteins released by astrocytes, or the "astrocyte secretome"

(Dowell et al., 2009; Keene et al., 2009; Moore et al., 2009). These approaches, in addition to the newly generated gene and secreted protein profiles of astrocytes, will be invaluable tools in proceeding forward in the identification of new astrocyte factors and their roles in synapse formation.

In the results presented here, we use a proteomic approach to separate and identify proteins released from astrocytes that increase GABAergic axon length, branching, and synaptogenesis. We show that astrocyte soluble proteins (or protein complexes) of high molecular weight affect these aspects of GABAergic neurons. Furthermore, we identify the protein composition of bioactive fractions using mass spectroscopy and computational analyses. Thirty-four proteins were selected as candidates for further analysis using literature searches and biological pathway analysis. I describe the approaches we are taking to evaluate these candidates as proteins that mediate the effects of astrocytes on GABAergic axon length, branching, and synaptogenesis. Taken together, these results show that we have identified a list of proteins that are released from astrocytes and that may modulate the formation and function of GABAergic circuitry.

Results

Gel filtration separates ACM proteins by size

We concentrated and separated ACM proteins (and protein complexes) by gel filtration (a typical chromatogram is shown in Fig. 1A). Silver staining of gel filtration fractions run on a denaturing SDS-Page gel showed that ACM are separated by size and individual fractions contain relatively small number of bands (Fig. 1B). The first fractions collected during gel filtration contained many high molecular weight bands but also several lower molecular weight bands (Fig. 1B). This indicates that smaller proteins (possibly contained within high molecular weight protein complexes) are present within large molecular weight fractions. These results show that proteins and protein complexes released by astrocytes can be separated based on their molecular weight.

ACM proteins in high molecular weight gel filtration fractions affect GABAergic neurons

In order to begin to characterize the protein(s) released from astrocytes that affect GABAergic axon length, branching and synaptogenesis, we treated neuron only cultures of dissociated hippocampal neurons with gel filtration fractions and examined the effects on GABAergic neurons. To assess whether fractionation by gel filtration affected the ability of ACM to affect GABAergic neurons, we recombined a small amount of each fraction into one pool (reconstituted ACM) and treated neuron only cultures. Reconstituted ACM increased GABAergic axon length, branching and presynaptic

terminal density to a similar extent as unmodified ACM (Fig. 2). These results show that ACM proteins retain their biological activity after separation by gel filtration.

To examine the size of the protein(s) that mediate the affects of ACM on GABAergic neurons, groups of 4 gel filtration fractions were pooled and tested in their ability to affect GABAergic neurons. Fractions containing proteins ranging in molecular mass of 2000+-860 kDa increased GABAergic axon length, branching, and presynaptic terminal density. Additionally, fractions with proteins ranging from 859-360 kDa increased GABAergic axon length and branching, whereas fractions with proteins ranging from 25-9 kDa only increased the number of GABAergic axon branches. These results show that the biological activity mediating the effects of astrocyte conditioned media on GABAergic neurons was separated into two fractions, a high molecular weight fraction (2000+ - 860 kDa) and a low molecular weight fraction (25 – 9 kDa), each having distinct biological activities.

Proteomic evaluation of biologically active gel filtration fractions

Biologically active ACM gel filtration fractions were analyzed by tandem mass spectrometry (MS/MS) to examine their protein composition. Gel/LC-MS/MS analysis identified a total of 772 unique proteins from three samples of high molecular weight ACM gel filtration fractions (Supp. Table 1). To specifically examine secreted proteins we evaluated the protein identifications using a multi-step computational workflow involving *in silico* cellular localization prediction algorithms and functional Gene

ontology (GO) classification. The computation algorithm SignalP (Bendtsen et al., 2004), which uses N-terminal signal peptides for subcellular localization prediction, predicted 186 proteins to contain an N-terminal signal peptide. To include secreted proteins that may lack an N-terminal signal, GO analysis was performed using Cytoscape network visualization software implementing the BiNGO plug-in. An additional 37 proteins were classified that lacked an identifiable signal peptide, but had been annotated to the extracellular region (GO: 5 576) or the cell surface (GO: 9 986).Together, these computational analyses identified 223 proteins as secreted proteins (Supp. Table 1).

Since fractions 1-8 increased GABAergic axon length, branching and synaptogenesis (see Fig. 2B), we examined the patterns of separation of secreted proteins to help narrow the list of potential candidates. From our experimental findings we predict that the protein(s) responsible for increasing GABAergic axon length, branching and synaptogenesis would be found in “all fractions” or “not separated” fractions. We found that 11 and 30 proteins were uniquely identified in pooled fractions 1-4 and 5-8, respectively, while, 39 proteins were identified in both pooled fractions1-4 and 5-8. The remaining 143 proteins were not separated into any of these three categories (Fig. 3A).

Biological pathway reconstruction provides powerful tools to analyze genomic and proteomic profiles (van Baarlen et al., 2008). Ingenuity Pathway Analysis (IPA) is a software tool that accelerates the identification of cellular pathways or processes by generating protein networks according to biological and functional categories. We selected six pathways identified by IPA as significantly represented in our samples (see

Fig. 3C) that may be important in neurite extension and synapse formation. Of the 223 secreted proteins, ~70 proteins were identified by IPA to be involved in these selected pathways. A large portion of these proteins are involved in neurite outgrowth and adhesion, whereas a smaller number of proteins are involved in axon guidance, long-term potentiation, glial migration, and synaptogenesis (Fig. 3C).

To prioritize this group of proteins for candidate testing we developed criteria to characterize and rank these potential candidates. Candidates were excluded if i) they lacked sufficient evidence of secretion (determined from literature searches, 16 candidates) or ii) the candidate was not found in more than one condition or experiment (8 candidates). To rank candidates we utilized, i) manual literature searches (presence or function within neurons or astrocytes) and ii) interest of candidate. Interest of a candidate was based on known protein function (determined by literature searches). Candidates were grouped into six categories: low interest, interest, high interest, highest interest, known candidate (candidate shown to be neuron or glial factor that affects neurite outgrowth or synaptogenesis), known candidate (candidate shown to be neuron-glial signaling factor that affects neurite outgrowth or synaptogenesis). Using these four criteria we identified and ranked 34 candidate proteins released by astrocytes that should be tested for their effects on GABAergic axon length, branching, and synaptogenesis (Table 2).

Computational and functional classification of potential candidates

Recently, two groups have generated a gene expression profile of astrocytes *in vitro* and *in vivo* (Lovatt et al., 2007; Cahoy et al., 2008). This astrocyte transcriptome provides a view into the global gene expression of astrocytes over development and can be compared to gene expression profiles of other cell types (see (Cahoy et al., 2008). We utilized this resource to further characterize the candidates we identified from bioactive gel filtration fractions (Fig. 3) in astrocytes *in vitro*, *in vivo*, and compared to other cell types. We examined the presence of the candidates in expression profiles (from (Cahoy et al., 2008) of *in vitro*, *in vivo* astrocytes and *in vivo* neurons. Two potential candidates were not evaluated in the gene expression profiles generated by Cahoy and colleagues (Neural cell adhesion molecule, complement component C3). Of the other candidates, 31 of the 32 candidates were expressed by astrocytes *in vivo*, the remaining candidate was found to be expressed by astrocytes *in vitro* (Table 2, presence or absence of gene was determined by methods described in (Cahoy et al., 2008)). We examined whether candidates were enriched in astrocytes compared to other cell types and conditions. We found that 33% of candidates are enriched in astrocytes compared to other cell types (neurons, oligodendrocytes), 19% are enriched in astrocytes *in vitro*, and 43% are enriched in astrocytes *in vivo*. These results suggest that all of our candidates are present in astrocytes and many are enriched in astrocytes *in vivo*.

To examine the difference between gene expression values to that of amount of secreted protein, we employed semi-quantitative MS based on label-free spectral counting. This method has been previously used as an effective means to estimate relative

protein abundance (Old et al., 2005). The number of redundant peptides (spectral counts) was normalized by the protein molecular weight for each identified protein. When the normalized spectral counts are compared to gene expression values (obtained from (Cahoy et al., 2008), some candidates with the highest normalized spectral counts are not genes that are highly expressed by astrocytes *in vitro* (examples: fibronectin, tenascin C). This finding suggests that even low expressed genes can produce large amounts of protein. Together, these results highlight the importance of the combination of proteomic and genomic approaches to characterizing the astrocyte genes and potential candidates for mediating the effects of astrocytes on GABAergic neurons.

Discussion

Here we demonstrate that astrocyte soluble factors can be separated by size exclusion chromatography, evaluated in a bioassay and identified by mass spectroscopic and computational techniques. These studies have generated a vast amount of information about the proteins that astrocytes release into the extracellular space as well as provided insights into potential candidate proteins that may mediate the effects of astrocytes on GABAergic neurons.

Candidates shown to mediate astrocytes effects on excitatory synaptogenesis

In the context of previous work, our proteomic analysis identifies several candidates known to mediate effects of astrocytes on excitatory synaptogenesis. Our analysis identified both thrombospondin-1 and -2 in the largest molecular weight gel filtration fractions; fractions that increased GABAergic axon length, branching, and synaptogenesis. While thrombospondins (TSPs) are released from astrocytes and increase excitatory synaptogenesis both *in vitro* and *in vivo* (Christopherson et al., 2005), we have previously shown that TSPs are not required for astrocytes to increase GABAergic axon length, branching or synaptogenesis (Hughes et al., submitted). We also identified apolipoprotein E (ApoE), which is important for mediating the effects of astrocyte cholesterol on excitatory presynaptic release (Mauch et al., 2001). However, we do not believe that ApoE mediates the effects of cholesterol to increase GABAergic synaptogenesis because we have shown that exogenous cholesterol does not increase

GABAergic synaptogenesis (Elmariah et al., 2005), see also (Hama et al., 2004; Christopherson et al., 2005). Two other candidates identified in our evaluation of bioactive gel filtration fractions are SPARC and SPARC-L1. Both SPARC and SPARC-L1 are released from glia and increase neurite outgrowth (Au et al., 2007) and recently have been implicated in inhibiting and promoting excitatory synaptogenesis respectively (Eroglu et al., 2007). Since SPARC-L1 increases excitatory synaptogenesis, we tested whether SPARC-L1 also increased inhibitory synaptogenesis. We added recombinant SPARC-L1 to neuron-only cultures and found no significant increases in GABAergic axon length, branching, or synaptogenesis (EGH and RBG unpublished observations) suggesting that SPARC-L1 does not mediate the affects of astrocytes on GABAergic neurons. Together, these findings suggest that proteins released from astrocytes that affect GABAergic neurons have not been previously implicated in mediating the effects of astrocytes on excitatory synaptogenesis.

Potential candidates for mediating the effects of astrocytes on GABAergic neurons

One potentially interesting candidate identified in the large molecular weight fractions that increase GABAergic axon length, branching and synaptogenesis is close homologue of L1 (CHL1). CHL1 is a transmembrane molecule that also can function as a soluble factor as it can be cleaved from the cell surface by metalloproteases (Naus et al., 2004). CHL1 is expressed by Bergmann glia in the cerebellum and organize inhibitory synapses onto Purkinje cell dendrites (Ango et al., 2008). CHL1-deficient mice have

increased numbers of inhibitory synapses and enhanced inhibitory synaptic transmission (Nikonenko et al., 2006). Together, these results suggest that CHL1 is important for the regulation of inhibitory synapse formation and function in the developing nervous system and make it an important candidate to evaluate whether it is mediating the effects of astrocytes on GABAergic neurons.

Another interesting candidate identified in bioactive gel filtration fractions is amyloid beta precursor protein (APP). APP has been intensively studied for its role in the pathogenesis of Alzheimer's disease, while its normal function is less understood. APP is an integral membrane protein expressed in neurons and glia which can undergo proteolytic processing to release soluble ectodomains. These soluble ectodomains are important for regulating neurite outgrowth during development (Qiu et al., 1995; Young-Pearse et al., 2008) and play roles in modulating synaptic transmission, by increasing the surface stability of NMDA receptors (Hoe et al., 2009b). Since APP is expressed by astrocytes and play roles in neurite outgrowth and synaptic transmission, it is another important candidate to determine whether it plays a role in mediating the effects of astrocytes on GABAergic neurons during development.

One alternative possibility is that multiple proteins interact to exert the effects of astrocytes on GABAergic neurons. Since only one large molecular weight fraction increases GABAergic axon length, branching, and synaptogenesis, this argues that the bioactive protein(s) are at least separated into the same gel filtration fraction. However, two proteins identified in this bioactive fraction, amyloid precursor protein (APP) and

Reelin, interact to increase neurite outgrowth (Hoe et al., 2009a). Other proteins found in bioactive fractions, such as TSP-1, ApoE, and VLDL, interact to play roles in neuronal migration (Blake et al., 2008). This evidence suggests that protein interaction and biological pathway analysis tools should be used to identify sets or pathways of proteins that could be tested to determine whether they regulate the ability of astrocytes to increase GABAergic axon length, branching and synaptogenesis.

Evaluating candidates and their affects on GABAergic neurons

With the discovery of large numbers of new candidates from genomic and proteomic profiles of astrocytes, the evaluation of many potentially interesting candidates will be necessary. Several groups have used large-scale screens to identify new molecules implicated in synapse formation and synapse specificity (Kurusu et al., 2008; Linhoff et al., 2009). One of these approaches was an unbiased expression screen, where a cDNA library screen yielded a new family of trans-synaptic molecules that mediate synapse formation (Linhoff et al., 2009). This type of approach on a large and small scale will be invaluable to evaluate large numbers of new candidates identified by the gene expression and secreted protein profiles of astrocytes.

We report the identification of astrocyte soluble proteins in gel filtration fractions that increase GABAergic axon length, branching, and presynaptic terminal density. Of the 223 identified secreted proteins we intend to focus on 34 candidates based on biological pathway analysis and literature searches. We plan to screen these candidates

individually by treating neuron only cultures with three different concentrations of the recombinant protein for three days and immunostaining these coverslips for GAD and VGAT to identify GABAergic neuron neurite morphology and presynaptic terminal density. In this manner, we will be able to evaluate these 34 candidates in a relatively short period of time. However, despite the reduction in secretome complexity and activity-based secretome fractionation using gel filtration, we cannot exclude the possibility that the biologically active proteins were not identified below the detection limits of the proteomic approach. Based on the initial candidate protein screen, the proteomics approach may require further optimization for increased depth of secretome analysis.

In the results presented here, we use a proteomic approach to separate and identify proteins released from astrocytes that increase GABAergic axon length, branching, and synaptogenesis. The studies described above begin to define the cellular and molecular mechanisms that underlie how astrocytes modulate GABAergic synapse formation, function and maintenance. These studies will be essential to understanding neuron-glial communication and the role in play in the development of neural circuits.

Materials and Methods

Cell cultures

Primary hippocampal neuronal cultures are prepared as previously described (Goslin et al., 1988). Hippocampi are dissected from embryonic day 18-19 mice, dissociated in Ca^{2+}- and Mg^{2+}-free HBSS containing 0.03% trypsin for 20 min., triturated in Dulbecco's Modified Eagle Medium (DMEM; Life Technologies) supplemented with 10% heat-inactivated fetal bovine serum (FBS) and plated at 100,000 cells per ml in DMEM supplemented with 10% FBS, 10% Ham's F12 (Life Technologies), and 1% Penicillin and Streptomycin (Life Technologies) on poly-L-lysine (PLL) coated coverslips in 12-well plates. For pure neuronal cultures, cytosine arabinoside (Ara-C; 10 μM) is added to cultures 18 – 20 hours after plating to prevent glial proliferation. Culture media is changed to Neuralbasal (Life Technologies) supplemented with B27 (Life Tech.) at 4 *div*. Cells are maintained at 37 °C, 5% CO_2, 95% humidity; medium is changed weekly.

Primary astrocyte cultures are prepared as described previously (Duan et al., 2003; Zhang et al., 2003). Briefly, hippocampi are dissected, rinsed in cold HEPES-buffered Earle's Balanced Salt Solution (EBSS), dissociated in 0.125% trypsin for 20 min., and plated in T25 flasks in modified Minimum Essential Medium (MMEM) supplemented with 10% heat-inactivated FBS, 2 mM L-glutamine, 14 mM sodium bicarbonate, 40 mM D-glucose, 1% sodium pyruvate and 1% Penicillin and Streptomycin. Astrocytes proliferate for 14 – 21 days; after reaching confluency, are rinsed in cold EBSS and shaken at 260 rpm for 18 - 20 hours in MMEM to remove neurons and other cells.

Purified astrocytes are then plated onto PLL-coated coverslips at 400,000 cells/ml in MMEM. Medium is changed to Neuralbasal Medium and coverslips used for neuron co-cultures or ACM treatments within 1 - 3 days. Coverslips are immunostained with an antibody against GFAP (Chemicon) to assess purity prior to use.

For pure neuronal cultures treated with ACM, neurons are plated in Neuralbasal Medium conditioned by astrocytes or fibroblasts (14-21 days old) during the previous 24-72 hours. Sterile inserts with 3 μm high pore density membranes (BD Labware) were placed into each well, and coverslips with astrocyte monolayers were inverted 0.9 mm above neurons. Inserts remain in place throughout the culture duration.

Immunostaining and confocal microscopy

Coverslips were fixed in 4% paraformaldehyde and 4% sucrose for 15 min., permeabilized with cold 0.25% Triton X-100 for 5 min., and blocked in 5% normal goat serum (Invitrogen) for 1 hour at RT. Triple labeling was performed with combinations of primary antibodies: GAD-6 (1:10, monoclonal; Developmental Studies Hybridoma Bank, Iowa), GFAP (1:1000, rabbit antiserum; Sigma), tau (1:1000, rabbit antiserum; gift of Dr. V. Lee), and VGAT-N (1:200, guinea pig antiserum; Synaptic Systems, Goettingen, Germany). Antibodies were visualized after staining with the appropriate FITC-, TRITC- or CY5-conjugated secondary antibodies (all used at 1:200, Jackson ImmunoResearch, Inc., West Grove, PA). Immunostaining was performed at 4, 7 and 10 *div* or later ages *in vitro* with antibodies against glutamic acid decarboxylase (GAD), the

synthetic enzyme for GABA, to identify GABAergic neurons, and tau, to visualize axons. Images were obtained using a confocal microscope (Leica TCS SP2). In each image, laser light levels and detector gain and offset were adjusted so that no pixel values were saturated in regions analyzed.

Quantification and statistical analysis for confocal images

For all experiments, 6-15 neurons in each condition were examined on each of 2-3 coverslips in 3-5 independent experiments**.** Neurons were randomly selected for analysis. GABAergic neurons were distinguished from glutamatergic neurons by anti-GAD immunoreactivity. In a majority of experiments, the number and proportion of glutamatergic and GABAergic neurons were determined by counting GAD+ and GAD- neurons in a minimum of 5 randomly chosen fields on each coverslip (750 x 750 microns). The number of immunostained presynaptic clusters was determined from confocal images using interactive software (custom-written ImageJ macros). Confocal images of neurons were threshold automatically using an iterative thresholding technique (Bergsman et al., 2006), and the number and area of individual clusters were determined using interactive software (custom-written ImageJ macros). Clusters with more than 20% pixel overlap of pre- and postsynaptic markers were considered colocalized and thus synaptic.

Values for axon length, branch number and cluster number were compared across conditions using the Kruskal-Wallis nonparametric ANOVA test followed by Dunn's

pairwise multiple comparison test, unless otherwise indicated. All values are presented as mean ± s.e.m.

Gel filtration

Concentrated ACM is filtered through 0.22 μm membranes, and injected on the HPLC for gel filtration analysis using an Agilent (Palo Alto, CA) 1100 series HPLC controlled by ChemStation software (Agilent). 1.2 mg of ACM in a total volume of 250 μl is resolved onto a Superdex 200 HR10/30 column (GE Healthcare Bio-Sciences, Uppsala, Sweden) for size exclusion chromatography (SEC) analysis. ACM proteins are resolved at a flow rate of 0.3 ml/min in 25 mM HEPES, pH 7.25, and 150 mM NaCl. Fractions (0.5 ml) are collected and concentrated with 5000 NMWL Ultrafree-MC filters (Millipore). The gel filtration column is calibrated using the following mixture of globular proteins standards: thyroglobulin (669 kDa, 85 Å), ferritin (440 kDa, 61 Å), catalase (232 kDa, 52.2 Å), aldolase (158 kDa, 48 Å), albumin (67 kDa, 35.5 Å), ovalbumin (43 kDa, 30.5 Å), chymotrypsin (25 kDa, 20.9 Å), and ribonuclease A (13.7 kDa, 16.4 Å). The void volume is determined from the elution migration of blue dextran (2000 kDa, 99 Å). Protein elution is monitored by UV absorbance at 275 nm. All experiments involving gel filtration chromatography are performed initially at RT. Fractionated samples are stored at -80 °C until use. Neurons are treated with fractions diluted 1:20 in NeuralBasal medium and assayed after 72 hours.

Electrospray Tandem MS Analysis of Astrocyte-conditioned Media

Tryptic digests of fractions from gel filtration (prepared as described in Zuo and Speicher, 2000) are analyzed on an LTQ linear IT mass spectrometer (Thermo Electron) coupled with a NanoLC pump (Eksigent Technologies, Livermore, CA) and autosampler. Tryptic peptides are separated by RP-HPLC on a nanocapillary column, 75 μm id x 20 cm PicoFrit (New Objective, Woburn, MA, USA), packed with MAGIC C_{18} resin, 5 μm particle size (Michrom BioResources, Auburn, CA). Solvent A is 0.58% acetic acid in Milli-Q water, and solvent B is 0.58% acetic acid in acetonitrile (ACN). Peptides are eluted into the mass spectrometer at 200 nL/min using an ACN gradient. Each RP-LC run consists of a 10 min. sample load at 1% B; a 75 min. total gradient consisting of 1–28% B over 50 min., 28–50% B over 14 min., 50–80% B over 5 min., 80% B for 5 min before returning to 1% B in 1 min. To minimize carryover, a 36 min. blank cycle is run between each sample. Hence, the total sample-to-sample cycle time is 121 min. The mass spectrometers are set to repetitively scan m/z from 375 to 1600 followed by data-dependent MS/MS scans, the ten most abundant ions with dynamic exclusion enabled.

Protein Identification and Validation

Proteins are identified from the MS/MS spectra using the SEQUEST Browser program (Thermo Electron). DTA files are generated from MS/MS spectra using an intensity threshold of 5000 and minimum ion count of 30. The DTA files generated are processed by the ZSA, CorrectIon, and IonQuest algorithms of the SEQUEST Browser

program, and searched against the NCBI non-redundant protein database [*www.ncbi.nlm.nih.gov/RefSeq/*]. Databases are indexed with the following parameters: average mass range of 500–3500, length of 6–100, tryptic cleavages with 1 internal missed cleavage sites, static modification of Cys by carboxyamidomethylation (+57 Da), and variable modification of methionine (+16 Da). The DTA files were searched with a 2.5 Da peptide mass tolerance and 0 Da fragment ion mass tolerance.

Potential sequence-to-spectrum peptide assignments generated by SEQUEST are loaded into Scaffold (version Scaffold-01_06_17, Proteome Software Inc., Portland, OR) to validate MS/MS based peptide and protein identifications as well as to compare protein identifications across experimental conditions. Peptide and protein probabilities were calculated by the Peptide and Protein Prophet algorithms, respectively. A protein identification is accepted if it meets one of the following three criteria: (1) ≥ 99.0% protein confidence and ≥ 3 unique peptides at 95% probability, (2) ≥ 99.0% protein confidence, 2 peptides at ≥ 50% probability, and satisfied (1) in another condition, or (3) ≥ 99.0% protein confidence, 1 peptide at ≥ 50% probability, and satisfied (1) in a biological duplicate. Proteins identifications not assigned are manually inspected.

Acknowledgements

We thank M. Maronski and M.O. Scott for technical assistance, S. Scherer, and members of the Balice-Gordon lab for helpful discussions. This work was supported by

grants from the NIH (NS046490 and MH057683) to R.B.-G. and an NIH NRSA (NS056549) to E.G.H.

Figures and Legends

Figure 3.1 Proteins in astrocyte conditioned media are separated based on molecular weight by gel filtration.

(A), UV spectra of eluted protein as astrocyte conditioned media was separated by size exclusion chromatography. Fractions (0.5 ml) were collected at the indicated times. Pooled (B) and individual (C) fractions (2.0 µl) were examined by SDS-Page followed by silver stain analysis.

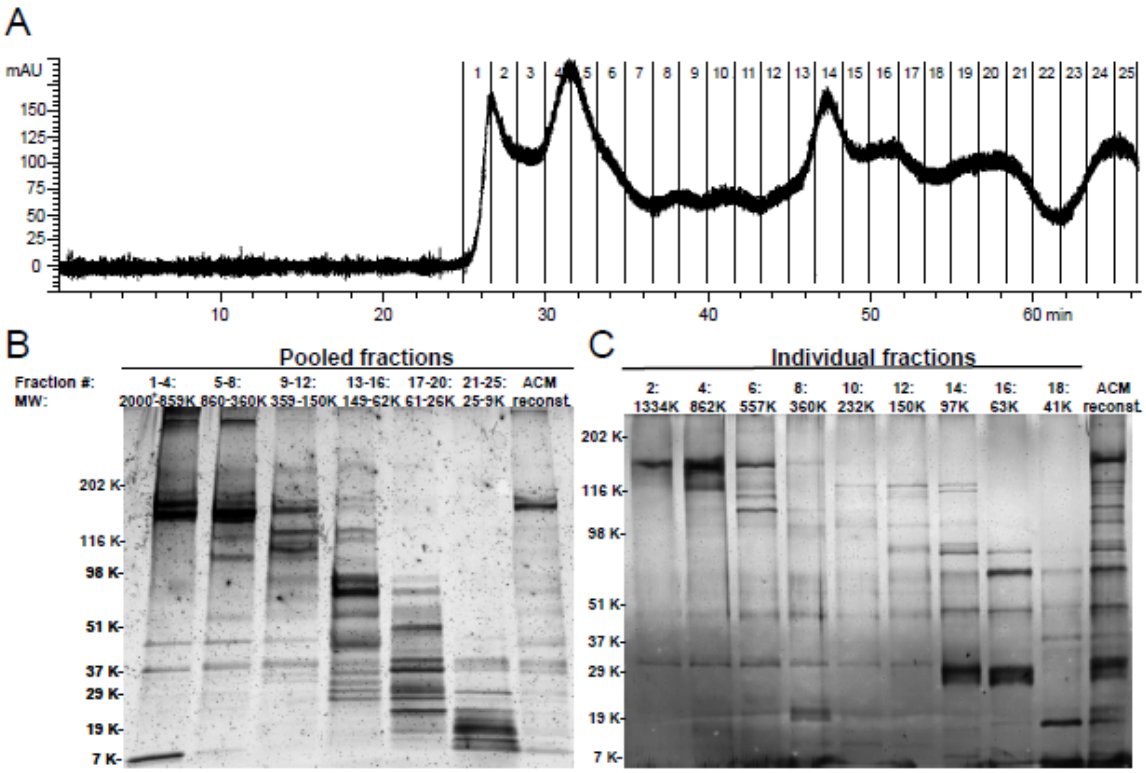
A
mAU
150
125
100
75
50
25
0
1 2 3 4 5 6 7 8 9 10 11 12 13 14 15 16 17 18 19 20 21 22 23 24 25
10
20
30
40
50
60 min
B
Pooled fractions
Fraction #:
MW:
1-4: 2000-858K
5-8: 860-360K
9-12: 359-150K
13-16: 149-62K
17-20: 61-26K
21-25: 25-9K
ACM reconst
202 K-
116 K-
98 K-
51 K-
37 K-
29 K-
19 K-
7 K-
C
Individual fractions
2: 1334K
4: 862K
6: 557K
8: 360K
10: 232K
12: 150K
14: 97K
16: 63K
18: 41K
ACM reconst
202 K-
116 K-
98 K-
51 K-
37 K-
29 K-
19 K-
7 K-

Figure 3.2 Large molecular weight gel filtration fractions increase GABAergic axon length, branching and synaptogenesis.

Hippocampal neurons were cultured alone, with astrocytes, ACM, or pooled gel filtration fractions for 3 days were immunostained at 4 *div* with antibodies against tau (red) and glutamic acid decarboxylase (GAD; green) and vesicular GABA transporter (VGAT, blue). (A), GABAergic axon length, branching, and presynaptic terminal density were significantly increased in neurons cultured with reconstituted ACM (far left) and high molecular weight fractions (middle left) compared to neurons cultured with mid-range molecular weight fractions (middle right) at 4 *div*. GABAergic axon branching was significantly increased in neurons cultured with low molecular weight fractions (far right) compared to neurons cultured with mid-range molecular weight fractions (middle right) at 4 *div*. Areas within white boxes are shown below at higher magnification. Scale bar = 25 (top), 10 (bottom) μm. (B), Quantification of the effect of astrocytes, ACM, reconstituted ACM, or ACM gel filtration fractions on GABAergic axon length (white), branching (black) or presynaptic terminal density (gray). Asterisk indicates significant difference compared to neuron-only cultures ($p < 0.001$).

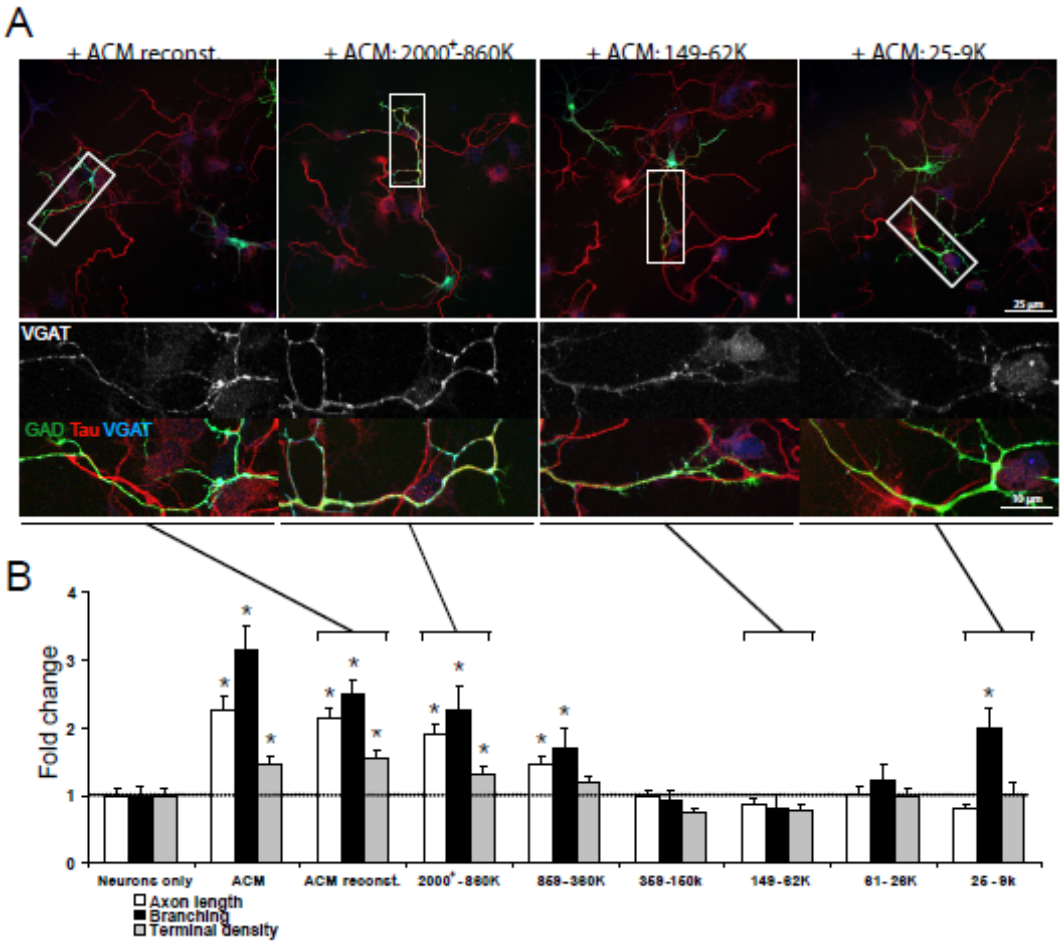
A
+ ACM reconst.
+ ACM: 2000+-860K
+ ACM: 149-62K
+ ACM: 25-9K
VGAT
GAD Tau VGAT
B
Fold change
Neurons only
ACM
ACM reconst.
2000+-860K
859-360K
359-160k
149-62K
61-28K
25-9k
Axon length
Branching
Terminal density

Figure 3.3 Proteomic evaluation of biologically active gel filtration fractions

(A), Mass spectroscopic analysis of bioactive fractions yielded approximately 800 proteins. Using a multi-step computational workflow we identified approximately 225 of these proteins to be secreted. (B), Histogram of the number of secreted proteins present in all fractions analyzed, only in fractions 1-4, or only in fractions 1-8. (C), The number of secreted proteins included identified by IPA to be important in six pathways important in neurite extension and synapse formation.

A

		2000⁺-360 kDa	2000⁺-860 kDa	859-360 kDa	
	Total	All fractions	Fractions 1-4	Fractions 5-8	Not Separated
# of Proteins	772	139	46	48	539
# of Secreted Proteins	223	39	11	30	143

B

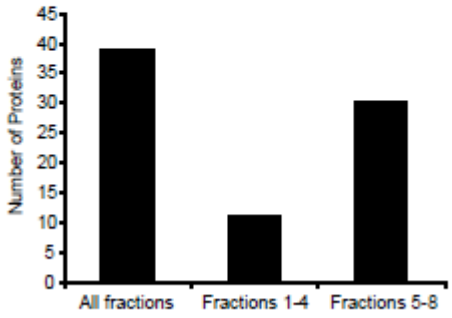

C

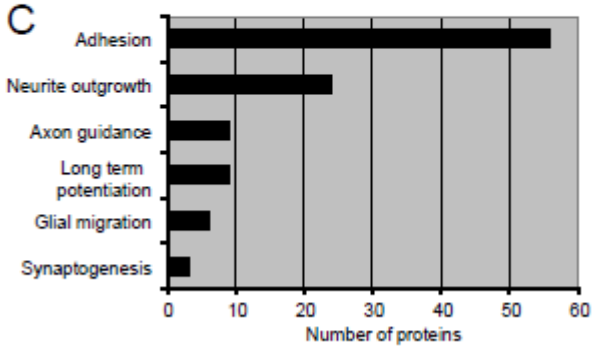

Table 3.1 Potential candidates of secreted astrocyte proteins that may mediate the effects of astrocytes on GABAergic neurons.

#	Cultured Astrocytes	P1 Astrocytes	Enriched in astrocytes	Enriched in vitro	Enriched in vivo	Gene Symbol	Gene Name	Fraction(s)	Norm. spectral counts	Interest	Cultured Astroglia	Cultured Astroglia
1	P	P	TRUE	TRUE	FALSE	Apoe	Apolipoprotein E	All	4.8		13.41	25227
2	P	P	TRUE	TRUE	FALSE	Sparcl1	SPARC-like 1 (Hevin)	-	3.6		11.70	7794
3	P	P	TRUE	FALSE	TRUE	Sparc	SPARC	All	1.5		12.85	15990
4	P	P	FALSE	FALSE	FALSE	Agrn	Agrin	-	1.2		10.75	2214
5	A	P	FALSE	FALSE	TRUE	Fn1	Fibronectin 1	All	5.3		6.18	32
6	A	P	FALSE	FALSE	FALSE	Vcan	Versican	-	4.4		6.26	255
7	A	P	TRUE	FALSE	TRUE	A2m	Alpha-2-macroglobulin	All	2.5		12.78	19331
8	P	P	FALSE	FALSE	FALSE	Chl1	Close homolog of L1	-	1.5		8.39	539
9	P	P	TRUE	TRUE	FALSE	Tgfb2	Transforming growth factor, beta 2	-	0.7		9.83	1162
10			FALSE	FALSE	FALSE	Ncam	Neuronal cell adhesion molecule	-	0.2			
11	A	P	FALSE	FALSE	TRUE	App	Amyloid beta (A4) precursor protein	-	4.5		7.06	32
12	P	P	FALSE	FALSE	TRUE	Csf1	Colony stimulating factor 1	-	4.4		10.62	3600
13	P	A	FALSE	FALSE	TRUE	Anxa1	Annexin A1	-	2.5		12.30	12171
14	A	P	FALSE	TRUE	FALSE	Reln	Reelin	Fractions 5-8	2.0		11.44	118
15	A	P	FALSE	TRUE	FALSE	Vldlr	Very low density lipoprotein receptor	-	1.7		5.85	34
16	P	P	TRUE	TRUE	FALSE	Lrp1	Alpha-2-macroglobulin receptor	All	1.6		9.81	1911
17	P	P	TRUE	FALSE	TRUE	Gpc4	Glypican 4	All	0.8		10.62	2602
18	P	P	TRUE	TRUE	FALSE	Psap	Prosaposin	All	0.4		10.29	1622
19	P	P	FALSE	FALSE	FALSE	Bmp1	Bone morphogenetic protein 1	Fractions 5-8	0.2		7.35	278
20	P	P	TRUE	FALSE	TRUE	Cdh2	N-cadherin	-	0.2		12.32	7999
21	P	P	FALSE	FALSE	FALSE	Sema3b	Semaphorin 3B	-	0.2		6.61	153
22	A	P	TRUE	FALSE	FALSE	Tnc	Tenascin C	All	2.3		5.67	22
23	P	P	FALSE	FALSE	FALSE	Lamc1	Laminin, gamma 1	-	1.7		9.14	498
24	P	P	TRUE	TRUE	FALSE	Bcan	Brevican	Fractions 5-8	1.3		10.72	4381
25	P	P	TRUE	TRUE	FALSE	Ptprz1	Phosphacan	-	0.9		12.01	8952
26	P	P	FALSE	FALSE	FALSE	Gas6	Growth arrest-specific 6	-	0.9		11.64	4089
27	P	P	FALSE	FALSE	FALSE	Igf2r	Insulin-like growth factor 2 receptor	-	0.9		7.39	258
28	P	P	TRUE	FALSE	TRUE	Igfbp2	Insulin-like Growth Factor Binding protein 2	-	0.3		13.32	24485
29	P	P	FALSE	FALSE	TRUE	Bgn	Biglycan	All	4.8		11.38	6889
30	P	P	TRUE	TRUE	FALSE	Clu	Clusterin	All	4.5		13.39	27435
31	P	P	FALSE	FALSE	TRUE	Ctgf	Connective tissue growth factor	Fractions 1-4	2.7		12.96	18808
32	P	P	FALSE	FALSE	TRUE	Fbln5	Fibulin 5	Fractions 5-8	0.6		12.37	14844
33	P	P	TRUE	FALSE	TRUE	Fstl1	Follistatin-like 1	Fractions 1-4	0.6		12.12	9888
34			FALSE	FALSE	FALSE	C3	Complement component C3	Fractions 5-8	0.6			

Legend

Cultured Astrocytes: A= Absent, P= Present

P1 Astrocytes: A= Absent, P= Present

Normalized spectral counts: highest, lowest

Interest: known candidate (both); known candidate (neuron effect or glial); highest interest; high interest; interest

Supplemental Table 1 Mass spectroscopic and computational analyses of biological active ACM gel filtration fractions.

An interactive excel spreadsheet containing all proteins identified by mass spectroscopic analysis.

To be submitted to Nature Medicine

Cellular and synaptic mechanisms of anti-NMDA receptor encephalitis

Ethan G. Hughes[1]*, Xiaoyu Peng[1]*, Amy J. Gleichman[2,3], Meizan Lai[3], Lei Zhou[3], Ryan Tsou[1], Thomas D. Parsons[4], David R. Lynch[2,3], Josep Dalmau[3] and Rita J. Balice-Gordon[1]

*EGH and XP contributed equally.

[1]Dept. of Neuroscience and [2]Neurology, University of Pennsylvania School of Medicine,

[3]Department of Pediatrics, Children's Hospital of Philadelphia

[4]Dept. of Clinical Studies – New Bolton Center, University of Pennsylvania School of Veterinary Medicine, Philadelphia, PA

Abstract / Intro / Methods / Figures: 247 / 397 / 1645 / 5

Supplemental Information: 8 Figures

Key Words: Autoimmune, encephalitis, NMDA receptor, paraneoplastic, antibodies

Address correspondence to: Rita J. Balice-Gordon, Ph.D., Professor of Neuroscience, Dept. of Neuroscience, University of Pennsylvania School of Medicine, 215 Stemmler Hall, Philadelphia, PA 19104-6074. (215) 898-1037; FAX (215) 573-9122, rbaliceg@mail.med.upenn.edu

Abstract

Autoimmunity to synaptic proteins is the cause of well known disorders of neuromuscular transmission, such as myasthenia gravis and Lambert-Eaton syndrome, but it is much less known as cause of central nervous system disorders. We recently described a severe, potentially lethal, but treatment responsive encephalitis associated with autoantibodies to the N-terminal extracellular domain of the NR1 subunit of the N-methyl-D-aspartate (NMDA) receptor. This disorder predominates in young women and children who develop a predictable set of symptoms, including prominent psychosis, bizarre behavior, and memory deficits, and frequently have an underlying tumor (mostly ovarian teratoma) that expresses NMDA receptors. Symptoms often respond to immunotherapy or tumor removal, suggesting an immune-mediated pathogenesis. Here we demonstrate, using *in vitro* studies, that patients' antibodies cause a decrease of surface density and synaptic localization of NMDA receptor clusters via antibody mediated capping and internalization. The magnitude of these changes correlates with antibody titer, and the effects are reversed when antibody titer is reduced. Moreover, patients' antibodies decrease NMDA but not AMPA receptor mediated synaptic currents, consistent with a selective loss of surface NMDA receptor clusters. We also demonstrate using *in vivo* studies that NMDA receptor cluster density is dramatically reduced in the hippocampus of rats infused with patients' antibodies as well as in the brain of autopsied patients with this disorder. These studies establish the cellular mechanisms by which antibodies of patients with anti-NMDA receptor encephalitis alter NMDA receptor

density, localization and function, which are critical for learning, memory and other behaviors.

Introduction

Synaptic plasticity is thought to underlie mechanisms of memory, learning, and cognition. Central to these neurological functions is the proper synaptic localization and trafficking of the excitatory glutamate NMDA and AMPA receptors. The roles of these receptors at the synaptic and cellular levels have been established through animal models in which the receptors have been genetically or pharmacologically altered (Jentsch and Roth, 1999; Mouri et al., 2007). In humans the role of these receptors in memory, learning, cognition and psychosis comes from more indirect approaches, such as pharmacological trials (e.g., NMDA receptor antagonists causing psychosis), and analysis of brain tissue from patients with Alzheimer's disease or schizophrenia in which several molecular pathways causing a downstream alteration of glutamate receptors are affected. We recently identified a disorder in which the NR1 subunit of the NMDA receptor is directly targeted by autoantibodies (Dalmau et al., 2007; Dalmau et al., 2008). Patients develop prominent psychiatric and behavioral symptoms, rapid memory loss, seizures, abnormal movements (dyskinesias), hypoventilation, and autonomic instability. In two series comprising 181 cases, there was a strong female predominance (ratio 8.5:1.5) and the median age of the patients was 19 years (23 months-75 years; 40% children). Most patients presented with bizarre behavior, agitation, delusions, hallucinations and catatonia, leading to admissions to psychiatric centers for suspected psychosis or schizophrenia. In 55% of the adults (less frequently in children), the disorder appears to be triggered by the presence of a tumor, mostly an ovarian teratoma that contains nervous

system tissue and expresses NMDA receptors. Despite the severity of the symptoms 75% of patients recover after receiving immunotherapy and, when appropriate, tumor removal, and 25% are left with memory and cognitive deficits, impulsiveness, inappropriate behavior, or, rarely, die of the disorder. The autoantibodies are present in patients' serum and cerebrospinal fluid (CSF), the latter usually showing intrathecal synthesis and high antibody concentration. All patients' antibodies recognize the N-terminal extracellular domain (amino-acid residues 25-380) of NR1, suggesting an antibody-mediated pathogenesis. We previously showed that patients' antibodies cause a decrease in surface NMDA receptor cluster density, but the underlying mechanisms were unexplored. Here we report *in vitro* and *in vivo* studies that establish the cellular mechanisms by which patients' antibodies lead to a reduction in surface and synaptic NMDA receptor density and function, likely underlying the learning, memory and other behavioral deficits observed in patients with anti-NMDA receptor encephalitis.

Results

Patients' antibodies reduce surface NMDA receptor clusters and protein in a titer dependent fashion

Rat hippocampal neurons were cultured for 14 days were treated 1 day with CSF or purified IgG containing anti-NR1 antibodies determined by ELISA (Dalmau et al., 2007) from 10 patients, followed by immunohistochemical and Western blot analyses of surface and total NR1 protein. Patients' antibodies decreased NR1 or NMDA receptor surface and total cluster density in a titer dependent fashion, compared to CSF or IgG from control patients (Fig. 1A, C). Similar results were obtained with Western blot analyses of cell surface and total NR1 protein (Fig. 1B, D). Moreover, Western blot analyses of the effect of patients' antibodies on NR2 subunits (which assemble with NR1 to form NMDA receptors) showed that patients' antibodies decreased surface and total NR2A and NR2B proteins in a titer dependent fashion (Supp. Fig. 1).

To determine whether the effects of patients' antibodies correlate with the change of titers during the course of the disease, hippocampal neurons were cultured with CSF samples obtained at two different time points of the disease of three patients. The initial CSF was obtained at the time of symptom presentation and the second sample during symptom improvement in two patients and symptom worsening in the third patient. In the first two patients the CSF obtained at symptom presentation had a higher NR1 antibody titer than the CSF obtained during symptom improvement, while in the third patient the

CSF obtained during symptom worsening had a higher antibody titer than the CSF obtained at symptom presentation. In all 3 patients, the CSF with higher NR1 antibody titer decreased NMDA receptor surface and total cluster density (or total NMDA receptor protein measured by Western blot) (Fig. 1E, F) to a greater extent than the CSF with the lower titer. Together, these results show that NR1 antibodies from patients with anti-NMDA receptor encephalitis decrease NMDAR surface cluster density and protein in a titer-dependent manner and that in each individual the effects of the antibodies vary with the change of titers during the course of the disease.

Patients' antibodies reversibly reduce synaptic NMDA receptor clusters without affecting the number of synapses and other synaptic components

Because patient antibodies decreased overall NMDA receptor surface cluster density and protein, we determined whether the antibodies also affected NMDA receptor synaptic localization, the number of synapses, and other synaptic components. Hippocampal neurons were cultured with CSF or purified IgG for 3 or 7 days, followed by immunostaining or Western blot analysis of NR1 and synaptic components such as presynaptic VGlut, postsynaptic PSD-95, AMPA receptor subunits GluR1 and GluR2, and GABA receptors. Patients' antibodies did not affect the number of excitatory synapses compared to controls (Fig. 2A, B). Moreover, patients' antibodies did not affect the density of postsynaptic PSD-95, GluR1, GluR2 or GABA receptor clusters, or the surface or total amount of these proteins (Supp. Fig. 2), dendritic branching, dendritic

spine density (Supp. Fig. 3, 4), or cell survival (Supp. Fig. 8). These results show that patient antibodies specifically affect NMDA receptors without affecting AMPA or GABA receptors, other synaptic proteins, the number of excitatory synapses, and neuronal morphology or viability.

While the overall structural integrity of excitatory neurons and synapses was not affected, we found that patients' antibodies dramatically reduced the synaptic localization of NMDA receptor clusters compared to controls (Fig. 2A, C), consistent with the overall decrease in surface NMDA receptor cluster density (Fig. 1). Since patients who receive early treatment often fully recover, we investigated whether the antibody-mediated decrease in NMDA receptor synaptic localization was reversible. Patient antibodies were removed from the culture medium after 3 days of treatment and neurons were cultured for 4 additional days. The density of synaptically localized NMDA receptor clusters returned to baseline levels 4 days after patient antibodies were removed (Fig. 2A, C). These results show that patients' antibodies cause a specific loss of NMDA receptors from excitatory synapses and that this loss is reversed after antibody removal.

Patients' antibodies selectively decrease synaptic NMDA currents

We next assessed the effects of patient antibodies on NMDA receptor function using whole-cell patch recordings of miniature excitatory postsynaptic currents (mEPSCs), which consist of a fast AMPA receptor-mediated current and a slow NMDA receptor current. Neurons were treated for 1 day with patient or control CSF and

spontaneous inward currents were recorded at -70 mV in a 0 Mg^{2+} extracellular solution to unmask synaptic NMDA receptor-mediated mEPSCs. CNQX was used to block AMPA receptor-mediated mEPSCs and APV was used to block NMDA receptor-mediated mEPSCs (Fig. 3A).

Patient antibody treatment did not affect mEPSC frequency or amplitude (Supp. Fig. 4), consistent with structural analyses that showed that patients' antibodies do not affect the number of excitatory synapses (mEPSC frequency) or the number of postsynaptic sites containing AMPA receptors (mEPSC amplitude).

In neurons treated for 1 day with CSF from control patients, CNQX blocked large, fast AMPA receptor mediated currents, revealing small, slower NMDA receptor mediated currents that were completely blocked by APV (Fig. 3A, left). In contrast, in neurons treated for 1 day with patient CSF, CNQX blocked all mEPSCs, and no further reduction was observed after APV (Fig. 3A, right). This result shows that there is very little NMDA receptor mediated current in neurons treated with patient antibodies.

To quantify the reduction in synaptic NMDA receptor mediated currents, currents were examined before and after APV application. In neurons treated for 1 day with CSF from control patients, APV reduced or abolished the late, slow NMDA receptor mediated component of the mEPSC (Fig. 3B, left; 3C, left). In contrast, in neurons treated for 1 day with patient CSF, APV application did not further reduce the NMDA receptor mediated component of the mEPSC (Fig. 3B, right; 3C, left). No difference was observed in the peak AMPA receptor mediated component of the mEPSC (Fig. 3C,

right). These results show that patients' antibodies specifically decrease synaptic NMDA receptor mediated currents and do not affect AMPA receptor mediated currents, consistent with the specific loss of surface, synaptically localized NMDA receptor clusters.

Patients' antibodies crosslink and internalize NMDA receptors

We next determined the mechanism by which patient antibodies decrease surface NMDA receptor cluster density and protein. The Fc IgG domain was enzymatically removed from patients' antibodies to generate Fab fragments. These Fab fragments, like intact patient IgG, bound to surface NR1 clusters identified with commercial anti-NR1 immunostaining (Supp. Fig. 5). Neurons were treated for 1 day with patients' antibody Fab fragments had the same NMDA receptor cluster density and surface protein as neurons treated with control IgG (Fig. 4A, B). In contrast, neurons treated for 1 day with patients' Fab fragments and anti-Fab secondary antibodies (linking two Fab fragments in a confirmation similar to unmodified patients' antibodies) had significantly lower NMDA receptor cluster density and surface protein as compared to neurons treated with control IgG (Fig. 4A, B). These results show that patients' antibodies mediate the loss of surface NMDA receptors in part by binding to, capping and crosslinking NMDA receptors, resulting in their internalization (Fig. 4C).

Patients' antibodies decrease NMDA receptor cluster density and protein in rodent and human hippocampus *in vivo*

Our results show that, *in vitro*, patients' anti-NR1 antibodies lead to a selective loss of surface NMDA receptor clusters and their function, without loss of other synaptic components or neuron viability. To determine the effects of patients' antibodies *in vivo*, CSF from patients with high titers of NR1 antibodies, or control CSF from individuals without NR1 antibodies, was infused directly into the hippocampus of adult rats for two weeks, followed by immunostaining for human IgG to examine the diffusion and deposition of patients' antibodies, immunostaining and Western blot analysis of NMDA receptors and other synaptic components to determine the effects of patients antibodies, and assessment of cell death using the TUNEL assay. Patient antibodies colocalized with NMDA receptor clusters *in vivo* as *in vitro* (Supp. Fig. 7). Moreover, infused patient IgG, but not control IgG, was found bound to rat hippocampus in a predictable pattern that was dependent on NMDA receptor density (e.g., high density in proximal dendrites of dentate gyrus, data not shown). This pattern was similar to the direct immunostaining of bound IgG reported in the autopsy of two patients with anti-NMDA receptor encephalitis (Dalmau et al., 2007).

Patients' CSF infusion into rat hippocampus caused deposition of human IgG in the hippocampus (Supp. Fig. 8). Moreover, in regions where human IgG was deposited, there was a significant decrease in NMDA receptor cluster density and intensity of NR1 immunostaining without affecting the number of synapses, the density of other synaptic

components (Fig. 5A-E; Supp. Fig. 8) or cell death (Supp. Fig. 8). The magnitude of the effects of each patient's CSF correlated with the titer of NR1 antibodies infused into rat brains (Fig. 5B), as demonstrated in *in vitro* studies (Fig. 1). Furthermore, the total amount of NR1 protein was reduced in rodent hippocampus infused with patient compared to control CSF (Fig. 5C).

To investigate whether NMDA receptor cluster density is reduced in the brains of patients with anti-NMDA receptor antibodies, paraffin-embedded sections of the hippocampus of two patients with anti-NMDA receptor encephalitis and the hippocampus of three age-matched, anti-NR1 negative, neurologically normal individuals were immunostained with anti-NR1 antibodies. The density of NMDA receptor clusters was substantially decreased in patients' hippocampus compared to controls (Fig. 5F-H). Moreover, deposits of human IgG, but not complement, were identified in some of the regions with reduced NMDA receptor clusters (data not shown). These data show that patient anti-NMDA receptor antibodies reduce NMDA receptor cluster in rodent neurons *in vitro* and *in vivo* as well as in patient brain.

Discussion

Anti-NMDA receptor encephalitis is a recently described disorder that is associated with antibodies against the NR1 subunit of the NMDA receptor and results in a well defined set of symptoms. Our previous studies noted that the resulting syndrome resembled the phenotype of animals in which the NMDA receptor function had been attenuated pharmacologically or genetically, suggesting that patients' antibodies decreased NMDA receptor levels. We now demonstrate using *in vitro* and *in vivo* studies that patients' antibodies decrease the surface density and synaptic localization of NMDA receptor clusters via antibody mediated capping and internalization, independent of the presence of complement, and without affecting other synaptic proteins, AMPA receptors or synapse density. The magnitude of these changes depends on antibody titer, and the effects are reversible when the antibody titer is reduced. Moreover, patients' NR1 antibodies decrease NMDA, but not AMPA, receptor mediated synaptic currents. Thus the selective loss of surface clusters abolishes NMDA receptor mediated synaptic currents. These findings indicate that NR1 antibodies from patients with anti-NMDA receptor encephalitis decrease glutamatergic synaptic function without a substantial loss of synapses.

This reversible loss of NMDA receptors, and the resulting synaptic dysfunction, may underlie the deficits of memory, behavior and cognition that are hallmarks of anti-NMDA receptor encephalitis (Dalmau et al., 2008). Indeed, a remarkable feature of this disorder is the frequent reversibility of symptoms, even when these are severe and

protracted. Previous studies showed a correlation between clinical outcome and antibody titer, which is usually higher in CSF than serum due to intrathecal antibody synthesis. The work we present here demonstrates that the effect of patients' CSF on surface NMDA receptors is correlated with the change of antibody titers and symptom severity during the course of the disease. When comparing different patients, a similar correlation was found between CSF antibody titers and the intensity of effects on NMDA receptors, but there was inter-patient variability between antibody titers and severity of patients' symptoms (data not shown). This variability is common to most autoimmune disorders, and is likely due to patient-specific related factors (e.g., age, fever, poorly controlled seizures) and the fact that analysis of CSF provides the closest, though imperfect, assessment of the immune response within the brain. In the current study, analysis of the hippocampus of two patients who died of this disorder showed a substantial decrease of NMDA receptor levels compared with the hippocampus of three age-matched, neurologically normal individuals. This decrease of NMDA receptors was comparable to that observed in rats infused with patients' antibodies. Moreover, we previously reported that patients' hippocampus showed deposits of IgG and absence of complement (Dalmau et al., 2007), consistent with the complement-independent antibody effects demonstrated in *in vitro* studies.

In the peripheral nervous system, immune-mediated disruption of synaptic structure and function results in well known disorders of neuromuscular transmission such as myasthenia gravis and Lambert-Eaton syndrome (Sanders, 2002; Conti-Fine et

al., 2006). Anti-NMDA receptor encephalitis provides a new model of central nervous system synaptic autoimmunity, antigenically different but mechanistically similar to Lambert-Eaton syndrome in which autoantibodies, but not monovalent Fab fragments, crosslink and internalize voltage-gated calcium channels, without complement activation. Both disorders may occur as paraneoplastic manifestation of a tumor that expresses neuronal proteins (e.g., small-cell lung cancer in Lambert-Eaton) or contains ectopic nervous tissue (e.g., teratoma in anti-NMDA receptor encephalitis). Moreover, in both disorders the immunological trigger of cases without tumor association is unknown, although a genetic predisposition to autoimmunity has been demonstrated or suggested. Although both disorders respond to immunotherapy and when appropriate tumor removal, the response of anti-NMDA receptor encephalitis is slower and less predictable, particularly in cases with delayed diagnosis or without a detectable tumor. These patients usually have persistently high CSF antibody titers, despite the effectiveness of plasma exchange or IVIg in reducing serum antibody titers. In these cases, symptoms frequently respond to cyclophosphamide, which crosses the blood-brain barrier, or rituximab, which depletes memory B-cells. As postulated in other disorders, these cells are able to cross the blood-brain-barrier, and are believed to undergo re-stimulation, antigen-driven affinity maturation, clonal expansion, and differentiation into antibody-secreting plasma cells.

NMDA receptor dysfunction has been implicated in several other cognitive disorders, including schizophrenia (Olney and Farber, 1995). Studies investigating the effects of phencyclidine and ketamine (noncompetitive antagonists of NMDA receptors)

in human subjects show these drugs induce behaviors similar to the positive and negative symptoms of schizophrenia, along with repetitive orofacial and limb movements, autonomic instability, and seizures (Luby et al., 1959; Krystal et al., 1994). In rodents, drugs that antagonize NMDA receptor function induce cataleptic freeze, and locomotor and stereotype behaviors, consistent with schizophrenia-like manifestations (Jentsch and Roth, 1999; Mouri et al., 2007). Furthermore, mice with decreased expression of NR1 have similar behavioral deficits, while mice lacking NR1 develop breathing problems and die in the perinatal period (Mohn et al., 1999). Interestingly, most patients with anti-NMDA receptor encephalitis present with acute schizophrenia-like symptoms and are admitted to psychiatric institutions before they develop catatonia, catalepsy, stereotyped movement disorders, and frequent autonomic instability and hypoventilation. The striking similarity between these phenotypes, the effect of patients' antibodies resulting in a dramatic decrease of surface NMDA receptor clusters and function, and the reduced levels of NMDA receptors in autopsied patients, support an antibody-mediated pathogenesis of anti-NMDA receptor encephalitis. The psychosis and cognitive and behavioral deficits in patients with anti-NMDA receptor encephalitis most likely result from NMDA receptor hypofunction, directly and indirectly affecting synapse and circuit structure and function in regions that bind anti-NR1 autoantibodies. Thus the findings we report here also support the hypothesis that NMDA receptor hypofunction underlies many manifestations of schizophrenia. Future studies will focus on the circuit-level dysfunction caused by patient antibodies in hippocampus and other brain regions, to

begin to connect synaptic and circuit dysfunction with the behavioral abnormalities that are hallmarks of this disorder.

Materials and Methods

Preparation of patient and control CSF and IgG

Patient or control cerebrospinal fluid (CSF) was collected and filtered using protein A/G sepharose columns. CSF was diluted 1:15-50 to treat neurons *in vitro*. In some experiments, IgG purified from serum was used to treat neurons (Fig. 1D, F; Fig. 4). Both patient CSF and patient IgG decreased surface and total NMDA receptors to the same extent (Supp. Fig. 6). Furthermore, the effects of patient CSF on NMDA receptor cluster density were not mediated by complement, because heat-inactivated patient CSF decreased NMDAR cluster density and localization to a similar extent as non-heat inactivated patient CSF (Supp. Fig. 6). Briefly, 10 ml of patient or control serum were incubated with a 5 ml column of protein A/G Sepharose beads (50:50) for 30 min. on an orbital shaker at 4 °C. After elution IgG was added to a bio-spin chromatography column (Bio-Rad) followed by 3 washes with PBS, eluted with 100 mM glycine, pH = 2.5 and neutralized with Tris-HCl, pH = 8.0, dialyzed against PBS and concentrated to stock solutions of 20 mg/ml and stored at -80 °C. IgG concentration (~1mg / ml) and pH (7.4) were adjusted prior to use. Each CSF or IgG preparation was tested for antibody reactivity by staining mouse or rat brain sections or HEK cells expressing NR1/NR2 heteromers of the NMDAR as previously described (Dalmau et al., 2007; Dalmau et al., 2008).

Cell culture and patient antibody treatment

Primary rat hippocampal neuron and astrocyte cultures were prepared from embryonic day 18-19 (Goslin et al., 1988). Briefly, hippocampi were in Ca^{2+} free HBSS containing 1% papain for 20 min., triturated in Basal Media Eagle (BME; Invitrogen) supplemented with B-27 (Life Technology) and plated at 100,000 or 400,000 (for biotinylation) cells per ml in Neural Basal (NB; Life Technologies) supplemented with 10% FBS (Hyclone), B-27, 1% penicillin and streptomycin (Life Technologies) and 1% L-Glutamine (Life Technologies) on poly-L-lysine coated (Sigma) coverslips in 24-well plates. Culture media was changed to NB supplemented with B27 at 4 *div*. Cells were maintained at 37 °C, 5% CO_2, 95% humidity; medium was changed weekly.

Immunostaining for pre- and postsynaptic components

To stain surface NMDAR clusters, control or treated neurons were washed in NB plus B27 and were incubated with patient CSF containing anti-NR1 antibodies for 30 min., washed and incubated with fluorescently conjugated anti-human secondary antibodies for 30 min., and washed in PBS. Neurons were then fixed in 4% paraformaldehyde, 4% sucrose in PBS, pH = 7.4 for 15 min., permeabilized with cold 0.25% Triton X-100 for 5 min., and blocked in 5% normal goat serum (Invitrogen) for 1 hour at RT. Additional immunostaining was performed with various combinations of primary antibodies: to label glutamate receptors, anti-NR1 (1:1000; Chemicon), anti-GluR1 (1:10; CalBioChem) or anti-GluR2/3 (1:100; Chemicon); to label dendrites, chicken anti-MAP2 (1:5000; AbCam); to label presynaptic terminals, mouse anti-SV2

(1:200; DHSB); guinea pig anti-VGLUT 1 (1:5000; Chemicon), or mouse anti-Bassoon (1:400; Stressgen Bioreagents). Antibodies were visualized after staining with the appropriate fluorescently conjugated secondary antibodies (1:200, Jackson ImmunoResearch).

Confocal imaging, image analysis and statistical analysis

For all experiments, 6-12 randomly selected pyramidal neurons, identified by morphology (Elmariah et al., 2004; Elmariah et al., 2005) in each condition were imaged using confocal microscopy (Leica TCS 4D system) on each of 2-3 coverslips in 3-5 independent experiments**.** Images were thresholded automatically using an iterative thresholding technique (Bergsman et al., 2006), and the number and area of individual immunostained pre- or postsynaptic clusters were determined using interactive software (custom-written ImageJ macros). Clusters with more than 20% pixel overlap of pre- and postsynaptic markers were considered colocalized and thus synaptic. Cluster density was compared among conditions using the Kruskal-Wallis nonparametric ANOVA test followed by Dunn's pairwise multiple comparison test, unless otherwise indicated. All values are presented as mean ± s.e.m.

Biotinylation of surface proteins and analysis by Western blot

Neurons were treated with 1 μg – 1 mg/ml IgG for 1 day, washed with PBS supplemented with 0.1 mM $CaCl_2$ and 1 mM $MgCl_2$ (rinsing buffer) and incubated for 30

min. at 4 °C with 1 mg/ml Sulfo-NHS-Biotin (Thermo Scientific) in rinsing buffer. Neurons were then washed with rinsing buffer + 100 mM glycine (quenching buffer), incubated in quenching buffer for 30 minutes at 4°C to quench excess biotin, then lysed in RIPA buffer (150 mM NaCl, 1 mM EDTA, 100 mM Tris HCl, 1% Triton X-100, 1% sodium deoxycholate, 0.1% SDS, pH 7.4, supplemented with 1:500 protease inhibitor cocktail III, Calbiochem) at 4 °C for 1 hour. Lysates were cleared of debris by centrifugation at 12400 x g for 20 min. An aliquot of the remaining supernatant was taken for the lysate fraction, and a second aliquot was incubated with avidin-linked agarose beads (Immobilized Monomeric Avidin, Thermo Scientific) overnight at 4 °C. After centrifugation, the supernatant was removed and the beads (surface fraction) were washed 1X RIPA buffer, 2X high-salt wash buffer (500 mM NaCl, 5 mM EDTA, 50 mM Tris, 0.1% Triton X-100, pH 7.5), and 1X no-salt wash buffer (50 mM Tris, pH 7.5). The surface fraction was eluted from the beads with 2X sample buffer and proteins separated on an 8% gel using SDS-PAGE. Samples were transferred to nitrocellulose membranes and probed for antibodies against NR1 (1:1000, 556308, BD Pharmingen), NR2A (1:1000, AB1555, Millipore; 1:500, MAB5216, Millipore; 1:500, A6473, Invitrogen), NR2B (1:1000, AGC-003, Alomone; 1:500, 06-600, Upstate), $GABA_AR\alpha1$ (1:1000, 06-868, Upstate), $GABA_AR\alpha2$ (1:500, AB5984, Chemicon), GluR 2/3 (1:1000, 07-598, Upstate), PSD-95 (1:1000, 610496, BD Pharmingen), and actin (1:2000, A2066, Sigma). Actin and $GABA_ARs$ were used as loading controls for total and surface fractions, respectively. Blots were incubated with HRP-conjugated goat anti-mouse or goat anti-

rabbit secondary antibodies (1:3000, Cell Signaling), and signals were visualized using chemiluminescence (SuperSignal Chemiluminescent Substrate, Thermo Scientific). All quantified films were in the linear range of exposure, were digitally scanned and signals quantified using NIH ImageJ.

Whole cell electrophysiological recordings of synaptic NMDA and AMPA receptor mediated currents

Whole cell voltage clamp recordings were performed as previously described (Elmariah et al., 2004; Elmariah et al., 2005) from 14 – 21 div pyramidal neurons treated for 24-48 hours with patient CSF containing anti-NR1 antibodies, control CSF or left untreated. Briefly, neurons were incubated in extracellular physiology solution without Mg^{2+} (in mM: 119 NaCl, 5 KCl, 2 $CaCl_2$, 30 Glucose, 10 HEPES, pH = 7.4). Voltage-clamp recordings were made at RT (22-25 °C) using glass microelectrodes (resistance 4-6 MΩ) filled with a Cesium substituted intracellular solution (in mM: 100 Cesium gluconate, 0.2 EGTA, 5 MgCl2, 2 ATP, 0.3 GTP, 40 HEPES, pH = 7.2). Pipette voltage offset was neutralized before the formation of a gigaohm seal. Membrane resistance, series resistance, and membrane capacitance were determined from current transients elicited by a 5 mV depolarizing step from a holding potential of -80 mV, using the whole cell application of HEKA software. Criteria for cell inclusion in the data set included a series resistance ≤ 30 MΩ and stability throughout the recording period. Currents were amplified, low-pass filtered at 2.5 kHz, and sampled at 5 Hz using HEKA software.

Miniature excitatory spontaneous currents (mEPSCs) were recorded at -70mV in the presence of TTX (1 μM) and Picrotoxin (10 μM). APV (50 μM) and CNQX (10 μM) were bath applied to block NMDAR and AMPAR mediated currents respectively. mEPSC events were detected and analyzed using MiniAnalysis (Synaptosoft, Leonia, NY), which employs a threshold-based event-detection algorithm. NMDAR and AMPAR components of mEPSCs were separated temporally by their distinct kinetics (Hestrin et al., 1990; Watt et al., 2000; Yang et al., 2003). The amplitude of the NMDAR mediated current was determined in a window between 15 and 25 ms after the peak of the AMPAR mediated component, which has a fast, < 1 ms rise time. All values are presented as mean ± s.e.m.

Fab fragments preparation and treatment

Fab fragments were prepared from serum IgG using a kit according to the manufacturer's directions (Fab preparation kit, Pierce Protein Research Products, Thermo Scientific). Briefly, serum IgG was digested for 2-4 hours at 37 °C with 1% (w/w) papain pH= 7.0 with 0.01 M cysteine, resulting in cleavage into Fab and Fc fragments. Fab fragments were then isolated by chromatography and concentration determined by absorption at 280 nm. Fab fragments were used to treat neurons at a concentration of 4 μg/ml. Control experiments showed that incubating neuron with patient Fab fragments for 30 min. resulted in surface staining of NR1 clusters (Supp. Fig. 5).

Alzet mini-pump placement, IgG infusion and sectioning

Young adult rats (6-8 weeks old) were anesthetized and a cannula placed into the left lateral ventricle using predetermined coordinates (AP 0.6 mm, lateral 1.6 mm to bregma and horizontal 2.0 mm to the dura mater). The cannula was attached to a head probe mounted to the skull. The cannula was attached to an Alzet minipump (Alzet brain infusion kit #3, pump model 2002) placed subcutaneously on the back and attached to the head probe via sterile tubing. Patient or control CSF was then delivered at a rate of 0.5 µl / hr for 2 weeks. Rats were then euthanized, brain tissue harvested, immersion fixed in 4% paraformaldehyde in PBS, pH = 7.4 for 15 min., cryoprotected in 30% sucruose in PBS, pH = 7.4 overnight at 4 °C, frozen in isopentane cooled in dry ice, and frozen sections obtained at 20 µm. Sections were immunostained using one or more of the primary and fluorescent secondary antibodies, confocally imaged and images thresholded and analyzed as described above.

Acknowledgements

We thank Drs. Marc Dichter, Myrna Rosenfeld and Steven Scherer for helpful discussions, Marion O. Scott and Margaret Maronski for technical assistance. This work was supported by grants from the NIH (NS046490 and MH057683 to R.B.-G.; CA89054 to J.D., NRSA NS056549 to E.G.H. and NRSA MH083395 to A.J.G.).

Figure Legends

Figure 4.1 Patient antibodies reduce surface NMDA receptor clusters and protein in a titer dependent fashion.

(a) Hippocampal neurons immunostained for surface, total NMDA receptor clusters and the presynaptic terminal marker Bassoon. Treatment with patient CSF for 1 day reduces the density of surface and total NMDA receptors without affecting presynaptic terminal density. Scale bar = 10 μm. **(b)** Immunoblots of surface and total NMDA receptor protein. Treatment with patient IgG (isolated from serum) reduces surface as well as total NMDA receptor protein. $GABA_A\alpha 1$ or actin are loading controls for the surface and total protein, respectively. Control NR1 levels have been overexposed in this image to visualize patient treated NR1 bands. **(c)** Quantification of surface (left) and total (right) NMDA receptor clusters after treatment with CSF from several patients with different antibody titers. CSF from patients with higher titer decrease surface and total NMDA receptor clusters to a greater extent. **(d)** Quantification of surface (left) and total (right) NMDA receptor protein after treatment with IgG from the same patient at two timepoints with different antibody titer. IgG isolated from patients with a higher antibody titer decreased surface and total NMDAR protein to a greater extent than IgG isolated from the same patient when a lower antibody titer was present.

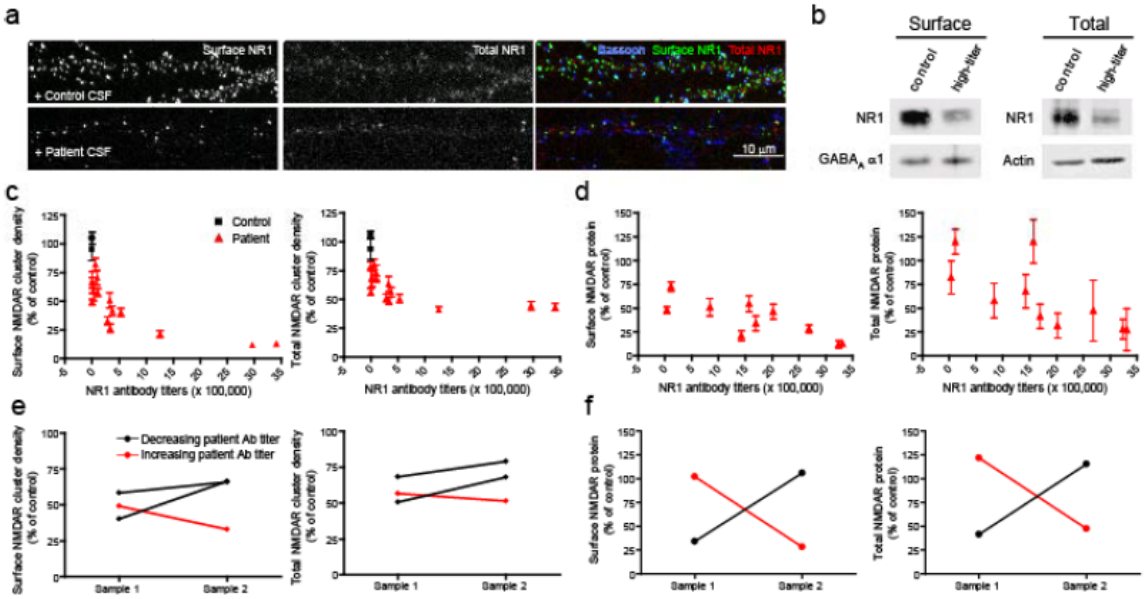
a
Surface NR1
Total NR1
Bassoon Surface NR1 Total NR1
+ Control CSF
+ Patient CSF
10 µm
b
Surface
Total
control
high-titer
NR1
GABA$_A$ α1
Actin
c
Control
Patient
Surface NMDAR cluster density (% of control)
Total NMDAR cluster density (% of control)
NR1 antibody titers (x 100,000)
d
Surface NMDAR protein (% of control)
Total NMDAR protein (% of control)
NR1 antibody titers (x 100,000)
e
Decreasing patient Ab titer
Increasing patient Ab titer
Surface NMDAR cluster density (% of control)
Total NMDAR cluster density (% of control)
Sample 1
Sample 2
f
Surface NMDAR protein (% of control)
Total NMDAR protein (% of control)
Sample 1
Sample 2

Figure 4.2 Patient antibodies reversibly reduce synaptic NMDA receptor clusters without affecting the number of synapses.

(a) Hippocampal neurons immunostained for total NMDA receptor clusters, a presynaptic glutamatergic terminal protein, VGlut, and a postsynaptic protein localized to glutamatergic synaspes, PSD-95. Treatment with patient CSF for 1 day reduces the density of synaptic NMDA receptor clusters without affecting the number of excitatory synapses. After removal of patient CSF, the proportion of NMDA receptor clusters localized to synapses returns to baseline. Scale bar = 10 μm. **(b)** Quantification of the colocalization of pre- and postsynaptic proteins at excitatory synapses. **(c)** Quantification of the density of NMDA receptor clusters at excitatory synapses (synaptic NR1). Asterisk indicates significant difference (Student's t test, $p < 0.001$).

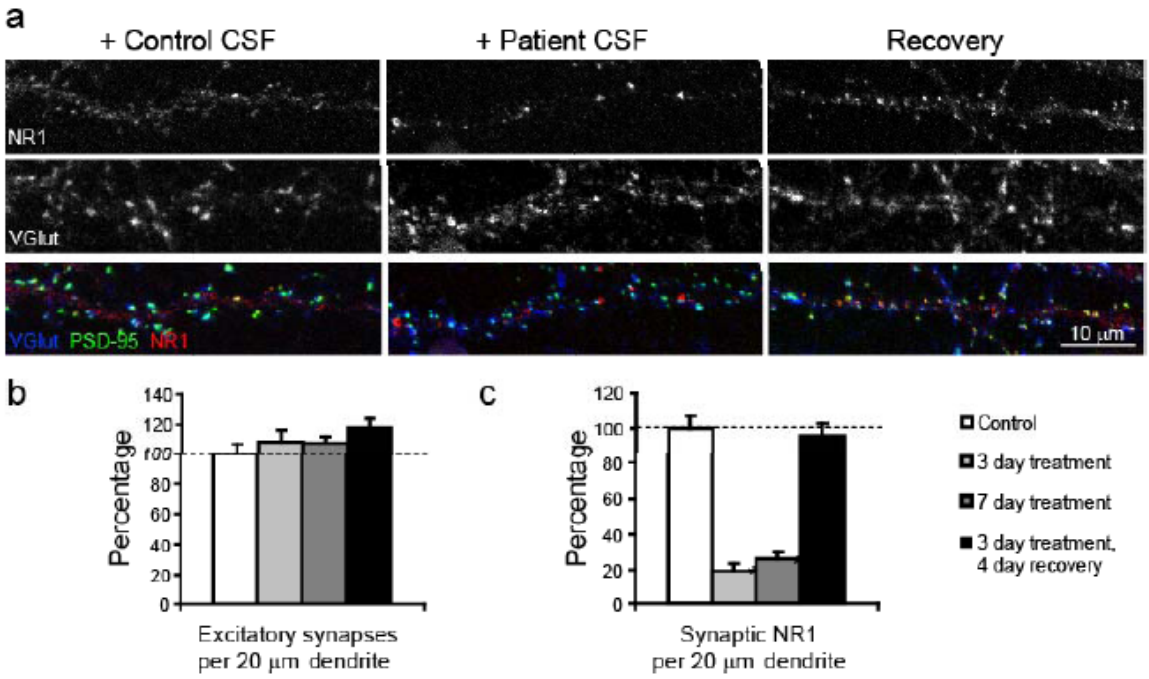
a
+ Control CSF
+ Patient CSF
Recovery
NR1
VGlut
VGlut PSD-95 NR1
10 µm
b
Percentage
140
120
100
80
60
40
20
0
Excitatory synapses
per 20 µm dendrite
c
Percentage
120
100
80
60
40
20
0
Synaptic NR1
per 20 µm dendrite
Control
3 day treatment
7 day treatment
3 day treatment,
4 day recovery

Figure 4.3 Patient antibodies selectively decrease synaptic NMDA currents.

(a) mEPSCs recorded in physiological saline with TTX, bicuculline, and 0 Mg^{2+} to isolate synaptic NMDA receptor mediated currents (left upper trace). APV, an NMDA receptor antagonist, blocks the slow decay of mEPSCs leaving only AMPA receptor mediated currents which account for the fast rise of mEPSCs (left upper middle trace). CNQX, an AMPA receptor antagonist, blocks the fast rise of mEPSCs, allowing NMDA receptor mediated currents to be isolated, as indicated by asterisks (left lower middle trace). Both AMPA and NMDA receptor mediated synaptic currents are blocked by CNQX plus APV (left bottom trace). Treatment of hippocampal neurons with patient CSF for 1 day dramatically reduces synaptic NMDA receptor mediated currents (right). **(b)** Representative average mEPSCs from neurons treated for 1 day with control CSF (left) or patient CSF (right). APV does not affect the slow decay of mEPSCs in neurons treated for 1 day with patient CSF, indicating that patient antibodies decrease NMDA receptor mediated synaptic currents. **(c)** Quantification of the effect of patient antibodies on NMDA (left) and AMPA (right) receptor mediated synaptic currents (right). Asterisk indicates significant difference (Student's t test, $p < 0.001$).

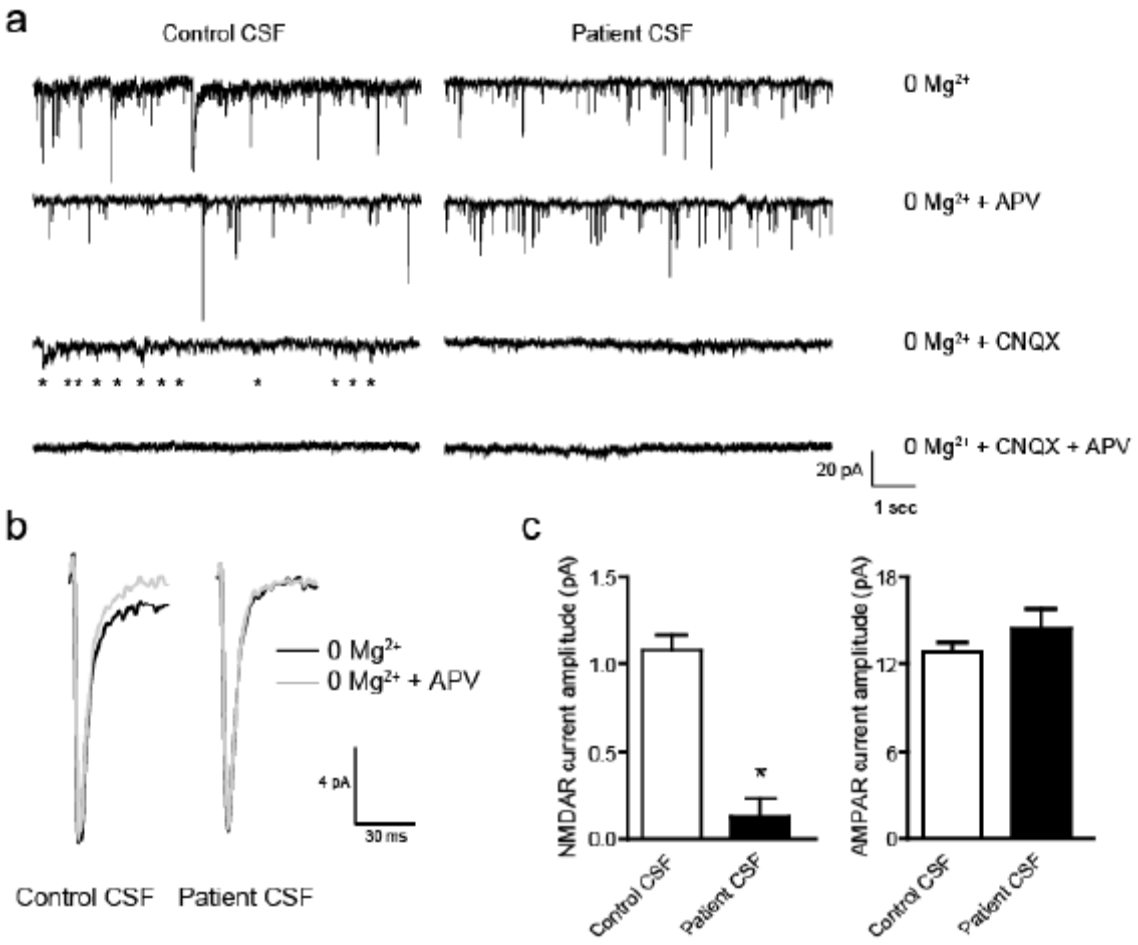
a
Control CSF
Patient CSF
0 Mg2+
0 Mg2+ + APV
0 Mg2+ + CNQX
0 Mg2+ + CNQX + APV
20 pA
1 sec
b
0 Mg2+
0 Mg2+ + APV
4 pA
30 ms
Control CSF
Patient CSF
c
NMDAR current amplitude (pA)
1.5
1.0
0.5
0.0
*
Control CSF
Patient CSF
AMPAR current amplitude (pA)
18
12
6
0
Control CSF
Patient CSF

Figure 4.4 Patient antibodies bind, crosslink and internalize NMDA receptors.

(a) Hippocampal neurons immunostained for surface and total NMDA receptor clusters. Treatment with patient IgG decreases and total NMDA receptor cluster density (middle left). Treatment with patient Fab fragments does not affect surface or total NMDA receptor cluster density (middle right), while treatment with reclustered patient Fab fragments decreases surface and total NMDA receptor cluster density (right). Scale bar = 10 μm. **(b)** Quantification of the effects of patient IgG, Fab fragments, and reclustered Fab fragments on surface and total NMDA receptor cluster density. Asterisk indicates significant difference (Student's t test, $p < 0.001$). **(c)** Schematic which outlines the effect of each treatment on surface receptor clusters.

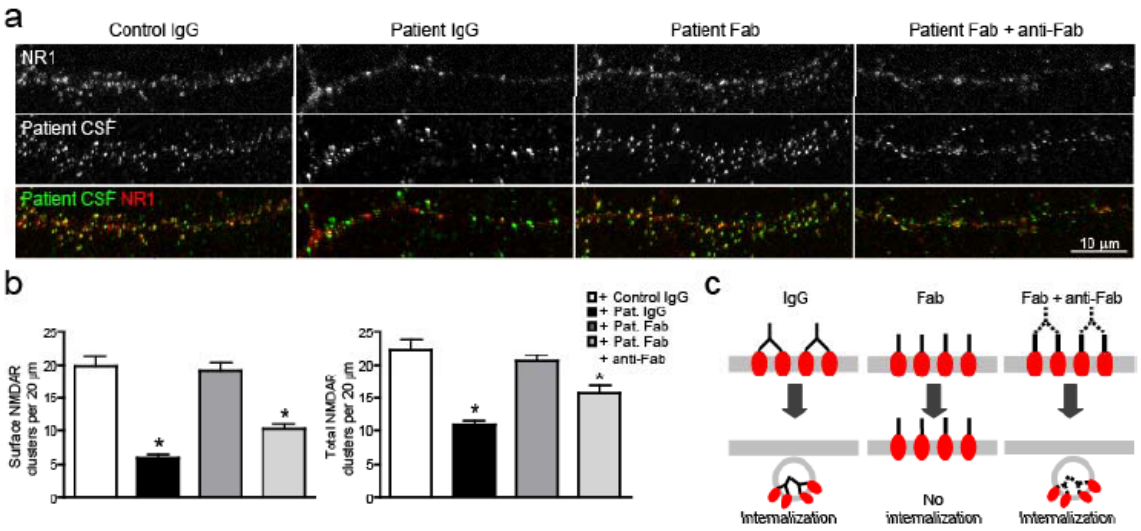
a
Control IgG
Patient IgG
Patient Fab
Patient Fab + anti-Fab
NR1
Patient CSF
Patient CSF NR1
10 µm
b
Surface NMDAR clusters per 20 µm
Total NMDAR clusters per 20 µm
+ Control IgG
+ Pat. IgG
+ Pat. Fab
+ Pat. Fab + anti-Fab
c
IgG
Fab
Fab + anti-Fab
Internalization
No internalization
Internalization

Figure 4.5 Patients' antibodies decrease NMDA receptor cluster density and protein in rodent and human hippocampus *in vivo*.

(a) After implanting a cannula into the CA1 region of hippocampus and infusing control or NMDA patient CSF at a rate of ~0.5 µl/hour for 8 days, rats were euthanized, frozen hippocampal sections prepared and immunostained with synaptic antibodies. Brain sections from rats infused with control CSF (top left) contain bright and clustered NMDA receptor staining in CA1, while brain sections from rats infused with patient CSF (top right) contain significantly reduced NMDA receptor staining. Staining for synapsin, a presynaptic terminal protein, is similar between control CSF and patient CSF injected rats (bottom left, right). Scale bar = 2 µm. **(b)** Quantification of the effect of infusion of patient CSF with varying antibody titer on NMDA receptor cluster density in CA1. Patient CSF with higher antibody titers reduce NMDA receptor cluster density to a greater extent than low titer samples. **(c)** Western blot analyses of NR1 protein in control and patient CSF infused rat hippocampus, ipsilateral (I) and contralateral (C) to infusion. NR1 protein is reduced in ipsilateral patient CSF infused hippocampus. **(d)** Quantification of the density of synapsin labeled clusters (Student's t test, $p > 0.5$). **(e)** Quantification of the density of excitatory synapses (colocalization between presynaptic synapsin and postsynaptic AMPA receptor clusters (Student's t test, $p > 0.5$). **(f)** Hippocampal tissue section from a control patient (left) and from patient with anti-NMDA receptor encephalitis (right) immunostained with a commercial anti-NR1 antibody. The intensity of NR1-immunoreactivity is dramatically reduced in the

hippocampi of anti-NMDA receptor encephalitis patients (N = 2) compared to hippocampi of control patients (N = 3). **(g)** Boxed areas in f shown at higher magnification. Scale bars = 1 mm (top); 25 μm (bottom). **(h)** Quantification of the intensity of NR1 immunostaining (Student's t test, $p < 0.001$).

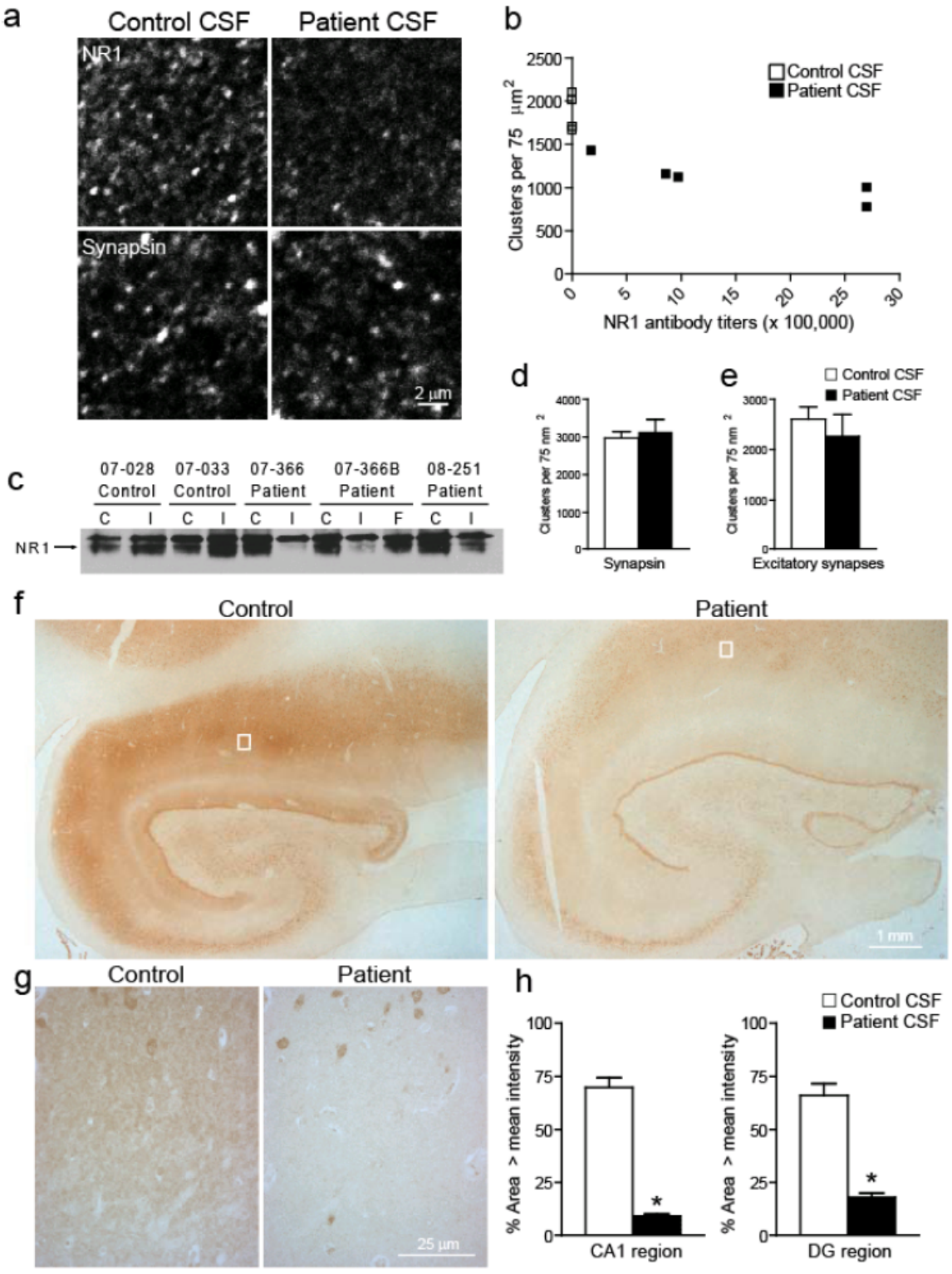
a
Control CSF
Patient CSF
NR1
Synapsin
2 µm
b
Control CSF
Patient CSF
Clusters per 75 µm2
NR1 antibody titers (x 100,000)
c
07-028 Control
07-033 Control
07-366 Patient
07-366B Patient
08-251 Patient
C I C I C I C I F C I
NR1
d
Clusters per 75 nm 2
Synapsin
e
Control CSF
Patient CSF
Clusters per 75 nm 2
Excitatory synapses
f
Control
Patient
1 mm
g
Control
Patient
25 µm
h
Control CSF
Patient CSF
% Area > mean intensity
CA1 region
DG region

Supplemental Figure 4.1 Patient IgG treatment decreases surface and protein of NMDA receptor NR2A/B subunits in a titer dependent fashion.

(a) Immunoblots of surface and total NMDA receptor NR2A and NR2B protein. Treatment with patient IgG reduced surface as well as total NMDA receptor NR2A protein. $GABA_A\alpha1$ and actin are loading controls for surface and total protein, respectively. **(b)** Quantification of surface (left) and total (right) NMDA receptor NR2A protein after treatment with IgG from several patients with different antibody titer. IgG from patients with higher titer resulted in a greater decrease in surface and total NMDA receptor NR2A and NR2B protein than patients with a lower titer. **(c)** Quantification of surface (left) and total (right) NMDA receptor NR2B protein after treatment with IgG from several patients with different antibody titer. IgG from patients with higher titer resulted in a greater decrease in surface and total NMDA receptor NR2B protein than patients with a lower titer.

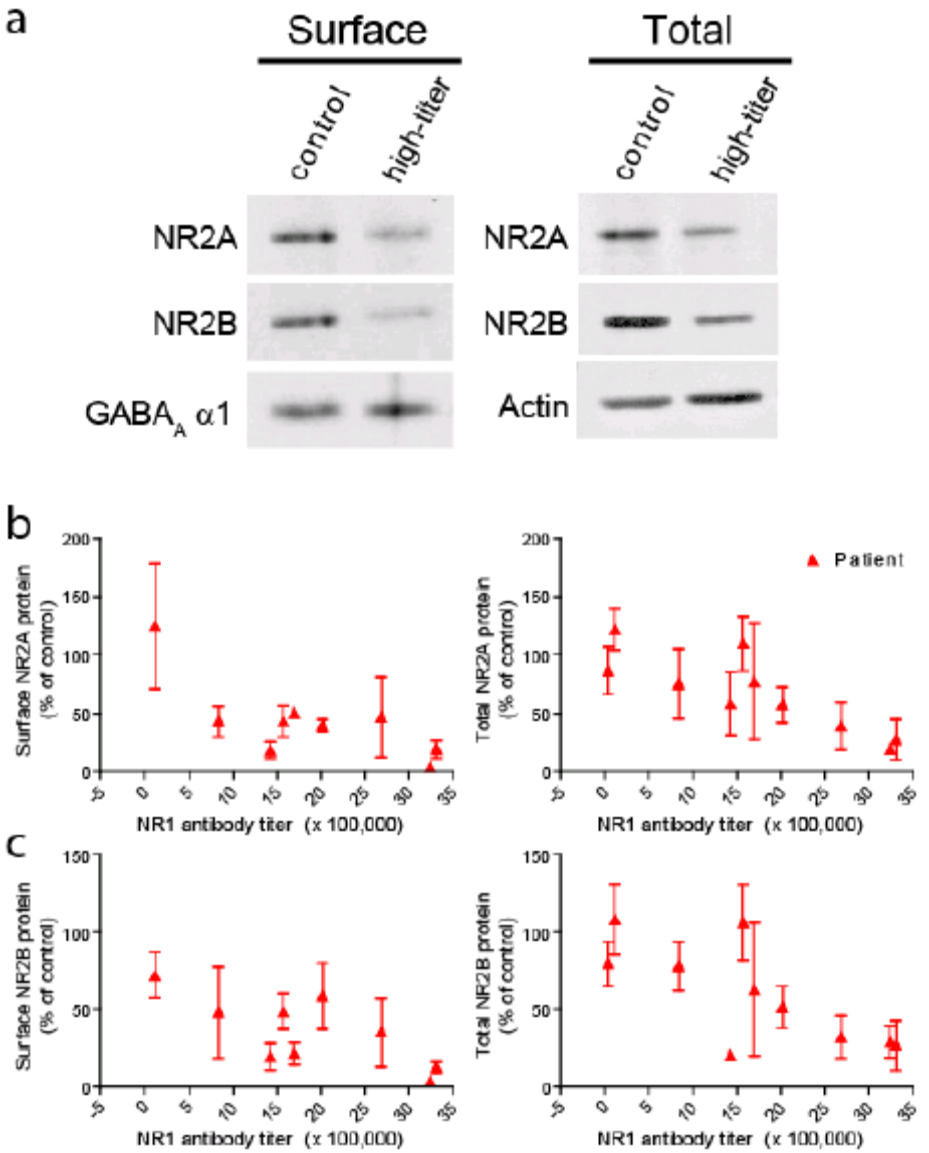
a
Surface
Total
control
high-titer
control
high-titer
NR2A
NR2B
GABA$_A$ α1
NR2A
NR2B
Actin
b
Surface NR2A protein (% of control)
Total NR2A protein (% of control)
Patient
NR1 antibody titer (x 100,000)
NR1 antibody titer (x 100,000)
c
Surface NR2B protein (% of control)
Total NR2B protein (% of control)
NR1 antibody titer (x 100,000)
NR1 antibody titer (x 100,000)

Supplemental Figure 4.2 Patient CSF treatment does not affect other synaptic components.

(a) Hippocampal neurons immunostained for an excitatory postsynaptic protein, PSD-95, excitatory presynaptic protein, VGlut, and surface clusters of AMPA receptor subunits GluR1 or GluR2. Scale bar = 10 μm. **(b)** Quantification of excitatory synaptic protein density. Treatment with patient CSF did not affect the density of these excitatory synaptic proteins. **(c)** Immunoblots of excitatory postsynaptic proteins, AMPA receptor subunits GluR2/3, excitatory postsynaptic protein PSD-95 and $GABA_A$ receptors. Treatment with patient IgG did not affect surface or total neurotransmitter receptor or excitatory synapse protein levels.

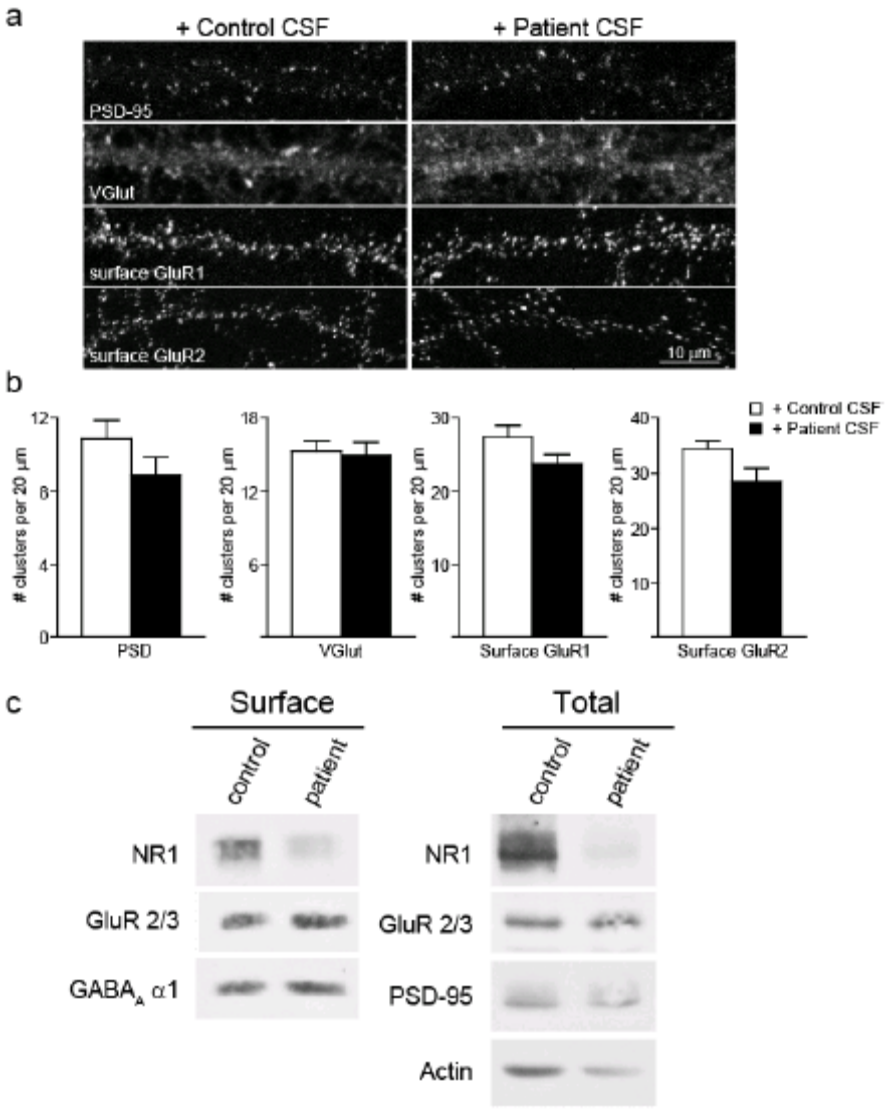
a
+ Control CSF
+ Patient CSF
PSD-95
VGlut
surface GluR1
surface GluR2
10 µm
b
+ Control CSF
+ Patient CSF
# clusters per 20 µm
PSD
VGlut
Surface GluR1
Surface GluR2
c
Surface
Total
control
patient
NR1
GluR 2/3
GABA$_A$ α1
PSD-95
Actin

Supplemental Figure 4.3 Patient CSF treatment does not affect dendritic spines or branching.

(a) Hippocampal neurons transfected with the fluorescent protein, Tomato-td, imaged before and after one day of treatment with control or patient CSF, and traced with NeuronJ. Control (top) or patient (bottom) CSF treatment did not affect dendritic branching or complexity. Scale bar = 100 μm. **(b)** Quantification of primary dendrite number. **(c)** Quantification of primary dendrite length (Student's t test, $p > 0.05$). **(d)** Sholl analysis of dendrite complexity before (white) and after (black) one day of control (left) or patient CSF (middle) treatment. Comparison of the difference before and after control and patient CSF treatment (right). **(e)** Hippocampal neurons transfected with Tomato-td and treated for one day with control or patient CSF. Control (top) or patient (bottom) CSF treatment did not affect dendritic protrusion density. Scale bar = 5 μm. **(f)** Quantification of the density of dendritic protrusions (Student's t test, $p > 0.05$).

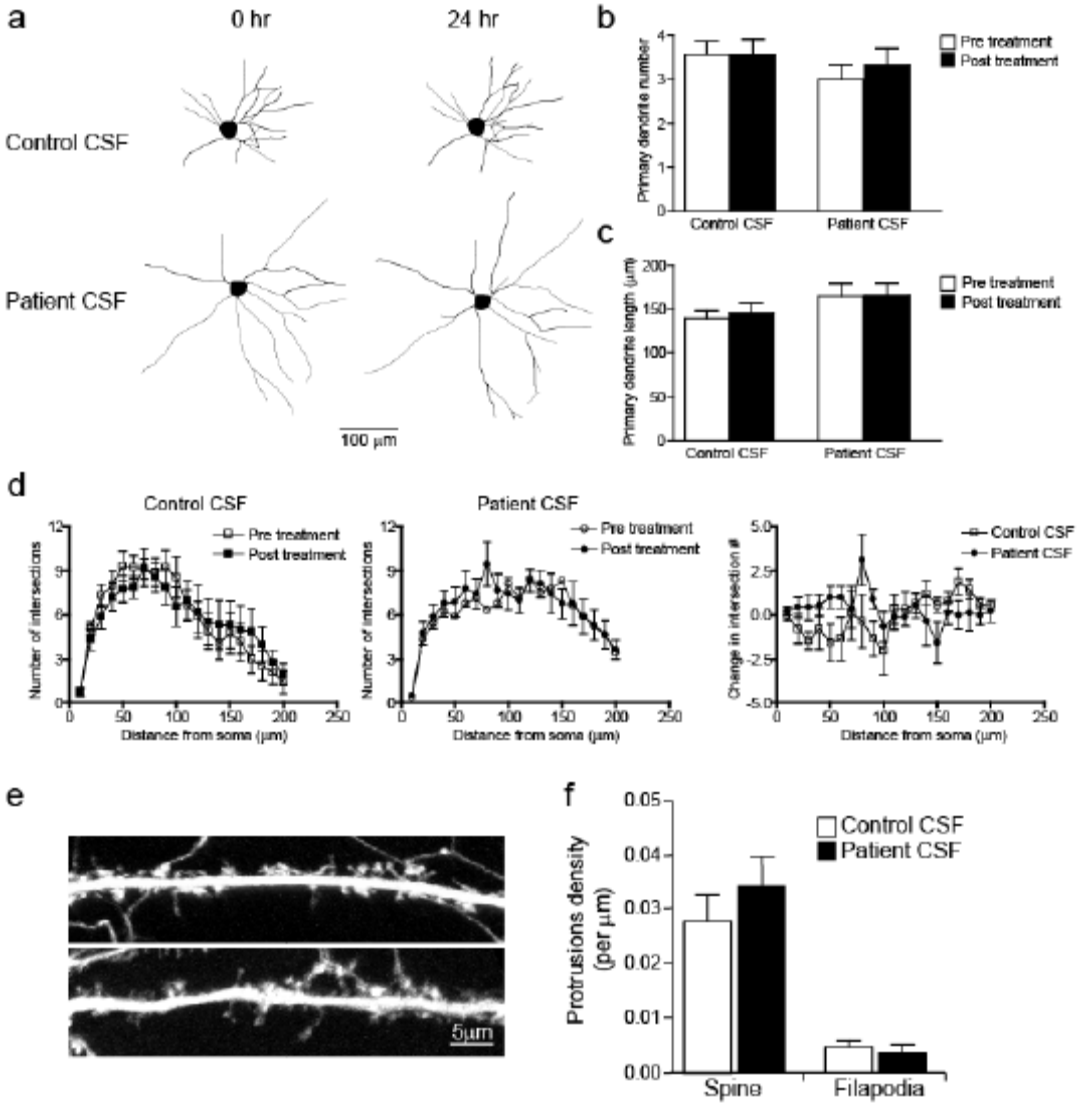
a
0 hr
24 hr
Control CSF
Patient CSF
100 µm
b
Primary dendrite number
Pre treatment
Post treatment
Control CSF
Patient CSF
c
Primary dendrite length (µm)
Pre treatment
Post treatment
Control CSF
Patient CSF
d
Control CSF
Patient CSF
Number of intersections
Pre treatment
Post treatment
Distance from soma (µm)
Change in intersection #
Control CSF
Patient CSF
e
5µm
f
Protrusions density (per µm)
Control CSF
Patient CSF
Spine
Filapodia

Supplemental Figure 4.4 Patient CSF treatment does not affect mEPSC frequency or amplitude.

(a) Quantification of mEPSC amplitude in neurons treated with and without control, patient CSF, and APV. The total mEPSC amplitude (which represents the amount of functional postsynaptic AMPA receptors) is not significantly different among control, patient CSF or APV conditions (Kruskal-Wallis nonparametric ANOVA test followed by Dunn's pairwise multiple comparison test). **(b)** Quantification of mEPSC frequency in neurons treated with and without control, patient CSF, and APV. The frequency of mEPSCs (which represents the number of excitatory synapses) is not significantly different between control, patient CSF or APV conditions (Kruskal-Wallis nonparametric ANOVA test followed by Dunn's pairwise multiple comparison test).

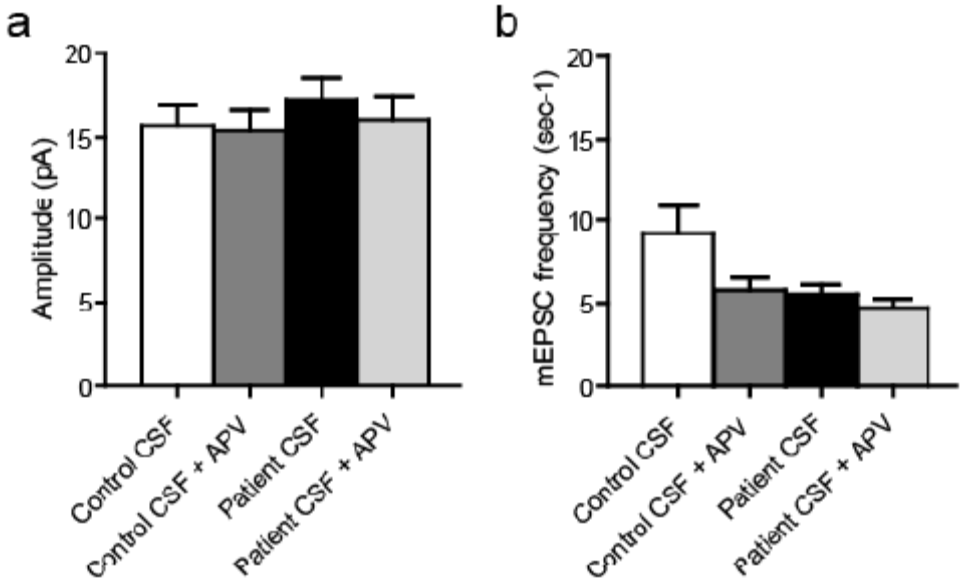
a
Amplitude (pA)
20
15
10
5
0
Control CSF
Control CSF + APV
Patient CSF
Patient CSF + APV
b
mEPSC frequency (sec-1)
20
15
10
5
0
Control CSF
Control CSF + APV
Patient CSF
Patient CSF + APV

Supplemental Figure 4.5 Patient antibody Fab fragments colocalize with NMDA receptor clusters.

(a) Hippocampal neurons immunostained for NMDA receptor clusters in neurons treated for 1 day with control IgG (top row), patient IgG (middle top), patient IgG clustered with anti-Fab secondary antibodies (middle), patient Fab fragments (middle bottom), patient Fab fragments reclustered with anti-Fab secondary antibodies (bottom). Color overlays of NR1 (red) and human IgG (green) are shown at right. While patient IgG and patient IgG + anti-Fab stain neurons more intensely, patient Fab fragments and patient Fab fragments + anti-Fab colocalize with NMDARs to a similar extent. Scale bar = 10 μm.

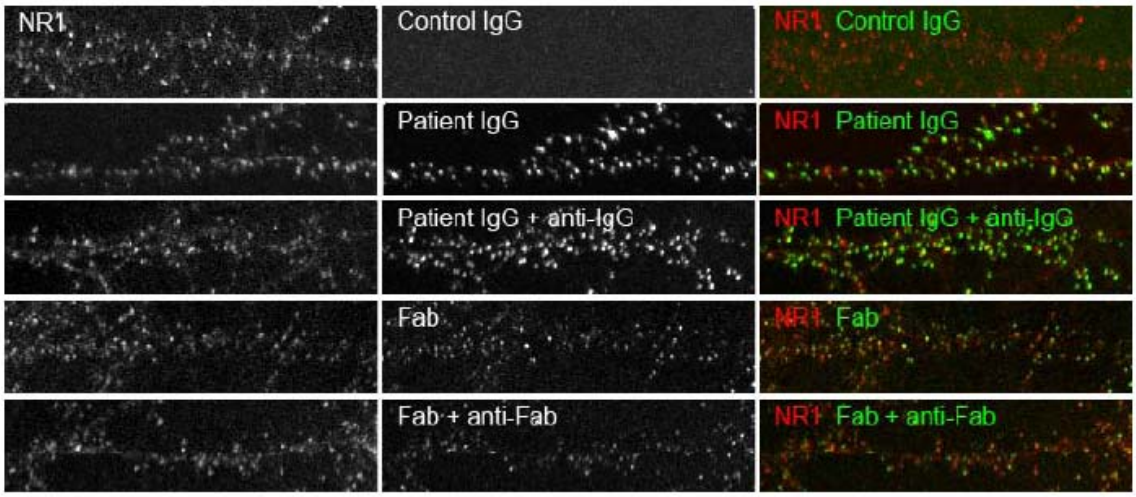
NR1
Control IgG
NR1 Control IgG
Patient IgG
NR1 Patient IgG
Patient IgG + anti-IgG
NR1 Patient IgG + anti-IgG
Fab
NR1 Fab
Fab + anti-Fab
NR1 Fab + anti-Fab

Supplemental Figure 4.6 Patient IgG and CSF treatment have similar effects and these effects are not mediated via the complement pathway.

(a) Quantification of hippocampal neurons immunostained for surface NMDA receptor clusters treated with Control IgG, CSF, patient IgG, CSF, and heat inactivated patient CSF. Treatment with patient IgG and CSF for one day decrease surface NMDARs to a similar extent. Heat inactivated patient CSF also decrease surface NMDARs to a similar extent as patient IgG and CSF, suggesting that these effects are not mediated by complement-mediated pathways. **(b)** Quantification of dissociated hippocampal neurons immunostained for total NMDARs treated with Control IgG, CSF, patient IgG, CSF, and heat inactivated patient CSF (Kruskal-Wallis nonparametric ANOVA test followed by Dunn's pairwise multiple comparison test)

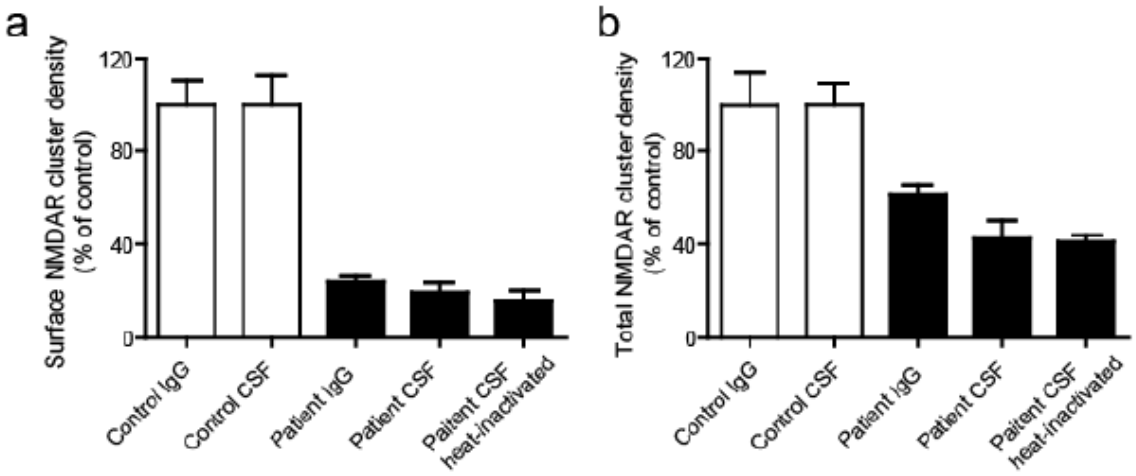
a
Surface NMDAR cluster density (% of control)
120
80
40
0
Control IgG
Control CSF
Patient IgG
Patient CSF
Paitent CSF heat-inactivated
b
Total NMDAR cluster density (% of control)
120
80
40
0
Control IgG
Control CSF
Patient IgG
Patient CSF
Paitent CSF heat-inactivated

Supplemental Figure 4.7 Patient CSF recognizes NMDA receptor clusters *in vivo*.

(a) Rat brain sections immunostained with patient CSF (top left), NMDA receptors (top middle), and a postsynaptic protein, PSD-95 (top right). Patient CSF clusters are highly colocalized with NMDARs (yellow puncta, bottom left). Patient CSF clusters colocalize with PSD-95 to a similar extent as NMDARs (compare bottom middle to bottom right).

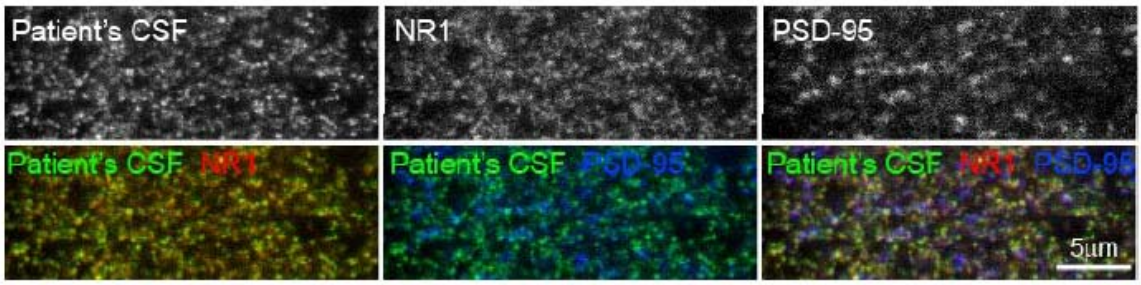
Patient's CSF
NR1
PSD-95
Patient's CSF NR1
Patient's CSF PSD-95
Patient's CSF NR1 PSD-95
5µm

Supplemental Figure 4.8 Infusion of patient CSF results in the deposition of human IgG in the hippocampus without increasing cell death.

(a) Brain sections from rats infused with control (left) or patient CSF (right) into one hippocampus, and immunostained with human IgG, NR1, and TO-PRO to label nuclei. The deposition of human IgG was seen in the hippocampus of rats infused with patient CSF but not control CSF**.** Below, higher magnification views of the CA1 region of the hippocampus show that areas with human IgG deposits have reduced NMDA receptor clusters (see Fig. 5) and decreased overall staining intensity. **(b)** Brain sections from rats infused with control or patient CSF and immunostained with NR1 to label NMDA receptors, TO-PRO to label nuclei, and TUNEL to label apoptotic cells. Infusion with control (left) or patient CSF (middle) did not cause significant cell death. While several apoptotic cells were found along the cannula tract (right), the total number and distribution did not differ between rats infused with control or patient CSF. **(b)** Quantification of the density of dissociated hippocampal cells *in vitro* between control or patient CSF treatment (left) and of the percent of TUNEL positive neurons *in vitro* (apoptotic cells). These measures were not significantly different between control or patient CSF treatment (Student's t test).

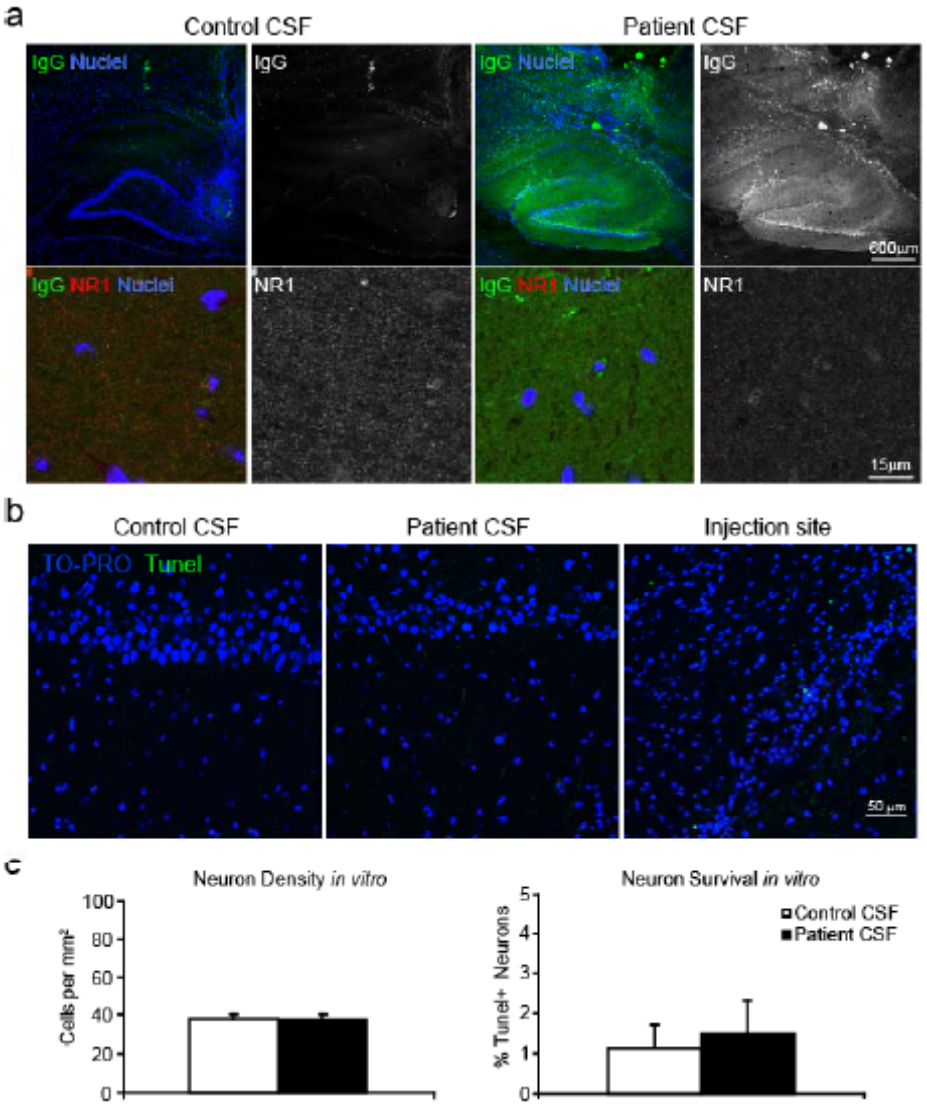
a
Control CSF
Patient CSF
IgG Nuclei
IgG
IgG Nuclei
IgG
600µm
IgG NR1 Nuclei
NR1
IgG NR1 Nuclei
NR1
15µm
b
Control CSF
Patient CSF
Injection site
TO-PRO Tunel
50 µm
c
Neuron Density in vitro
Cells per mm²
100
80
60
40
20
0
Neuron Survival in vitro
% Tunel+ Neurons
5
4
3
2
1
0
Control CSF
Patient CSF

Conclusions

The work described in the previous chapters extends our understanding of how neuron-glia signaling modulates GABAergic synapse formation in the developing CNS and how autoantibodies in patients with anti-NMDAR encephalitis disrupt synapse maintenance in the diseased nervous system. In particular, I have demonstrated that proteins secreted from astrocytes specifically increase GABAergic axon length, branch, and synaptogenesis and identified the astrocyte soluble proteins in size fractions that promote these effects. I have also shown that antibodies from anti-NMDAR encephalitis patients reversibly alter the number and distribution of glutamate receptors in neurons, resulting in a decrease in excitatory synapse function which most likely underlies the cognitive dysfunctions that characterize this immune-mediated encephalitis. Thus, these findings extend our understanding of how neuron-glial communication modulates the formation of synapses and how the disruption of synapse maintenance may underlie cognitive deficits in the diseased nervous system.

This work raises important questions for future research into the formation of GABAergic synapses. First, the differential regulation of glutamatergic and GABAergic synaptogenesis by astrocytes (Chapter 2) highlights the need for more in depth research into the mechanisms underlying synapse formation of different cell types. Recent work identifying transcription factors and secreted and cell adhesion molecules that specifically regulate GABAergic synapse development (Paradis et al., 2007; Ango et al., 2008; Lin et

al., 2008) has set the stage for understanding how astrocytes differentially modulate glutamatergic and GABAergic synaptogenesis. Second, the generation of a transgenic mouse model with astrocytes in which exocytosis is deficient (Pascual et al., 2005) provides a new tool to begin to examine the mechanisms governing the release of proteins from astrocytes that affect GABAergic neurons and synapses. Since astrocyte calcium elevations have been implicated in mediating the release of transmitters from astrocytes that affect neurons (Scemes and Giaume, 2006)); but also see ((Fiacco et al., 2007), it will also be important to investigate how astrocyte activity may play a role in the release of proteins that increase GABAergic synaptogenesis. Third, studies have shown that astrocytes from different regions differ in their ability to modulate neurite outgrowth (Qian et al., 1992), therefore it will be important to examine whether local astrocytes support synaptogenesis in a manner distinct from target-derived or other cues. In addition, it will be important to evaluate the ability of both immature and mature astrocytes to affect GABAergic neurons. Recent work has shown that only immature astrocytes express thrombospondins, which have been shown to increase excitatory synaptogenesis (Christopherson et al., 2005). This future work will be critical to understanding how astrocytes modulate synaptic connections in the developing and mature brain and will ultimately contribute to neurodevelopmental disorders such as epilepsy, autism and mental retardation, in which synapse formation, function, maintenance are aberrant or reduced.

The identification of proteins contained within gel filtration fractions that increase GABAergic axon length, branching, and synaptogenesis (Chapter 3) lays the foundation for several future experiments, with the ultimate goal of evaluating the effects of astrocytes on the development of GABAergic synapses *in vivo*. The 34 candidates identified in the bioactive fractions of astrocyte conditioned media can be individually tested by treating neuron only cultures with three different concentrations of the recombinant protein for three days. These cultures will be immunostained for GAD and VGAT to identify GABAergic neuron neurite morphology and presynaptic terminal density. In this manner, these candidates can be evaluated in a relatively short period of time. Once a candidate is confirmed in these *in vitro* assays, the role of that candidate in mediating the effects of astrocytes *in vivo* can be examined using transgenic and knock-out mouse models. Recently, several groups have used different approaches to identified single candidates or families of proteins from large groups of potential candidates (Kurusu et al., 2008; Linhoff et al., 2009). These approaches and others will be necessary as proteomic and genomic techniques provide increasingly detailed information about the processes that underlie synapse formation and development.

The identification of cellular mechanisms underlying anti-NMDAR encephalitis (Chapter 4) raises many important questions for future research into this and another diseases that cause synapse dysfunction. The most important future goal is to confirm the repertoire of pathogenic affects of autoantibodies in in vivo models of anti-NMDAR encephalitis. The generation of an animal model with similar features of the human

disease, including production of autoantibodies and disruption of blood-brain barrier integrity to allow antibodies access to the CNS, will allow further examination of the key mechanisms of this disorder. One issue of interest is to determine what effect anti-NMDAR autoantibodies have on hippocampal circuit plasticity, in particular LTP and LTD, and to attempt to directly relate this to behavior in *in vivo* models. It will also be essential to investigate the immunological mechanisms of disease onset, in particular to understand the parameters that affect continued intrathecal production of antibodies observed in patients with this and related disorders. Research into new treatments that may interfere with the pathogenic properties or actions of autoantibodies against the NMDA receptors will help provide better outcomes to patients. Ultimately, understanding the cellular, synaptic and circuit mechanisms and consequences of anti-NMDAR encephalitis will provide important information that can be leveraged to make progress in other psychiatric disorders involving glutamate receptor dysfunction, such as schizophrenia.

References

Ango F, Wu C, Van der Want JJ, Wu P, Schachner M, Huang ZJ (2008) Bergmann glia and the recognition molecule CHL1 organize GABAergic axons and direct innervation of Purkinje cell dendrites. PLoS Biol 6:e103.

Aoyagi A, Nishikawa K, Saito H, Abe K (1994) Characterization of basic fibroblast growth factor-mediated acceleration of axonal branching in cultured rat hippocampal neurons. Brain Res 661:117-126.

Au E, Richter MW, Vincent AJ, Tetzlaff W, Aebersold R, Sage EH, Roskams AJ (2007) SPARC from olfactory ensheathing cells stimulates Schwann cells to promote neurite outgrowth and enhances spinal cord repair. J Neurosci 27:7208-7221.

Beattie EC, Stellwagen D, Morishita W, Bresnahan JC, Ha BK, Von Zastrow M, Beattie MS, Malenka RC (2002) Control of synaptic strength by glial TNFalpha. Science 295:2282-2285.

Benfey M, Aguayo AJ (1982) Extensive elongation of axons from rat brain into peripheral nerve grafts. Nature 296:150-152.

Bergsman JB, Krueger SR, Fitzsimonds RM (2006) Automated criteria-based selection and analysis of fluorescent synaptic puncta. J Neurosci Methods 152:32-39.

Bezzi P, Gundersen V, Galbete JL, Seifert G, Steinhauser C, Pilati E, Volterra A (2004) Astrocytes contain a vesicular compartment that is competent for regulated exocytosis of glutamate. Nat Neurosci 7:613-620.

Blake SM, Strasser V, Andrade N, Duit S, Hofbauer R, Schneider WJ, Nimpf J (2008) Thrombospondin-1 binds to ApoER2 and VLDL receptor and functions in postnatal neuronal migration. EMBO J 27:3069-3080.

Bushong EA, Martone ME, Jones YZ, Ellisman MH (2002) Protoplasmic astrocytes in CA1 stratum radiatum occupy separate anatomical domains. J Neurosci 22:183-192.

Cahoy JD, Emery B, Kaushal A, Foo LC, Zamanian JL, Christopherson KS, Xing Y, Lubischer JL, Krieg PA, Krupenko SA, Thompson WJ, Barres BA (2008) A transcriptome database for astrocytes, neurons, and oligodendrocytes: a new resource for understanding brain development and function. J Neurosci 28:264-278.

Christopherson KS, Ullian EM, Stokes CC, Mullowney CE, Hell JW, Agah A, Lawler J, Mosher DF, Bornstein P, Barres BA (2005) Thrombospondins are astrocyte-secreted proteins that promote CNS synaptogenesis. Cell 120:421-433.

Coesmans M, Smitt PA, Linden DJ, Shigemoto R, Hirano T, Yamakawa Y, van Alphen AM, Luo C, van der Geest JN, Kros JM, Gaillard CA, Frens MA, de Zeeuw CI (2003) Mechanisms underlying cerebellar motor deficits due to mGluR1-autoantibodies. Ann Neurol 53:325-336.

Cohen-Cory S, Fraser SE (1995) Effects of brain-derived neurotrophic factor on optic axon branching and remodelling in vivo. Nature 378:192-196.

Colon-Ramos DA, Margeta MA, Shen K (2007) Glia promote local synaptogenesis through UNC-6 (netrin) signaling in C. elegans. Science 318:103-106.

Conti-Fine BM, Milani M, Kaminski HJ (2006) Myasthenia gravis: past, present, and future. J Clin Invest 116:2843-2854.

Dalmau J, Gleichman AJ, Hughes EG, Rossi JE, Peng X, Lai M, Dessain SK, Rosenfeld MR, Balice-Gordon R, Lynch DR (2008) Anti-NMDA-receptor encephalitis: case series and analysis of the effects of antibodies. Lancet Neurol 7:1091-1098.

Dalmau J, Tuzun E, Wu HY, Masjuan J, Rossi JE, Voloschin A, Baehring JM, Shimazaki H, Koide R, King D, Mason W, Sansing LH, Dichter MA, Rosenfeld MR, Lynch DR (2007) Paraneoplastic anti-N-methyl-D-aspartate receptor encephalitis associated with ovarian teratoma. Ann Neurol 61:25-36.

DeFreitas MF, Yoshida CK, Frazier WA, Mendrick DL, Kypta RM, Reichardt LF (1995) Identification of integrin alpha 3 beta 1 as a neuronal thrombospondin receptor mediating neurite outgrowth. Neuron 15:333-343.

DeGiorgio LA, Konstantinov KN, Lee SC, Hardin JA, Volpe BT, Diamond B (2001) A subset of lupus anti-DNA antibodies cross-reacts with the NR2 glutamate receptor in systemic lupus erythematosus. Nat Med 7:1189-1193.

Dowell JA, Johnson JA, Li L (2009) Identification of Astrocyte Secreted Proteins with a Combination of Shotgun Proteomics and Bioinformatics. J Proteome Res. [Epub ahead of print]

Doyle JP, Dougherty JD, Heiman M, Schmidt EF, Stevens TR, Ma G, Bupp S, Shrestha P, Shah RD, Doughty ML, Gong S, Greengard P, Heintz N (2008) Application of a translational profiling approach for the comparative analysis of CNS cell types. Cell 135:749-762.

Drachman DB, Angus CW, Adams RN, Michelson JD, Hoffman GJ (1978) Myasthenic antibodies cross-link acetylcholine receptors to accelerate degradation. N Engl J Med 298:1116-1122.

Duan S, Anderson CM, Keung EC, Chen Y, Swanson RA (2003) P2X7 receptor-mediated release of excitatory amino acids from astrocytes. J Neurosci 23:1320-1328.

Elmariah SB, Crumling MA, Parsons TD, Balice-Gordon RJ (2004) Postsynaptic TrkB-mediated signaling modulates excitatory and inhibitory neurotransmitter receptor clustering at hippocampal synapses. J Neurosci 24:2380-2393.

Elmariah SB, Oh EJ, Hughes EG, Balice-Gordon RJ (2005) Astrocytes regulate inhibitory synapse formation via Trk-mediated modulation of postsynaptic GABAA receptors. J Neurosci 25:3638-3650.

Feng Z, Ko CP (2008) Schwann cells promote synaptogenesis at the neuromuscular junction via transforming growth factor-beta1. J Neurosci 28:9599-9609.

Fiacco TA, McCarthy KD (2004) Intracellular astrocyte calcium waves in situ increase the frequency of spontaneous AMPA receptor currents in CA1 pyramidal neurons. J Neurosci 24:722-732.

Fiacco TA, Agulhon C, Taves SR, Petravicz J, Casper KB, Dong X, Chen J, McCarthy KD (2007) Selective stimulation of astrocyte calcium in situ does not affect neuronal excitatory synaptic activity. Neuron 54:611-626.

Fox MA, Sanes JR, Borza DB, Eswarakumar VP, Fassler R, Hudson BG, John SW, Ninomiya Y, Pedchenko V, Pfaff SL, Rheault MN, Sado Y, Segal Y, Werle MJ, Umemori H (2007) Distinct target-derived signals organize formation, maturation, and maintenance of motor nerve terminals. Cell 129:179-193.

Gomez CM, Richman DP (1985) Monoclonal anti-acetylcholine receptor antibodies with differing capacities to induce experimental autoimmune myasthenia gravis. J Immunol 135:234-241.

Goslin K, Schreyer DJ, Skene JH, Banker G (1988) Development of neuronal polarity: GAP-43 distinguishes axonal from dendritic growth cones. Nature 336:672-674.

Graf ER, Zhang X, Jin SX, Linhoff MW, Craig AM (2004) Neurexins induce differentiation of GABA and glutamate postsynaptic specializations via neuroligins. Cell 119:1013-1026.

Haber M, Zhou L, Murai KK (2006) Cooperative astrocyte and dendritic spine dynamics at hippocampal excitatory synapses. J Neurosci 26:8881-8891.

Hama H, Hara C, Yamaguchi K, Miyawaki A (2004) PKC signaling mediates global enhancement of excitatory synaptogenesis in neurons triggered by local contact with astrocytes. Neuron 41:405-415.

Hanly JG, Robichaud J, Fisk JD (2006) Anti-NR2 glutamate receptor antibodies and cognitive function in systemic lupus erythematosus. J Rheumatol 33:1553-1558.

Harrison MJ, Ravdin LD, Lockshin MD (2006) Relationship between serum NR2a antibodies and cognitive dysfunction in systemic lupus erythematosus. Arthritis Rheum 54:2515-2522.

Hartman KN, Pal SK, Burrone J, Murthy VN (2006) Activity-dependent regulation of inhibitory synaptic transmission in hippocampal neurons. Nat Neurosci 9:642-649.

Heck N, Garwood J, Schutte K, Fawcett J, Faissner A (2003) Astrocytes in culture express fibrillar collagen. Glia 41:382-392.

Heiman M, Schaefer A, Gong S, Peterson JD, Day M, Ramsey KE, Suarez-Farinas M, Schwarz C, Stephan DA, Surmeier DJ, Greengard P, Heintz N (2008) A translational profiling approach for the molecular characterization of CNS cell types. Cell 135:738-748.

Hestrin S, Nicoll RA, Perkel DJ, Sah P (1990) Analysis of excitatory synaptic action in pyramidal cells using whole-cell recording from rat hippocampal slices. J Physiol 422:203-225.

Hochstim C, Deneen B, Lukaszewicz A, Zhou Q, Anderson DJ (2008) Identification of positionally distinct astrocyte subtypes whose identities are specified by a homeodomain code. Cell 133:510-522.

Hoe HS, Lee KJ, Carney RS, Lee J, Markova A, Lee JY, Howell BW, Hyman BT, Pak DT, Bu G, Rebeck GW (2009a) Interaction of reelin with amyloid precursor protein promotes neurite outgrowth. J Neurosci 29:7459-7473.

Hoe HS, Fu Z, Makarova A, Lee JY, Lu C, Feng L, Pajoohesh-Ganji A, Matsuoka Y, Hyman BT, Ehlers MD, Vicini S, Pak DT, Rebeck GW (2009b) The effects of amyloid precursor protein on postsynaptic composition and activity. J Biol Chem 284:8495-8506.

Iizuka T, Sakai F (2008) [Anti-nMDA receptor encephalitis--clinical manifestations and pathophysiology]. Brain Nerve 60:1047-1060.

Jentsch JD, Roth RH (1999) The neuropsychopharmacology of phencyclidine: from NMDA receptor hypofunction to the dopamine hypothesis of schizophrenia. Neuropsychopharmacology 20:201-225.

Kang J, Jiang L, Goldman SA, Nedergaard M (1998) Astrocyte-mediated potentiation of inhibitory synaptic transmission. Nat Neurosci 1:683-692.

Keene SD, Greco TM, Parastatidis I, Lee SH, Hughes EG, Balice-Gordon RJ, Speicher DW, Ischiropoulos H (2009) Mass spectrometric and computational analysis of cytokine-induced alterations in the astrocyte secretome. Proteomics 9:768-782.

Kessels HW, Malinow R (2009) Synaptic AMPA receptor plasticity and behavior. Neuron 61:340-350.

Kilman V, van Rossum MC, Turrigiano GG (2002) Activity deprivation reduces miniature IPSC amplitude by decreasing the number of postsynaptic GABA(A) receptors clustered at neocortical synapses. J Neurosci 22:1328-1337.

Kim YI, Neher E (1988) IgG from patients with Lambert-Eaton syndrome blocks voltage-dependent calcium channels. Science 239:405-408.

Krystal JH, Karper LP, Seibyl JP, Freeman GK, Delaney R, Bremner JD, Heninger GR, Bowers MB, Jr., Charney DS (1994) Subanesthetic effects of the noncompetitive NMDA antagonist, ketamine, in humans. Psychotomimetic, perceptual, cognitive, and neuroendocrine responses. Arch Gen Psychiatry 51:199-214.

Kurusu M, Cording A, Taniguchi M, Menon K, Suzuki E, Zinn K (2008) A screen of cell-surface molecules identifies leucine-rich repeat proteins as key mediators of synaptic target selection. Neuron 59:972-985.

Lai M, Hughes EG, Peng X, Zhou L, Gleichman AJ, Shu H, Mata S, Kremens D, Vitaliani R, Geschwind MD, Bataller L, Kalb RG, Davis R, Graus F, Lynch DR, Balice-Gordon R, Dalmau J (2009) AMPA receptor antibodies in limbic encephalitis alter synaptic receptor location. Ann Neurol 65:424-434.

Lapteva L, Nowak M, Yarboro CH, Takada K, Roebuck-Spencer T, Weickert T, Bleiberg J, Rosenstein D, Pao M, Patronas N, Steele S, Manzano M, van der Veen JW, Lipsky PE, Marenco S, Wesley R, Volpe B, Diamond B, Illei GG (2006) Anti-N-methyl-D-aspartate receptor antibodies, cognitive dysfunction, and depression in systemic lupus erythematosus. Arthritis Rheum 54:2505-2514.

Le R, Esquenazi S (2002) Astrocytes mediate cerebral cortical neuronal axon and dendrite growth, in part, by release of fibroblast growth factor. Neurol Res 24:81-92.

Lennon VA, Lambert EH (1981) Monoclonal autoantibodies to acetylcholine receptors: evidence for a dominant idiotype and requirement of complement for pathogenicity. Ann N Y Acad Sci 377:77-96.

Levite M, Ganor Y (2008) Autoantibodies to glutamate receptors can damage the brain in epilepsy, systemic lupus erythematosus and encephalitis. Expert Rev Neurother 8:1141-1160.

Levite M, Fleidervish IA, Schwarz A, Pelled D, Futerman AH (1999) Autoantibodies to the glutamate receptor kill neurons via activation of the receptor ion channel. J Autoimmun 13:61-72.

Lin Y, Bloodgood BL, Hauser JL, Lapan AD, Koon AC, Kim TK, Hu LS, Malik AN, Greenberg ME (2008) Activity-dependent regulation of inhibitory synapse development by Npas4. Nature 455:1198-1204.

Linhoff MW, Lauren J, Cassidy RM, Dobie FA, Takahashi H, Nygaard HB, Airaksinen MS, Strittmatter SM, Craig AM (2009) An unbiased expression screen for synaptogenic proteins identifies the LRRTM protein family as synaptic organizers. Neuron 61:734-749.

Liu QY, Schaffner AE, Li YX, Dunlap V, Barker JL (1996) Upregulation of GABAA current by astrocytes in cultured embryonic rat hippocampal neurons. J Neurosci 16:2912-2923.

Liu QY, Schaffner AE, Chang YH, Vaszil K, Barker JL (1997) Astrocytes regulate amino acid receptor current densities in embryonic rat hippocampal neurons. J Neurobiol 33:848-864.

Lovatt D, Sonnewald U, Waagepetersen HS, Schousboe A, He W, Lin JH, Han X, Takano T, Wang S, Sim FJ, Goldman SA, Nedergaard M (2007) The transcriptome and metabolic gene signature of protoplasmic astrocytes in the adult murine cortex. J Neurosci 27:12255-12266.

Luby ED, Cohen BD, Rosenbaum G, Gottlieb JS, Kelley R (1959) Study of a new schizophrenomimetic drug; sernyl. AMA Arch Neurol Psychiatry 81:363-369.

Martens H, Weston MC, Boulland JL, Gronborg M, Grosche J, Kacza J, Hoffmann A, Matteoli M, Takamori S, Harkany T, Chaudhry FA, Rosenmund C, Erck C, Jahn R, Hartig W (2008) Unique luminal localization of VGAT-C terminus allows for selective labeling of active cortical GABAergic synapses. J Neurosci 28:13125-13131.

Marty S, Wehrle R, Sotelo C (2000) Neuronal activity and brain-derived neurotrophic factor regulate the density of inhibitory synapses in organotypic slice cultures of postnatal hippocampus. J Neurosci 20:8087-8095.

Matthiessen HP, Schmalenbach C, Muller HW (1989) Astroglia-released neurite growth-inducing activity for embryonic hippocampal neurons is associated with laminin bound in a sulfated complex and free fibronectin. Glia 2:177-188.

Mauch DH, Nagler K, Schumacher S, Goritz C, Muller EC, Otto A, Pfrieger FW (2001) CNS synaptogenesis promoted by glia-derived cholesterol. Science 294:1354-1357.

Mazzanti M, Haydon PG (2003) Astrocytes selectively enhance N-type calcium current in hippocampal neurons. Glia 41:128-136.

McAllister AK, Katz LC, Lo DC (1996) Neurotrophin regulation of cortical dendritic growth requires activity. Neuron 17:1057-1064.

McAllister AK, Katz LC, Lo DC (1997) Opposing roles for endogenous BDNF and NT-3 in regulating cortical dendritic growth. Neuron 18:767-778.

Meiners S, Powell EM, Geller HM (1995) A distinct subset of tenascin/CS-6-PG-rich astrocytes restricts neuronal growth in vitro. J Neurosci 15:8096-8108.

Mohn AR, Gainetdinov RR, Caron MG, Koller BH (1999) Mice with reduced NMDA receptor expression display behaviors related to schizophrenia. Cell 98:427-436.

Moore NH, Costa LG, Shaffer SA, Goodlett DR, Guizzetti M (2009) Shotgun proteomics implicates extracellular matrix proteins and protease systems in neuronal development induced by astrocyte cholinergic stimulation. J Neurochem 108:891-908.

Mothet JP, Pollegioni L, Ouanounou G, Martineau M, Fossier P, Baux G (2005) Glutamate receptor activation triggers a calcium-dependent and SNARE protein-dependent release of the gliotransmitter D-serine. Proc Natl Acad Sci U S A 102:5606-5611.

Mouri A, Noda Y, Noda A, Nakamura T, Tokura T, Yura Y, Nitta A, Furukawa H, Nabeshima T (2007) Involvement of a dysfunctional dopamine-D1/N-methyl-d-aspartate-NR1 and Ca2+/calmodulin-dependent protein kinase II pathway in the impairment of latent learning in a model of schizophrenia induced by phencyclidine. Mol Pharmacol 71:1598-1609.

Murai KK, Nguyen LN, Irie F, Yamaguchi Y, Pasquale EB (2003) Control of hippocampal dendritic spine morphology through ephrin-A3/EphA4 signaling. Nat Neurosci 6:153-160.

Nagler K, Mauch DH, Pfrieger FW (2001) Glia-derived signals induce synapse formation in neurones of the rat central nervous system. J Physiol 533:665-679.

Naus S, Richter M, Wildeboer D, Moss M, Schachner M, Bartsch JW (2004) Ectodomain shedding of the neural recognition molecule CHL1 by the metalloprotease-disintegrin ADAM8 promotes neurite outgrowth and suppresses neuronal cell death. J Biol Chem 279:16083-16090.

Neugebauer KM, Emmett CJ, Venstrom KA, Reichardt LF (1991) Vitronectin and thrombospondin promote retinal neurite outgrowth: developmental regulation and role of integrins. Neuron 6:345-358.

Nikonenko AG, Sun M, Lepsveridze E, Apostolova I, Petrova I, Irintchev A, Dityatev A, Schachner M (2006) Enhanced perisomatic inhibition and impaired long-term potentiation in the CA1 region of juvenile CHL1-deficient mice. Eur J Neurosci 23:1839-1852.

Nishida H, Okabe S (2007) Direct astrocytic contacts regulate local maturation of dendritic spines. J Neurosci 27:331-340.

Old WM, Meyer-Arendt K, Aveline-Wolf L, Pierce KG, Mendoza A, Sevinsky JR, Resing KA, Ahn NG (2005) Comparison of label-free methods for quantifying human proteins by shotgun proteomics. Mol Cell Proteomics 4:1487-1502.

Olney JW, Farber NB (1995) Glutamate receptor dysfunction and schizophrenia. Arch Gen Psychiatry 52:998-1007.

Olney JW, Newcomer JW, Farber NB (1999) NMDA receptor hypofunction model of schizophrenia. J Psychiatr Res 33:523-533.

Paradis S, Harrar DB, Lin Y, Koon AC, Hauser JL, Griffith EC, Zhu L, Brass LF, Chen C, Greenberg ME (2007) An RNAi-based approach identifies molecules required for glutamatergic and GABAergic synapse development. Neuron 53:217-232.

Pascual O, Casper KB, Kubera C, Zhang J, Revilla-Sanchez R, Sul JY, Takano H, Moss SJ, McCarthy K, Haydon PG (2005) Astrocytic purinergic signaling coordinates synaptic networks. Science 310:113-116.

Pfrieger FW, Barres BA (1997) Synaptic efficacy enhanced by glial cells in vitro. Science 277:1684-1687.

Pleasure D (2008) Diagnostic and pathogenic significance of glutamate receptor autoantibodies. Arch Neurol 65:589-592.

Poon VY, Klassen MP, Shen K (2008) UNC-6/netrin and its receptor UNC-5 locally exclude presynaptic components from dendrites. Nature 455:669-673.

Qian JA, Bull MS, Levitt P (1992) Target-derived astroglia regulate axonal outgrowth in a region-specific manner. Dev Biol 149:278-294.

Qiu WQ, Ferreira A, Miller C, Koo EH, Selkoe DJ (1995) Cell-surface beta-amyloid precursor protein stimulates neurite outgrowth of hippocampal neurons in an isoform-dependent manner. J Neurosci 15:2157-2167.

Rao A, Cha EM, Craig AM (2000) Mismatched appositions of presynaptic and postsynaptic components in isolated hippocampal neurons. J Neurosci 20:8344-8353.

Rich MM, Colman H, Lichtman JW (1994) In vivo imaging shows loss of synaptic sites from neuromuscular junctions in a model of myasthenia gravis. Neurology 44:2138-2145.

Rogers SW, Andrews PI, Gahring LC, Whisenand T, Cauley K, Crain B, Hughes TE, Heinemann SF, McNamara JO (1994) Autoantibodies to glutamate receptor GluR3 in Rasmussen's encephalitis. Science 265:648-651.

Rolls A, Shechter R, Schwartz M (2009) The bright side of the glial scar in CNS repair. Nat Rev Neurosci 10:235-241.

Rutherford LC, DeWan A, Lauer HM, Turrigiano GG (1997) Brain-derived neurotrophic factor mediates the activity-dependent regulation of inhibition in neocortical cultures. J Neurosci 17:4527-4535.

Sanders DB (2002) The Lambert-Eaton myasthenic syndrome. Adv Neurol 88:189-201.

Scemes E, Giaume C (2006) Astrocyte calcium waves: what they are and what they do. Glia 54:716-725.

Seil FJ, Drake-Baumann R (2000) TrkB receptor ligands promote activity-dependent inhibitory synaptogenesis. J Neurosci 20:5367-5373.

Shen K, Bargmann CI (2003) The immunoglobulin superfamily protein SYG-1 determines the location of specific synapses in C. elegans. Cell 112:619-630.

Shen K, Fetter RD, Bargmann CI (2004) Synaptic specificity is generated by the synaptic guidepost protein SYG-2 and its receptor, SYG-1. Cell 116:869-881.

Sillevis Smitt P, Kinoshita A, De Leeuw B, Moll W, Coesmans M, Jaarsma D, Henzen-Logmans S, Vecht C, De Zeeuw C, Sekiyama N, Nakanishi S, Shigemoto R (2000) Paraneoplastic cerebellar ataxia due to autoantibodies against a glutamate receptor. N Engl J Med 342:21-27.

Silver J, Miller JH (2004) Regeneration beyond the glial scar. Nat Rev Neurosci 5:146-156.

Smith-Thomas LC, Fok-Seang J, Stevens J, Du JS, Muir E, Faissner A, Geller HM, Rogers JH, Fawcett JW (1994) An inhibitor of neurite outgrowth produced by astrocytes. J Cell Sci 107 (Pt 6):1687-1695.

Smith GM, Miller RH, Silver J (1986) Changing role of forebrain astrocytes during development, regenerative failure, and induced regeneration upon transplantation. J Comp Neurol 251:23-43.

Spiegel I, Adamsky K, Eisenbach M, Eshed Y, Spiegel A, Mirsky R, Scherer SS, Peles E (2006) Identification of novel cell-adhesion molecules in peripheral nerves using a signal-sequence trap. Neuron Glia Biol 2:27-38.

Stevens B, Allen NJ, Vazquez LE, Howell GR, Christopherson KS, Nouri N, Micheva KD, Mehalow AK, Huberman AD, Stafford B, Sher A, Litke AM, Lambris JD, Smith SJ, John SW, Barres BA (2007) The classical complement cascade mediates CNS synapse elimination. Cell 131:1164-1178.

Theodosis DT, Poulain DA (2001) Maternity leads to morphological synaptic plasticity in the oxytocin system. Prog Brain Res 133:49-58.

Tomaselli KJ, Neugebauer KM, Bixby JL, Lilien J, Reichardt LF (1988) N-cadherin and integrins: two receptor systems that mediate neuronal process outgrowth on astrocyte surfaces. Neuron 1:33-43.

Tuzun E, Scott BG, Goluszko E, Higgs S, Christadoss P (2003) Genetic evidence for involvement of classical complement pathway in induction of experimental autoimmune myasthenia gravis. J Immunol 171:3847-3854.

Twyman RE, Gahring LC, Spiess J, Rogers SW (1995) Glutamate receptor antibodies activate a subset of receptors and reveal an agonist binding site. Neuron 14:755-762.

Ullian EM, Sapperstein SK, Christopherson KS, Barres BA (2001) Control of synapse number by glia. Science 291:657-661.

Ullian EM, Harris BT, Wu A, Chan JR, Barres BA (2004) Schwann cells and astrocytes induce synapse formation by spinal motor neurons in culture. Mol Cell Neurosci 25:241-251.

van Baarlen P, van Esse HP, Siezen RJ, Thomma BP (2008) Challenges in plant cellular pathway reconstruction based on gene expression profiling. Trends Plant Sci 13:44-50.

Varoqueaux F, Jamain S, Brose N (2004) Neuroligin 2 is exclusively localized to inhibitory synapses. Eur J Cell Biol 83:449-456.

Ventura R, Harris KM (1999) Three-dimensional relationships between hippocampal synapses and astrocytes. J Neurosci 19:6897-6906.

Vicario-Abejon C, Collin C, McKay RD, Segal M (1998) Neurotrophins induce formation of functional excitatory and inhibitory synapses between cultured hippocampal neurons. J Neurosci 18:7256-7271.

Watson R, Jiang Y, Bermudez I, Houlihan L, Clover L, McKnight K, Cross JH, Hart IK, Roubertie A, Valmier J, Hart Y, Palace J, Beeson D, Vincent A, Lang B (2004) Absence of antibodies to glutamate receptor type 3 (GluR3) in Rasmussen encephalitis. Neurology 63:43-50.

Watt AJ, van Rossum MC, MacLeod KM, Nelson SB, Turrigiano GG (2000) Activity coregulates quantal AMPA and NMDA currents at neocortical synapses. Neuron 26:659-670.

Yamada M, Numakawa T, Koshimizu H, Tanabe K, Wada K, Koizumi S, Hatanaka H (2002) Distinct usages of phospholipase C gamma and Shc in intracellular signaling stimulated by neurotrophins. Brain Res 955:183-190.

Yang Y, Ge W, Chen Y, Zhang Z, Shen W, Wu C, Poo M, Duan S (2003) Contribution of astrocytes to hippocampal long-term potentiation through release of D-serine. Proc Natl Acad Sci U S A 100:15194-15199.

Young-Pearse TL, Chen AC, Chang R, Marquez C, Selkoe DJ (2008) Secreted APP regulates the function of full-length APP in neurite outgrowth through interaction with integrin beta1. Neural Dev 3:15.

Zhang JM, Wang HK, Ye CQ, Ge W, Chen Y, Jiang ZL, Wu CP, Poo MM, Duan S (2003) ATP released by astrocytes mediates glutamatergic activity-dependent heterosynaptic suppression. Neuron 40:971-982.

Zuliani L, Sabater L, Saiz A, Baiges JJ, Giometto B, Graus F (2007) Homer 3 autoimmunity in subacute idiopathic cerebellar ataxia. Neurology 68:239-240.